



THE AUSTRALIAN NATIONAL UNIVERSITY

ACCOMMODATING CONGESTION AND FADING
IN MOBILE AD HOC NETWORKS
Routing Protocol Design and Optimization

Xiaoqin Chen
B.E.

A THESIS SUBMITTED FOR THE DEGREE OF
DOCTOR OF PHILOSOPHY
OF THE AUSTRALIAN NATIONAL UNIVERSITY

Department of Engineering
The Australian National University

September 2008



THE AUSTRALIAN NATIONAL UNIVERSITY

ACCOUNTING EDUCATION AND READING

IN MODEL ACCOUNTING

Robert F. Johnson



Xiropia (Jan)

E.S.

A THESIS SUBMITTED FOR THE DEGREE OF
DOCTOR OF PHILOSOPHY
BY THE AUSTRALIAN NATIONAL UNIVERSITY

THE AUSTRALIAN NATIONAL UNIVERSITY

Canberra

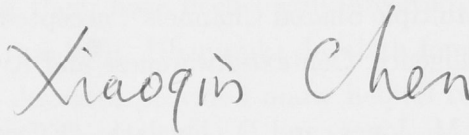
Declaration

I declare that the contents of this thesis are the results of original research and they do not include any material previously submitted for a degree or diploma in any university or institution.

Xiaoqin Chen

National ICT Australia

Department of Engineering, The Australian National University
Canberra, ACT, Australia

A handwritten signature in black ink that reads "Xiaoqin Chen". The signature is written in a cursive style with a large, prominent 'C' at the end.

Publications

- X. Chen, H. M. Jones, and D. Jayalath, “Channel-Aware Routing in MANETs with Route Handoff”, submitted to IEEE Transactions on mobile computing.
- X. Chen, D. Jayalath, and L. Hanlen, “Cooperative Routing for Wireless Networks with Multiple Shared Channels”, accepted by 2009 International Symposium on Intelligence, Context-Awareness and Autonomy in Wireless Networks.
- X. Chen, H. M. Jones, and D. Jayalath, “Effective Link Operation Duration: a New Routing Metric for Mobile Ad Hoc Networks”, in Proc. of ICSPCS, pp 315-320, December 2007.
- X. Chen, H. M. Jones, and D. Jayalath, “Congestion-Aware Routing Protocol for Mobile Ad Hoc Networks”, in Proc. of VTC-Fall 2007, pp 21-25, October 2007.
- X. Chen, D. Jayalath, and H. M. Jones, “A Cross-Layer Design for Mobile Ad Hoc Networking in Fast Fading Channels”, in Proc. of WITSP'05, pp 159-164, December 2005.

Acknowledgements

There are many people guiding and supporting me in the preparation of this thesis. I would like to sincerely express my gratitude to them.

I would like to thank my supervisors, Dr. Dhammika Jayalath, Dr. Haley Jones, and Dr. Leif Hanlen. All of them have been highly involved in the preparation of this thesis. I would like to thank Dr. Dhammika Jayalath for his valuable guidance and constant support. Dr. Jayalath provided many helpful references and friendly encouragement, and gave me great help on how to do the research. I have benefited greatly from his extensive knowledge and technical insight. I am truly grateful for the advice and direction from Dr. Haley Jones, which guided me towards areas of fruitful research. Dr. Jones used her experienced research knowledge to help me place the work in its proper context, and provided extensive comments both on technical and language details on this work. The preparation of this thesis is also benefited from the guidance of Dr. Leif Hanlen, who gave valuable suggestions and comments on my work. I would also like to thank Professor Rod Kennedy for serving as my Ph. D. advisor.

I would like to thank all of my colleagues and friends in Wireless Signal Processing (WSP) group, for the valuable discussions during group meetings and seminars. I also thank all the people at the research school of information sciences and engineering (RSISE) and the people at the faculty of engineering (FEIT), where I always have felt at home. In addition, I am grateful for the financial support from National ICT Australia (NICTA), which was crucial to the successful completion of this work.

Most of all, I am grateful to my family for their support and encouragement of pursuing this research. This work is dedicated to all of you.

Abstract

Mobile ad hoc network (MANET), with decentralized and easily deployed architecture, is an attractive approach to provide flexible and fast data exchange. The proliferation of personal communication devices has promoted a variety of potential military and commercial applications of MANETs. However, the communication capabilities of MANETs are strongly limited by the issues of topology dynamics, traffic congestion, and fading on the mobile radio channel. Random node mobility leads to unpredictable fluctuations on network connectivity. As the limited resources are shared by a large number of nodes in MANETs, congestion is one of the main causes of packet loss, especially when large-scale traffic is present. Moreover, the most important constraint of MANETs comes from the underlying radio channels that exhibit time-varying fading effects. This thesis argues that the efficiency of a routing protocol for MANETs is heavily dependent on the ability to react to variations in network topology, the ability to bypass congested nodes, and the ability to manage radio links which are subject to fading and interference.

The primary aim of this work is to design and optimise routing protocols in order to accommodate congestion and channel fading in MANETs. Specifically, we address two important routing mechanisms: congestion-aware routing and channel-aware routing. And two types of channel-aware routing schemes are taken into consideration, namely channel-adaptive routing and diversity-based routing.

We analyse a range of issues that potentially result in congestion in MANETs. Then we propose a congestion-aware routing protocol which tackles congestion via several approaches, taking into account causes, indicators and effects. The protocol makes localised routing decisions to diffuse traffic evenly among the nodes to combat congestion. Our study shows that routing protocols possessing congestion adaptability are able to improve network performance.

To mitigate time-varying radio fluctuations, we implement two channel-adaptive

routing algorithms. In the first approach, we investigate the interrelationship between link reliability and node mobility as well as radio variations. Based on the observations, we propose an innovative routing metric which combines link lifetime and channel fading to measure link reliability. It is shown in the simulations that the routing protocol implemented with the proposed metric copes well with the channel unreliability in a variety of situations and achieves better performance than the conventional topology-based routing protocols. In the second approach, we examine the second-order statistical characteristics of channel fading, and devise a novel channel-adaptive routing protocol which utilizes multiple channel adaptation schemes to fully exploit channel state information. An analytical model is also developed to derive theoretical expressions for path break probability, throughput and control overhead, to give us particular insights into the workings of the protocol. Such insights will be invaluable for future studies in MANETs. Simulation results show that the proposed routing protocol improves network performance by decreasing the amount of path re-establishment. The simulations also verify the theoretical analysis.

In seeking a better approach to combat fading, we investigate the feasibility of exploiting network diversities. A new diversity-based routing protocol is proposed consequently for MANETs with multiple channels. This protocol makes use of a clustering hierarchy to perform local relay selection and dynamic channel assignment. Then packets are transmitted cooperatively at each hop to take advantage of the multiple channels. A detailed theoretical analysis is also presented to model the behaviours of the routing protocol. The simulation results demonstrate that the protocol achieves diversity gains across a variety of scenarios. The theoretical analysis is consistent with the simulation results.

Keywords: mobile ad hoc network, routing protocol, channel-aware routing, congestion-aware routing

Contents

List of Figures	ix
List of Tables	xiii
Glossary	xv
List of symbols	xviii
1 Introduction	1
1.1 Characteristics of Mobile Ad Hoc Networks	2
1.2 Issues in Routing Protocol Design	3
1.2.1 Dynamic Topology	3
1.2.2 Traffic Congestion	4
1.2.3 Channel Fading	4
1.3 Thesis Motivation and Original Contributions	7
1.3.1 Motivation	7
1.3.2 Original Contributions and Relevant Publications	7
1.4 Organization of the Thesis	11
2 Background	12
2.1 Introduction	12
2.2 Characteristics of Routing Categories	13
2.3 Topology-Based Routing Protocols	14
2.3.1 Dynamic Destination-Sequenced Distance-Vector Routing Protocol	15
2.3.2 Ad hoc On-Demand Distance-Vector Routing Protocol	16
2.3.3 Dynamic Source Routing Protocol	17
2.3.4 Greedy Perimeter Stateless Routing Protocol	18

2.4	Congestion-Aware Routing Protocols	19
2.4.1	Congestion-Adaptive Routing Protocol	19
2.5	Channel-Aware Routing Protocols and Techniques	20
2.5.1	Channel-Adaptive Routing Protocols and Techniques	21
2.5.2	Diversity-Based Routing Protocols and Techniques	24
2.6	Mobile Radio Propagation	27
2.7	Mobile-to-Mobile Channel	29
2.7.1	Channel Model	29
2.7.2	Statistical Characteristics of Mobile-to-Mobile Channel	31
2.8	Conclusion	33
3	Congestion-Aware Routing Protocol for MANETs	35
3.1	Introduction	36
3.2	Review of IEEE 802.11 MAC	37
3.2.1	IEEE 802.11 DCF	37
3.2.2	Multi-rate Transmission in IEEE 802.11 MAC	38
3.3	Congestion in Multi-rate Ad Hoc Networks	39
3.3.1	MAC Control Overhead in Congestion	39
3.3.2	Mismatched Link Data-Rate Routes	41
3.4	Congestion-Aware Routing Metric	41
3.5	Congestion-Aware Routing Protocol	43
3.5.1	Addressing Mismatched Data-Rate Routes	43
3.5.2	Route Discovery	45
3.6	Simulations	46
3.6.1	Simulation Setup	46
3.6.2	Packet Delivery Ratio	47
3.6.3	Average End-to-End Delay	48
3.6.4	Normalized Routing Control Overhead	49
3.7	Conclusion	50
4	Channel-Adaptive Routing Metric: Effective Link Operation Duration	51
4.1	Introduction	52
4.2	Effective Link Operation Duration	53
4.3	Calculation the ELOD	53
4.3.1	Channel Model	53

4.3.2	Effective Link Operation Duration Estimation	54
4.4	Routing Protocol with ELOD	56
4.4.1	Routing Metric	57
4.4.2	The Proposed Routing Protocol	58
4.5	Simulations	58
4.5.1	Varying Node Mobility	59
4.5.2	Varying Traffic Load	61
4.6	Conclusion	63
5	Channel-Aware Routing in MANETs with Route Handoff	66
5.1	Introduction	66
5.2	Review of AOMDV	67
5.3	Mobile-to-Mobile Channel Model	67
5.3.1	Average Non-Fading Duration	68
5.3.2	Average Fading Duration	70
5.3.3	Channel Prediction Using Time Correlation	70
5.4	Channel-Aware AOMDV Protocol	72
5.4.1	Route Discovery in CA-AOMDV	73
5.4.2	Path Maintenance in CA-AOMDV	75
5.4.3	Choosing Prediction Length	77
5.5	Theoretical Analysis	78
5.5.1	Network Model	78
5.5.2	Single Path Lifetime Statistics	80
5.5.3	Multiple Path Lifetime in AOMDV	81
5.5.4	Multiple Path Downtime in CA-AOMDV	83
5.5.5	Multiple Path Lifetime in CA-AOMDV	84
5.5.6	Comparison of Multiple Path System Lifetimes of AOMDV and CA-AOMDV	85
5.5.7	Performance Analysis of AOMDV and CA-AOMDV	87
5.6	Simulation Results	93
5.6.1	Scenario to Evaluate the use of the ANFD in Routing	93
5.6.2	Varying Node Mobility	94
5.6.3	Varying Traffic Load	98
5.6.4	Validation of the Theoretical Model	99
5.7	Conclusion	101

6	Multiple Shared Channels Cooperative Routing	103
6.1	Introduction	104
6.2	System Model and Network Architecture	105
6.2.1	System Model	105
6.2.2	Network Architecture	105
6.2.3	Frequency Reuse	106
6.3	Multiple Shared Channels Cooperative Routing	107
6.3.1	Path Selection	108
6.3.2	Relay Selection Algorithm	108
6.3.3	Routing Protocol Design	109
6.4	Protocol Analysis	111
6.4.1	Network Model	112
6.4.2	Subchannel Collision Probability	112
6.4.3	Location Distribution of the Co-channel Transmitters	113
6.4.4	Average Packet Reception Rate on a Subchannel	114
6.4.5	Average End-to-End Packet Reception Rate	115
6.5	Simulation Results	116
6.5.1	Approximate for Theoretical Analysis	116
6.5.2	Comparing MSCC with GRID	118
6.6	Conclusion	121
7	Conclusions and Future Work	123
7.1	Thesis Summary	123
7.2	Thesis Contributions	124
7.3	Topics for Future Research	126
A	Review of OFDMA	128
A.0.1	OFDMA Modulation	129
	Bibliography	131

List of Figures

1.1	An example of infrastructure wireless network and mobile ad hoc network.	1
2.1	Routing categorization in MANETs. Protocols listed in orange refer to contributions from this thesis.	13
2.2	Example of movement of two nodes, A and B , and the relative distances between them at time t_0 and t	27
2.3	The fluctuations of the received signal power for a radio connection, where both large-scale path loss and small-scale fading are included.	28
2.4	An example of mobile-to-mobile channel.	29
2.5	The relationship between normalized level crossing rate and the ratio of the signal threshold and the root mean square received signal amplitude, $\rho = R_{th}/R_{rms}$, for various $\mu = v_R/v_T$, for the mobile-to-mobile channel from (2.7.8).	32
2.6	The relationship between normalized average fading duration and the ratio of the signal threshold and the root mean square received signal amplitude, $\rho = R_{th}/R_{rms}$, for various $\mu = v_R/v_T$, for the mobile-to-mobile channel from (2.7.9).	33
3.1	The standard transmission sequence in IEEE 802.11 DCF	38
3.2	Two scenarios with the same overall delay but different MAC and transmission delays due to different data-rates and congestion levels.	40
3.3	An example of an 802.11b multi-rate ad hoc network.	42
3.4	Comparison of packet delivery ratio (PDR) with increasing packet rates from 10 to 80 per second for CARM , CARMdelay and DSR.	48
3.5	Comparison of end-to-end delay with increasing packet rates from 10 to 80 per second for CARM, CARMdelay and DSR.	49

3.6	Comparison of normalized control overhead with increasing packet rates from 10 to 80 per second for CARM, CARMdelay and DSR.	50
4.1	Example of movement, V_A and V_B , and the relative distances between nodes A and node B at times t_1 and t_2	54
4.2	Throughput comparison under increasing node mobility.	59
4.3	Normalized routing control overhead comparison under increasing node mobility.	61
4.4	Average end-to-end delay comparison under increasing node mobility.	62
4.5	Average route discovery frequency comparison under different node mobility.	63
4.6	Packet delivery ratio comparison under increasing traffic load.	64
4.7	Average end-to-end delay comparison under increasing traffic load.	65
5.1	Two link-disjoint paths in AOMDV from Source to Destination via nodes BCEG and ACDF, respectively.	68
5.2	The relationship between normalized average non-fading duration and the ratio of the signal threshold and the root mean square received signal amplitude, $\rho = R_{th}/R_{rms}$, for various $\mu = v_R/v_T$, for the mobile-to-mobile channel from (5.3.1).	69
5.3	Handoff in CA-AOMDV. Node F has predicted a forthcoming fade for its link with node D and has generated a HREQ. Having no alternative paths to choose from, node D forwards the HREQ to node C which may then be able to handoff to the path with node E as the next node.	75
5.4	Ratio of multiple path system lifetime for CA-AOMDV to AOMDV for increasing values of link fading threshold parameter ρ , for $L = 3$ links per path, for $N_p = 2, 3, 4, 5, 6$ paths.	86
5.5	Ratio of multiple path system lifetime for CA-AOMDV to AOMDV for increasing values of link fading threshold parameter ρ , for $L = 6$ links per path, for $N_p = 2, 3, 4, 5, 6$ paths.	87
5.6	Ratio of multiple path system lifetime for CA-AOMDV to AOMDV for increasing values of link fading threshold parameter ρ , for $N_p = 6$ paths, for $L = 3, 4, 5, 6$ links per path.	88
5.7	Ratio of multiple path system lifetime for CA-AOMDV to AOMDV for increasing values of link fading threshold parameter ρ , for $N_p = 2$ paths, for $L = 3, 4, 5, 6$ links per path.	89

5.8	Link throughput vs. μ , $\mu = v_B/v_A$, v_A is fixed at 1 m/s, for communicating nodes, A and B , moving in parallel directions, separated by 70 m, initially.	94
5.9	Network throughput comparison between CA-AOMDV and AOMDV with increasing node mobility.	95
5.10	Average end-to-end delay comparison between CA-AOMDV and AOMDV with increasing node mobility.	96
5.11	Normalized routing control overhead comparison between CA-AOMDV and AOMDV with increasing node mobility. Overhead is normalized with respect to delivered data packets.	97
5.12	Throughput comparison between CA-AOMDV and AOMDV with increasing packet rate.	98
5.13	Normalized routing control overhead comparison between CA-AOMDV and AOMDV with increasing packet rate. Overhead is normalized with respect to delivered data packets.	99
5.14	Routing control overhead comparison between theoretical and simulated results with increasing average path lifetime. Theoretical values evaluated from (5.5.26) and (5.5.27).	100
5.15	Packet delivery ratio comparison between theoretical and simulated results with increasing average path lifetime. Theoretical values evaluated from (5.5.31) and (5.5.32).	101
6.1	OFDMA ad hoc network with clustering architecture. Each hexagon is with a radius of ℓ and represents a cluster. A triple of $(a, b; E_j)$ uniquely identifies a cluster, which means that the cluster centre is located at (a, b) , and the subchannel set allocated to that cluster is E_j , ($j = 0, \dots, 6$).	106
6.2	Cooperative routing strategy in MSCC, where SR is the source, D is the destination, CHs are cluster heads, R s are relay nodes, and each green line represents a communicating link.	107
6.3	The frame of a slot in data transmission state, where s_i $\{i = 1, \dots, 4\}$ represents the i th sub-slot, HA is the head advertisement packet, CMA is cluster member advertisement packet, and SHA is the second head advertisement packet.	110

6.4	Average end-to-end packet reception rate, $\delta_{\mathcal{H}}$, comparison between theoretical and simulated results with increasing C/I from 2 to 10 dB, where the theoretical values were evaluated from (6.4.10).	117
6.5	Average end-to-end packet reception rate comparison between theoretical and simulated results with increasing cluster radius from 60 to 300 m, where the theoretical values were evaluated from (6.4.10). . .	118
6.6	PDR comparison between MSCC and GRID with increasing nodes in the network from 80 to 280.	119
6.7	Average end-to-end delay comparison between MSCC and GRID with increasing nodes in the network from 80 to 280.	120
6.8	PDR comparison between MSCC and GRID with increasing C/I from 2 to 16 dB.	121
6.9	Average end-to-end delay comparison between MSCC and GRID with increasing C/I from 2 to 16 dB.	122
A.1	A Baseband OFDM system	129

List of Tables

- 3.1 Simulation parameters 47
- 5.1 Comparison of routing table entry structures in AOMDV and CA-AOMDV. 74
- 5.2 Parameters used in the analysis 79
- 6.1 Parameters used in the analysis 111
- 6.2 Simulation parameters for OFDMA physical layer 116

Glossary

AARF	Adaptive Auto-Rate Feedback
ABR	Associativity-Based Routing protocol
ACK	Acknowledgement frame
AFD	Average Fading Duration
ANFD	Average Non-Fading Duration
AODV	Ad hoc On-demand Distance-Vector routing protocol
AOMDV	Ad hoc On-demanding Multipath Distance-Vector routing protocol
BGCA	Bandwidth Guarded Channel Adaptive routing protocol
CA-AOMDV	Channel-Aware AOMDV routing protocol
CAR	Channel-Adaptive Relaying
CARM	Congestion-Aware Routing protocol for Mobile ad hoc networks
CBR	Constant Bit Rate
CCI	Co-Channel Interference
CDF	Cumulative Distribution Function
CRP	Congestion-adaptive Routing Protocol
CSI	Channel State Information
CSMA/CA	Carrier Sense Multiple access with Collision Avoidance
CTS	Clear-To-Send
DCF	Distributed Coordination Function
DIFS	Distributed Inter Frame Space
DLAR	Dynamic Load-Aware Routing protocol

DSDV	dynamic Destination-Sequenced Distance-Vector routing protocol
DSR	Dynamic Source Routing protocol
ELDC	Effective Link Data-rate Category
ELOD	Effective Link Operation Duration
ETX	Expected Transmission count metric
FORP	Flow Oriented Routing Protocol
GPS	Global Positioning System
GPSR	Greedy Perimeter Stateless Routing
HREQ	Handoff REQuest
LAR	Location-Aided Routing
LCR	Level Crossing Rate
LMMSE	Linear Minimum Mean Square Error
LMR	Lightweight Mobile Routing algorithm
MAC	Medium Access Control
MANET	Mobile Ad hoc NETwork
MC-CDMA	Multi-Carrier Code Division Multiple Access
MDRR	Mismatched Data-Rate Route
MOAR	Multi-channel Opportunistic Auto Rate
MP-AOMDV	Mobility Prediction Ad hoc On-demand multipath Distance Vector
MSCC	Multiple Shared Channels Cooperative Routing
MSR	Multipath Source Routing protocol
MTM	Medium Time Metric
NAV	Network Allocation Vector
OFDMA	Orthogonal Frequency Division Multiple Access

OLSR	Optimized Link State Routing protocol
PDF	Probability Density Function
PDR	Packet Delivery Ratio
PHY	PHYSical layer
R-DSDV	Randomized Destination-Sequenced Distance Vector routing protocol
RABR	Route lifetime Assessment Based Routing protocol
RBAR	Receiver Based Auto Rate
RERR	Route ERRor
RICA	Receiver-Initiated Channel Adaptive routing protocol
rms	root mean square
ROP	Route Outage Probability
RREP	Route REPLY
RREQ	Route REQuest
RTS	Request-To-Send
SDF	Selection Diversity Forwarding
SIFS	Short Inter Frame Space
SMR	Split Multipath Routing protocol
SNR	Signal-to-Noise Ratio
TORA	Temporally Ordered Routing Algorithm
WCD	Weighted Channel Delay
ZRP	Zone Routing Protocol

List of symbols

B	average number of connections over a given link
C	number of source-destination connections in a network
G_0	path gain
N	number of nodes in an ad hoc network
N_R	number of allowed retransmissions
N_{rd}	average number of route discovery processes during a particular period
N_{rq}	average number of RREQs during each path repair
N_a	maximum number of nodes in packet deliveries
P_r	received signal power
P_t	transmitted signal power
R	node transmission range
T_f	link lifetime
Γ	throughput
Ω	number of route discoveries per second per pair
Ω_A	average route discovery frequency in AOMDV
Ω_C	average route discovery frequency in CA-AOMDV
Φ^d	average delay for each route discovery
Ψ	packet delivery ratio
Υ	routing control overhead
Υ^d	route discovery overhead
Υ^r	route repair overhead
\bar{P}_s	average packet reception rate on a path
$\bar{\chi}$	average fading duration
$\bar{\vartheta}$	average non-fading duration

$\delta_{\mathcal{H}}$	average packet reception rate in a route
δ_h^i	average packet reception rate at the i th relay on hop h
\mathcal{D}	path duration
\mathcal{D}_{ap}	advertised path duration
\mathcal{G}_n	power of AWGN (additive white Gaussian noise)
\mathcal{O}_ℓ	effective link operation duration
\mathcal{O}_r	effective path operation duration
$\hat{\mathcal{H}}$	expected number of hops for a path
$\hat{\mathcal{I}}$	expected number of hops to deliver a HREQ
μ	ratio of the receiver velocity to that of the transmitter
ρ	ratio between the signal threshold and the rms value of the received signal
ε	node spatial intensity in a network
d	signal propagating distance
f_R	maximum Doppler frequency of the receiver
f_T	maximum Doppler frequency of the transmitter
q_o	probability that the channel won't be occupied by a node's neighbours

Chapter 1

Introduction

A major focus of recent network research has been on wireless communications. By taking advantage of wireless mobile communications, a node is able to maintain its communication connections during the movement [1]. There are two main classes of wireless networks: infrastructure wireless networks and infrastructureless wireless networks. Infrastructure wireless networks, such as cellular networks, apply pre-configured infrastructure to provide wireless connectivity within the coverage areas [2]. The major drawback of infrastructure wireless networks is that the communication connection is limited by the availability of the infrastructure. In contrast, infrastructureless wireless networks are able to operate independently of any infrastructure. Examples of infrastructureless wireless networks include sensor networks and mobile ad hoc networks (MANETs). In this study we will focus on MANETs.

An illustration of an infrastructure wireless network and a mobile ad hoc network is given in Figure 1.1. The history of MANETs dates back to 1970's. They have their

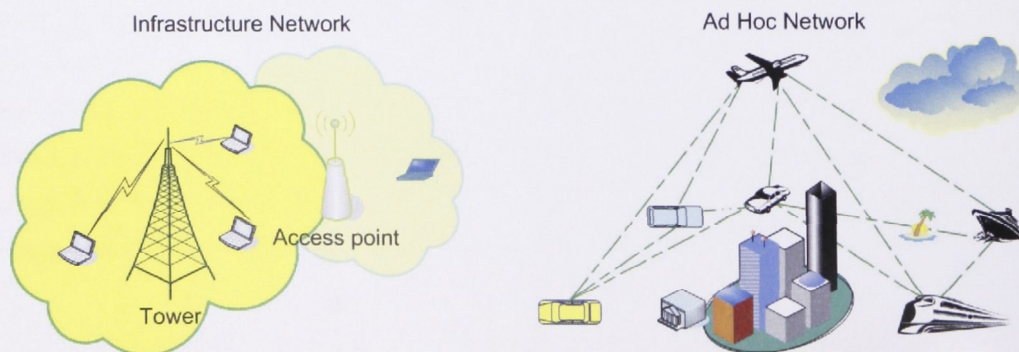


Figure 1.1: An example of infrastructure wireless network and mobile ad hoc network.

root in packet radio networks (PRNs), originating from the single hop ALOHNET network at the University of Hawaii [3]. Then, the DARPA-sponsored Packet Radio Network (PRNET) project stretched the single hop PRNs into multi-hop networks in the 1980's [3, 4].

In MANETs, there are no pre-existing infrastructures or central configuration authorities, thus mobile nodes can be deployed flexibly and instantly. This distributed and easily deployed architecture permits MANETs to provide flexible and fast data exchange in a wide range of network conditions. Such a feature makes MANETs very useful in environments where fixed infrastructures are difficult to implement, or where networks are needed to be constructed immediately. Generally, the proliferation of personal communication devices has promoted a variety of potential military and commercial applications of MANETs, such as battlefield, emergencies (e.g., natural disaster), public safety, conferences, intelligent transportation systems, and wideband wireless access to the Internet.

1.1 Characteristics of Mobile Ad Hoc Networks

Firstly, the main trait of MANETs is its dynamic network topology. In a MANET, all the mobile nodes can move randomly around the network. The random node movement leads to time-varying node geographical locations and link distances. Node transmission range in MANETs is restricted by wireless radios that have low transmission power and limited bandwidth, consequently, network connectivity fluctuates with the node movement. Moreover, during wireless transmissions, node mobility can introduce high packet delivery errors that could effectively disconnect a communicating link. The unstable mobile radio communication causes unpredictably changing network topology.

Secondly, the distributed architecture determines inherent multihop transmission nature of MANETs. Limited by radio transmission range, a source node in MANETs might not be able to directly send a packet to its chosen destination. MANETs use collaborative communications to connect the whole network, in which all the mobile nodes simultaneously take the roles of data source and intermediate relay [5]. A node is able to communicate with indirectly connected nodes by relaying packets via other nodes in the network. This distributed multihop packet transmission feature makes routing a critical issue in MANETs. With the absence of a centralized administrator, it is necessary for MANETs to employ routing protocols to build reliable paths for

1.2 Issues in Routing Protocol Design

packet delivery.

Finally, the most important constraint of MANETs comes from the underlying unreliable wireless channels that exhibit time-varying fading effects. It is well known that path unreliability distinguishes MANETs from other types of networks. MANETs exploit multihop paths to route packets. The successful transmission probability of packets on a given path depends on the reliability of the radio link at each hop. However, path loss and multipath fading additively distort the radio connections, causing them to fluctuate frequently and be unstable [6]. Another factor that significantly impairs link stability in MANETs is node mobility. The presence of rapid node movement at the edges of a radio link (or in the surrounding environment) can introduce a large Doppler spread and result in rapid channel variations [7]. When a channel falls into a deep fade, the instantaneous signal-to-noise ratio (SNR) can be lower than a specified threshold and cause high packet transmission errors or even link disconnection. In summary, wireless transmission and node movement make channel fading the most crippling element to overall network capacity of MANETs.

1.2 Issues in Routing Protocol Design

In MANETs, routing protocols are used to establish and maintain paths (which normally consist of multiple hops) to efficiently direct packet transmission. Due to the aforementioned characteristics of MANETs, three of the main challenges in routing protocol design are to

- *adapt to* **dynamic topology**,
- *combat* **traffic congestion**,
- *and accommodate* **channel fading**.

Let us look at each of these challenges and some of the existing solutions in more detail.

1.2.1 Dynamic Topology

In order to ensure a high level of packet delivery, routing protocols must be competent enough to address the fluctuating network topology. The appropriate routing protocols should be able to establish the connection between a source and its destination

in a timely manner once some paths are present between them [3]. However, the paths might be composed of multiple nodes that are in random motions. Although it is expected the paths remain stable for a period of time, movement of nodes at the ends of a link might change link connectivity and disconnect previously established paths via that link. Consequently, the routing protocol should also have the ability to recover the source-destination connection in case the existing path is broken.

1.2.2 Traffic Congestion

As the limited available resources are shared by a large number of nodes in MANETs, minimizing traffic congestion is an important issue in routing protocol design. Specifically, a routing protocol might build paths via some “hotspots” that participate in many routes. It might lead to a congestion around these nodes once excessive number of packets flow through them. Moreover, in MANETs, because the nodes within each other’s transmission range share the wireless channel, congestion around a single node can affect the operations of all of its neighbouring nodes. This problem becomes more serious in networks with intensive traffic transmission, such as in multimedia. Congestion can lead to high levels of packet collisions, massive packet losses, high routing overhead, long delays, and costly wastage of time and energy on congestion recovery [8]. By combining congestion control with dynamic topology management, congestion-aware routing schemes can mitigate congestion by bypassing the overloaded links.

1.2.3 Channel Fading

In MANETs with highly volatile radio links, it is necessary to accommodate channel variations to maintain path reliability. The conventional solutions to multihop routing problems in MANETs are mostly based on knowledge of topology which is built on the “disk model” [9, 10]. The disk model is a deterministic network model where a node’s communication range is bounded within a circle with a fixed radius irrespective of channel variations [11]. This model neglects the impact of channel fading, so signal power is assumed to simply be attenuated with transmission distance due to path loss. However, in MANETs, network connectivity inevitably fluctuates with channel fading. A link might go into a deep fade and be disconnected even if the geographical location does not change much. Thus, volatility of the channel cannot be ignored and routing protocols solely built on the disk model are naive. In order

1.2 Issues in Routing Protocol Design

to overcome the shortcomings of wireless communication and to combat dynamic topology, routing protocol design should take into account both the node mobility and the radio variations [12, 13]. The ability to combat channel fading is one of the most important factors in determining the efficiency of routing protocols.

Adaptation and diversity, which are two of the essential techniques used to mitigate radio fluctuations in the presence of multipath fading and interference [14], have practical applications in channel-aware routing schemes.

Channel-Adaptive Routing

The potential of adaptive transmission was recognized 30 years ago by Cavers [15] to take advantage of the predictable channel state information (CSI) [16]. Channel-adaptive techniques mostly make use of the evaluation of radio link quality based on a statistical measurement from *a priori* knowledge of the expected channel characteristics [7].

In MANETs, the measures of topology dynamics (link connectivity, node mobility, etc.) are mostly interrelated with channel propagation parameters (signal strength, level cross rate, etc). Therefore, it is advisable to introduce an awareness of channel characteristics into routing protocols. Channel-adaptive routing protocols discover the best relays with the strongest propagating parameters to address link feature like node mobility, transmission distance and fading [17]. In general, channel-adaptive routing protocols utilize methods that can provide an estimation or prediction of the CSI for mobile nodes to monitor the instantaneous link conditions. With knowledge of channel behaviours, nodes can adaptively choose the best available links to build a path, or preemptively change a failing connection to a new one with more favourable channel conditions. In this way, the channel-adaptive schemes implemented in the network layer generally achieve network diversity gains as well [18]. Research shows that, combined with adaptive techniques in the physical layer, channel-adaptive routing protocols can improve the information efficiency of a network by a factor of four to five in Rayleigh fading and log-normal channels [19].

Diversity-based Routing

In environments rich in resources, diversity is one of the most powerful technologies to exploit channel randomness. Diversity in this context is defined as the method of conveying information through multiple independent instantiations of random channels

[20]. In MANETs, the communication links can vary widely from directly line-of-sight to severely obstructed, with each of them fluctuating with the movement of the nodes at the ends of the links or in the surrounding environment. The presence of multiple users experiencing independent channel fading means that MANETs possess abundant sources of diversity, such as multi-user diversity, multiple path diversity, and frequency diversity.

Multihop transmission feature means that MANETs are rich with multi-user diversity. In MANETs, each node, whether it is a source or an intermediate relay, can have access to multiple independently faded next-hop choices, possibly some of them in good channel conditions. An appealing approach to exploit multi-user diversity is cooperative routing [21], in which a packet is transmitted via several relays at each hop. As illustrated in recent research, cooperative routing provides diversity gains on the order of the number of relays in the network [22]. The research of exploiting multi-user diversity in MANETs has its root in the work of [23].

In addition to multi-user diversity, another widely available diversity in MANETs is multiple path diversity. The multihop transmission characteristic and distribution mechanism provide many potential alternative paths between a source and its chosen destination node. These paths may be link- or node-disjoint, with each route composed of partially or completely different nodes. The disjoint alternative paths can have independent fading statistics.

Also it is of benefit to exploit frequency diversity. In the MANETs with multicarrier communication systems such as Orthogonal Frequency Division Multiple Access (OFDMA) [24] or orthogonal Multi-Carrier Code Division Multiple Access (MC-CDMA) [25, 26], the frequency band is split into multiple narrowband subcarriers such that there are multiple orthogonal frequency channels present in each link. In a multipath fading ¹ environment, which happens in most packet transmissions on MANETs, if frequency separation between two orthogonal channels is greater than the coherence bandwidth ², these channels will experience uncorrelated fading. In such networks, an appealing approach to mitigate adverse channel fading is to exploit frequency diversity by transmitting packets via multiple carefully selected channels,

¹The wireless signals usually reach the receiver via multiple propagation paths, each with independently time-varying path gain due to the particular obstacles and interference on that path [27].

²The different time delays in the multiple propagation paths can cause independent statistical properties for two signals with different carrier frequencies. The maximum frequency separation for which the signals are still significantly correlated is called the coherence bandwidth of a mobile radio channel [7].

1.3 Thesis Motivation and Original Contributions

each with independent fading.

Section Summary *The ability to react to variations in network topology, the ability to bypass congested nodes, and the ability to manage radio links which are subject to fading and interference, are the necessary concerns of efficient routing protocol design.*

1.3 Thesis Motivation and Original Contributions

1.3.1 Motivation

The main purpose of this doctoral research is to design and optimise routing protocols to accommodate congestion and channel fading in MANETs. Routing protocol design for MANETs has attracted research attention for many years with significant achievements. To the best of our knowledge, most of these studies are focused on the areas of how to deal with node mobility and topology dynamics. Issues of congestion and channel fading control are neglected in most routing protocol designs with limited outcomes, and still require further work.

The first important purpose of this work is to propose a congestion-aware routing protocol for MANETs. Congestion has a determining role in the packet losses of MANETs, especially where large-scale traffic transmissions are involved. It is necessary to combine routing schemes with congestion control mechanisms to provide congestion adaptability in the network layer.

Moreover, as we discussed in previous sections, the mobile radio channel places a fundamental limitation on network performance. Routing protocols which ignore the impact of channel variations cannot effectively address adverse conditions in MANETs. An attractive solution is to introduce an awareness of the channel characteristics into the routing protocols. The second purpose of this research is to design and optimise routing protocols to include adaptation to the underlying time-varying channels by making use of channel-adaptive and diversity schemes.

1.3.2 Original Contributions and Relevant Publications

Based on the main themes of the thesis, the major original contributions of this research are the designs of routing protocols with congestion awareness, and channel awareness to improve network performance. The details are as follows:

- We first propose an attractive congestion-aware routing metric, the Weighted Channel Delay (WCD) [28], which employs data transmission delay, the Medium Access Control (MAC) overhead, and buffer queuing delay, with preference given to less congested high throughput links, avoiding the most congested ones.

Then we propose the Congestion-Aware Routing protocol for multi-rate Mobile ad hoc networks (CARM) [28]. CARM utilizes two mechanisms to improve the routing protocol adaptability to congestion. Firstly, the WCD is used to select high throughput routes with low congestion. The second mechanism that CARM employs is the avoidance of mismatched link data-rate routes via the use of Effective Link Data-rate Categories (ELDCs). Generally, the protocol tackles congestion via several approaches, taking into account causes, indicators and effects. The localised routing decisions support to diffuse traffic evenly among the nodes to combat congestion.

The simulation results demonstrate that CARM can improve network performance across a wide range of scenarios when compared with the traditional Dynamic Source Routing (DSR) [29] protocol. The congestion adaptability allows CARM an increase on packet delivery ratio, a decrease on average end-to-end delay, and a decrease on routing control overhead.

- Secondly, we introduce an innovative channel-adaptive routing metric to measure link reliability. We propose that the stability of a link should be represented by the time for which the link is up, which is not simply the duration in which the nodes are within each other's transmission range, but the one in which the nodes are within each other's transmission range with no fading. We call this new metric Effective Link Operation Duration (ELOD) [30]. To estimate the ELOD, first, the proposed scheme makes use of node mobility to predict link lifetime; then it combines the link lifetime with channel fading statistics to obtain the ELOD. Thus, applying ELOD as a routing metric addresses issues caused by node mobility as well as those caused by channel fading.

We then introduce the ELOD into a routing protocol to perform channel-adaptive routing [30]. The simulation results show that the routing protocol implemented with the proposed channel-adaptive metric can cope well with the channel unreliability in various environments, and achieve a higher throughput, a lower end-to-end delay, and a lower routing control overhead than conventional topology-based routing protocols.

1.3 Thesis Motivation and Original Contributions

- Thirdly, we propose a novel channel-adaptive routing protocol which extends the Ad-hoc On-Demand Multipath Distance Vector routing protocol (AOMDV) [31] with multiple channel adaptation schemes to accommodate channel fading. The proposed Channel-Aware AOMDV (CA-AOMDV) [32] makes use of channel state information (CSI) in both the route discovery and path maintenance phases to improve path stability:
 - Route discovery: In CA-AOMDV, the average channel non-fading duration (ANFD) is combined with the hop-count criterion from AOMDV to serve as a metric with which to select short but stable paths instead of simply choosing the shortest path, as in AOMDV. Therefore, CA-AOMDV targets paths taking into account both the stability and the length, to improve overall path quality.
 - Route maintenance: Assuming independently time-varying path characteristics, CA-AOMDV uses predicted signal strength to trigger a handoff before a fade occurs, reducing the source-destination connection failure rate. The channel average fading duration (AFD) for the breaking link is also recorded, so that the channel may be utilized again once it comes out of the fade.

Furthermore, we develop a theoretical model to analyse the network performance of MANETs. This model first derives the theoretical expressions for the probability density functions (PDFs) of the lifetimes of a single path and multiple paths. The performance in terms of routing control overhead and throughput of both AOMDV and CA-AOMDV based on the link lifetime distributions are then analysed [32].

Simulation results show that CA-AOMDV can improve network performance by decreasing the frequency of path re-establishment. When compared with AOMDV, CA-AOMDV has an improved throughput, a decreased routing control overhead, and a decreased average end-to-end delay. Simulations verify the theoretical analysis.

- Finally, we propose a new diversity-based routing protocol, Multiple Shared Channels Cooperative Routing (MSCC) [33], for MANETs. The proposed MSCC protocol has a clustering hierarchy. A bandwidth reuse scheme is applied among the clusters to reduce inter-cluster Co-Channel Interference (CCI).

Moreover, within each cluster, a set of subchannels are distributed to cluster members in a no-colliding way, therefore, intra-cluster CCI can be eliminated. Packets are transmitted cooperatively at each hop. Specifically, when a cluster has a packet to deliver, the cluster head will select several relays from the cluster members that with good channel conditions. Then these relays forward the packet via the subchannels allocated to them respectively. Generally, MSCC takes advantage of diversity in a multiple shared channel environment, while reduces the CCI as well.

We derive theoretical expressions to analyse the performance of this protocol [33]. The simulation results indicate that the exploitation of diversity leads to an increase in throughput. The theoretical analysis is consistent with the simulation results.

Characteristics and Applications of the Proposed Routing Protocols

With regard to the four proposed routing protocols, CARM, ELOD, CA-AOMDV and MSCC, each of them is in possession of a unique design and with distinguishing characteristics, thus, has applications in particular environments, respectively.

- In CARM, congestion control mechanisms are combined with routing schemes to mitigate congestion in MANETs. The congestion awareness feature leads CARM competent in networks with large-scale traffic transmission, such as in multimedia. However, the impact of channel variations is ignored in CARM.
- ELOD and CA-AOMDV seek the approach of adaptation to address channel fluctuations. ELOD achieves adaptability by employing a channel-adaptive routing metric. While CA-AOMDV incorporates several channel adaptation approaches to ameliorate channel fading. It makes use of channel state information in both route discovery and route maintenance phases. With better knowledge of channel behaviours, CA-AOMDV can more accurately choose the best links to build a path, or adaptively switch a failing connection to a new one with more favourable channel conditions. However, these schemes works well only if the CSI is kept up-to-date. CA-AOMDV requires continually monitoring instantaneous link conditions to trigger a handoff once a fade occurs. In a highly mobile environment, the channel probing would be rather high and counteract adaptation gains.

- MSCC takes advantage of network diversities instead of adaptation techniques to combat channel fading. In environments rich in sources of diversity, it is powerful to exploit channel randomness by cooperatively transmitting via multiple relays.

1.4 Organization of the Thesis

The remaining chapters of this thesis are structured into four parts. In the first part, Chapter 2 provides research background material in both routing protocols and wireless channel characteristics. In particular, this chapter first performs a literature survey on recent advances in the routing protocols of MANETs. The second half of this chapter is dedicated to a brief review of mobile wireless channel models and their statistical characteristics. The results of the investigation on radio transmission motivate the proposals of channel awareness schemes to constitute channel-aware routing protocols in the third part of the thesis.

The second part of the thesis mainly concerns of congestion-aware routing scheme. A detailed description of the proposed congestion-aware routing protocol, CARM, is provided in Chapter 3.

In the third part of the thesis, we present the proposed channel-aware routing protocols. And two types of channel-aware routing protocols are taken into consideration, namely channel-adaptive routing protocol and diversity-based routing protocol. This part is organized as follows. The channel-adaptive routing protocols are developed in Chapter 4 and Chapter 5. Specifically, Chapter 4 addresses the issue of reliable path selection, and a novel channel-adaptive routing metric, ELOD, is presented. Chapter 5 introduces the proposed channel-adaptive routing protocol, CA-AOMDV. A theoretical model is also presented in this chapter to characterise the performance of CA-AOMDV. The diversity-based routing protocol, MSCC, is described in Chapter 6 to achieve both frequency and multi-user diversity gains in MANETs. The theoretical analysis of MSCC is also developed in this chapter.

Finally, we draw our conclusions, and discuss future research topics in Chapter 7.

Chapter 2

Background

2.1 Introduction

This chapter provides background material in both routing protocols and wireless channel characteristics. We start with a brief review of the routing protocols and routing techniques that have been proposed for MANETs in recent years. These protocols and techniques will be grouped into three categories with respect to their routing characteristics, and a detailed description of each routing category will be presented. The second part of this chapter conducts a literature survey on the models which are commonly used to describe the radio channels of mobile communications. The results motivate the proposals of channel awareness schemes to constitute channel-aware routing protocols in the third part of this thesis.

The layout of this chapter is as follows. It begins with the categorisation of routing protocols and techniques in Section 2.2, which is followed by the detailed description of each routing protocol category. Specifically, Section 2.3 presents topology-based routing protocols. Congestion-aware routing protocols are described in Section 2.4, and channel-aware routing protocols and metrics are explained in Section 2.5. In the second part of this chapter, an overview of typical mobile radio propagation models is provided in Section 2.6. Section 2.7 presents a related fading channel model, the mobile-to-mobile channel, and its statistical characteristics. Finally, conclusions are drawn in Section 2.8.

2.2 Characteristics of Routing Categories

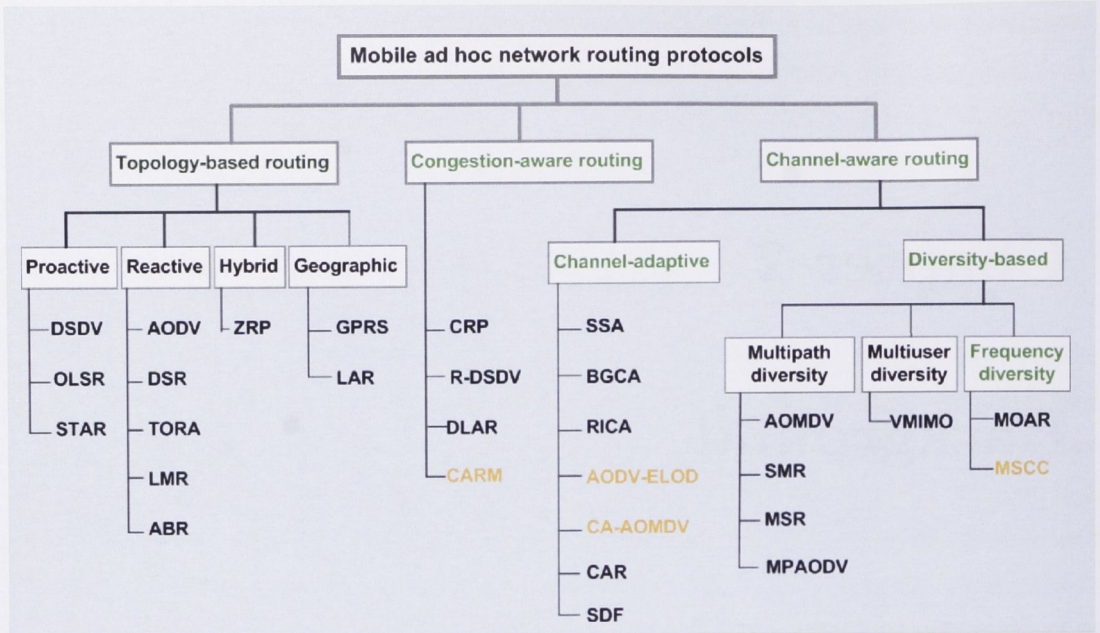


Figure 2.1: Routing categorization in MANETs. Protocols listed in orange refer to contributions from this thesis.

2.2 Characteristics of Routing Categories

With respect to the routing characteristics discussed in Chapter 1, the routing protocols and techniques proposed for MANETs typically fall into three categories: topology-based routing protocols, congestion-aware routing protocols, and channel-aware routing protocols. Channel-aware routing protocols are further divided into two sub-categories: channel-adaptive routing protocols and diversity-based routing protocols. The categorisation of routing protocols for MANETs is illustrated in Figure 2.1.

Not surprisingly, in topology-based routing protocols, topology information is of primary concern in making routing decisions. The integration of routing mechanisms with congestion control techniques permits congestion-aware routing protocols with the ability to react to congestion measurement. In channel-aware routing protocols, channel state information is combined with topology information to combat channel fading as well as network dynamics. Each of these routing categories will be discussed in detail in the following sections.

2.3 Topology-Based Routing Protocols

The most of conventional routing protocols proposed for MANET are designed to deal with network dynamics and node mobility. They are traditionally classified as proactive (or table-driven), reactive (or on-demand), or hybrid routing protocols. Geographic routing (or position-based routing) protocols are proposed for networks where geographical information is available.

In proactive routing protocols, each node has a routing table in which to record paths to other nodes in the network. Nodes exchange routing information periodically to ensure their routing tables up-to-date. Proactive routing protocols continuously maintain any possible connections within the network, so that routes are established prior to the arrival of data packets. In this way any arriving packet can be routed immediately. However, if the rate of topology change in a network is fast, periodically maintained paths are prone to being out-of-date. Thus proactive routing protocols only have limited applications in MANETs. Typical proactive routing protocols include Destination-Sequenced Distance-Vector (DSDV) [34], and Optimized Link State Routing (OLSR) [35]. Particularly, DSDV uses an enhanced distance-vector routing method by optimising the classical Distributed Bellman-Ford (DBF) algorithm [36], while OLSR follows the link-state route computation approach.

Reactive routing protocols establish a path only if that path is of requisite in certain packet transmissions. The path discovery process is initiated by a source node to broadcast a route request through the entire network. The reactive routing mechanisms result in much lower levels of routing control overhead than proactive routing protocols. However, generally there is a delay of route computation in reactive routing protocols. Moreover, in a highly volatile network environment, broadcasts in route discovery process may be unreliable. Typical examples of reactive routing protocols include Ad hoc On-demand Distance-Vector (AODV) [37], Dynamic Source Routing (DSR) [29], Lightweight Mobile Routing (LMR) [38], Temporally Ordered Routing Algorithm (TORA) [39], and Associativity-Based Routing (ABR) [40]. Specifically, in AODV, each intermediate relay contains only next-hop routing information. While DSR uses a source-based routing scheme in which a source node learns the complete path to a particular destination. As compared with AODV, DSR generates more routing overheads and scales worse with the network size. LMR and TORA follow the link-reversal routing algorithm. Instead of collecting global routing formation to support shortest-path computation, as what happens in AODV or DSR, they are only

2.3 Topology-Based Routing Protocols

aware of connections to adjacent nodes to build the Directed Acyclic Graphs (DAGs) rooted at the destination nodes. In contrast to following a failure-query/reply round in LMR to repair a link failure, the route maintenance in TORA involves only a single phase (update). LMR is intended for applications in networks where the rate of change is not too fast or too slow, to achieve a balance between shortest-path routing and flooding. TORA is suitable for application in large-scale, dynamic heterogeneous networks where a multitude of Radio Access Technologies (RATs) is available. Finally, ABR employs node associativity to select long-lived paths in terms of link stability. It is favourable to support conference-size MANETs.

The constraints of proactive and reactive routing mechanisms determine that they can work efficiently only within a limited range of network conditions, for example, in networks with a relatively small number of nodes. In large-scale networks, two important means of increasing network scalability are hybrid routing and geographic (or position-based) routing. Hybrid routing protocols, such as Zone Routing Protocol (ZRP) [41], make use of clustering hierarchy to take advantage of local proactive routing and global reactive routing. In networks that are equipped with a location service, such as Global Positioning System (GPS), geographic routing is another important way to increase scalability. Geographic routing protocols achieve routing efficiency by exploiting geographical information, and routing decisions are performed based on the geographical location of each relay node. Examples of geographic routing protocols include Greedy Perimeter Stateless Routing (GPSR) [42], and Location-Aided Routing (LAR) [43]. GPSR allows greedy forwarding using the geographical information of a node's immediate neighbours, while LAR uses location information to restrict the search of a new route within a "request zone" in the network.

We now give details of some typical topology-based routing protocols.

2.3.1 Dynamic Destination-Sequenced Distance-Vector Routing Protocol

In the dynamic Destination-Sequenced Distance-Vector routing protocol (DSDV) [34], each node maintains a routing table to direct packet transmission. Packets are routed to a given destination node along the path stored in the routing tables for that destination with the highest sequence number. If saved paths to the destination have the same sequence number, the one with the smallest hopcount is used.

To maintain up-to-date routing tables, nodes periodically broadcast routing advertisement packets. Two types of advertising schemes are in use. The first is a full dump in which all of the available routing information is broadcast. The other is an incremental broadcast which only includes the routing information that has changed since the last full dump. Typically a full dump is arranged when network topology has changed significantly. This is of benefit to reducing the amount of routing information carried in the next incremental broadcast. Whenever a node receives an advertisement packet, it will compare the routing information carried in the advertisement with those recorded in its routing table. If a newly received route for a given destination has a higher sequence number than an existing one, or if it has a sequence number equal to an existing route but with a shorter hopcount, the new route is selected. The routing table is updated and route changes are broadcast to neighbouring nodes immediately.

Shortly, DSDV continuously maintains connections within a network, thus a route can be put into use immediately once it is in need. However, the protocol must advertise route changes often enough to keep routing tables up-to-date. If the rate of topology change in the network is fast, the periodic advertisement may cause a broadcast “storm”, and the amount of routing overhead can be very huge even unacceptable.

2.3.2 Ad hoc On-Demand Distance-Vector Routing Protocol

The Ad hoc On-demand Distance-Vector routing protocol (AODV) [37] discovers a path reactively. The protocol follows a two-phase routing procedure of route request (RREQ)/route reply (RREP) in response to route discovery. When a node has packets to deliver while no routes are available, it broadcasts a RREQ to its neighbours. Similarly to DSDV, AODV maintains a routing table at each node. When a neighbouring node receives a RREQ, it first will check whether it has seen the RREQ before. If the node has seen the RREQ before, it discards the broadcasting packet. Otherwise, the node updates its routing table and sets up a reverse route entry for the source. Moreover, the node will search its routing table for a path to that destination. If there is no path present, it increments the RREQ’s hopcount then broadcasts the packet further. While if the node is the destination, or if it has a path to the destination with a sequence number at least as high as that of the RREQ, it returns a RREP to the source.

2.3 Topology-Based Routing Protocols

A RREP is forwarded back to the source node along reverse route. When an intermediate node receives a RREP, it sets up a forward path entry for the destination in the route table. If a node receives more than one RREPs for a given destination, generally only the first one is forwarded to the source. A later received RREP will be delivered only if it has a greater destination sequence number or a smaller hopcount than any previously forwarded ones. The source begins transmission as soon as the first RREP arrives, and it can choose a new path later if it receives further RREPs.

If a link on a path (or multiple paths) is broken, a Route Error (RERR) message is generated by the upstream node of the broken link. The RERR lists all the destinations that are now unreachable because of the link breakage. If the upstream node has any precursor nodes listed in its route table for these disconnected destinations, it delivers the RERR to them. When a neighbour receives the RERR, it marks the routes to those destinations as invalid and forwards the RERR further if it still has precursor nodes for the destinations. When a source node receives the RERR, it can re-initiate a route discovery if it still needs that route.

Generally, in AODV each intermediate relay contains only the next-hop routing information, thus the protocol yields low levels of routing overhead and scales well with the network size. However, the reactive route discovery mechanism may result in a route computation delay.

2.3.3 Dynamic Source Routing Protocol

The Dynamic Source Routing protocol (DSR) [29] utilises a reactively source routing scheme. In packet delivery, a source node places the entire route which contains the sequence of hops that a packet should follow in the packet header. Another important component of DSR is route cache. Each node overhears routing information from the packets (including the source routes, RREQs, RREPs, etc.) that pass through it to maintain its route cache. Typically, a node first will search its route cache for a path when it has packets to deliver. If no path is found, the node initiates a route discovery by broadcasting a RREQ. When an intermediate node receives a RREQ that it didn't see before, the node appends its address to the RREQ and forwards it further if it has no route to the destination node. Otherwise, if a route is found in the cache, or if the node is the destination, the node generally responds by sending a RREP back to the source.

The route maintenance of DSR is similar to that of AODV. Each node along a

route monitors its next-hop link during transmissions. Route maintenance is initiated by the node which has detected a disconnected link, and a RRER is returned to the source node. The source node will search its route cache for an alternative route to deliver subsequent packets. If no route is found, the source node invokes another route discovery process to find a new one.

In short, the cached routing information permits DSR to establish or repair a route quickly when topology changes. This results in a decrease in path connection delay. However, the cached paths are prone to being stale in a highly volatile environment, and the source routing mechanism in which the entire route is placed in a packet header can result in high levels of routing overhead.

2.3.4 Greedy Perimeter Stateless Routing Protocol

The Greedy Perimeter Stateless Routing (GPSR) protocol [42] exploits geographical information to achieve scalability. In GPSR, nodes are assumed to be equipped with a location service to determine their location. Each node periodically broadcasts beacons to maintain a list of one-hop neighbouring nodes. Usually a “greedy” routing scheme is used to forward packets to the neighbour node which is with closest location to the destination node, until the destination is reached finally. While the greedy routing works well for dense network environments, it may fail when the packet reaches a node with a “void”, which occurs in sparse conditions. The perimeter routing, which is based on the right-hand rule, is used to route packets around voids. The greedy routing and perimeter routing are combined as follows. Whenever a packet reaches an intermediate node which has no neighbour closer to the destination, the perimeter routing replaces greedy routing and the packet is forwarded according to the right-hand rule. The routing scheme returns back to the greedy routing once the packet reaches a node which is closer to the destination than the perimeter entry point, where the perimeter is the sequence of edges found by using the right-hand rule.

Section Summary *In this section, we give a brief review of topology-based routing schemes, which include proactive, reactive, hybrid, and geographic routing. Proactive routing protocols use periodical broadcast to continuously maintain connections. They take advantage of low path connection delay, but the periodical routing information advertisement may cause a broadcast storm. The reactive routing protocols establish a path only if necessary. The reactive routing mechanisms result in much lower routing*

2.4 Congestion-Aware Routing Protocols

control overhead than that of proactive routing protocols, but with a delay for path discovery. Both proactive and reactive routing schemes work efficiently only in networks with relatively small size. In large-scale networks, hybrid routing, which combines the proactive and reactive routing approaches, and geographic routing, where geographical information is used to assist routing, are proposed to increase network scalability.

2.4 Congestion-Aware Routing Protocols

Congestion is one of the main causes of packet loss in MANETs. With a lack of congestion adaptability, routing schemes may establish paths via some links prone to being congested. Thus, it is of benefit to introduce congestion awareness into routing protocols. Specifically, congestion-aware routing schemes [44, 45] take account of the congestion status when choosing a new route, where routing metric is partly treated as a function of congestion measurements. Several proposed congestion aware routing protocols are Congestion-Adaptive Routing (CRP) [46], Dynamic Load-Aware Routing (DLAR) [47], and Randomized Destination-Sequenced Distance Vector (R-DSDV) [48]. Particularly, CRP uses a “bypass” route to split traffic on the primary route to mitigate congestion. Taking advantage of adaptive control mechanisms in response to congestion, the protocol reduces the chance of congestion occurrence. However, CRP costs some routing overhead to maintain bypass routes. In DLAR, the traffic load of a node is of primary concern in route selection. The protocol also monitors the congestion level of routes and repairs a route once congestion occurs. While DLAR only takes account of the impact of traffic load, other factors potentially resulting in congestion are ignored. R-DSDV is an enhancement of the DSDV routing protocol. Instead of on a periodic basis as in DSDV, it broadcasts routing messages probabilistically. The proactive routing mechanism leads R-DSDV unsuitable for highly volatile environments.

We now take the Congestion-Adaptive Routing protocol as an example and present it in details.

2.4.1 Congestion-Adaptive Routing Protocol

The Congestion-Adaptive Routing protocol (CRP) [46] prevents congestion preemptively by reducing the amount of the incoming traffic on congested routes. The protocol classifies nodes into three types: “green” (far from congested), “yellow” (likely

congested), or “red” (congested), based on node congestion level which is measured by checking node buffer occupancy. There are two types of routes in CRP, namely primary route and bypass route. The first path established via a route discovery process is the primary route. A bypass is composed of some less-congested nodes around the primary route. In CRP, each node periodically advertises its congestion status by broadcasting update (UDT) packets to its neighbours. When a node receives a UDT packet from its next primary node indicating that a link on the primary route is congested, the node starts to discover a bypass route toward the next “green” node on the primary route. Once the bypass is established, the node splits the incoming traffic on the primary route and switches part of the traffic to the bypass route based on the congestion levels of both routes.

Generally, with the availability of a bypass route, CRP can prevent congestion preemptively by splitting traffic over the primary route and the bypass route. The adaptive congestion control scheme allows CRP to reduce the chance of congestion occurrence. However it costs routing overhead to maintain bypass routes.

***Section Summary** At the network layer, congestion-aware routing is one of effective means to reduce packet losses. To introduce congestion awareness into routing protocols, a routing metric is partly treated as a function of congestion measurements. The congestion-aware metric then is combined with congestion control mechanisms to change path establishment. Generally, in congestion-aware routing protocols, congestion control schemes are combined with mobility and topology control mechanisms to improve network robustness. However, it costs some routing overheads to implement congestion-aware mechanisms in routing process.*

2.5 Channel-Aware Routing Protocols and Techniques

Not only intending to combat topology dynamics, channel-aware routing schemes also attempt to accommodate channel fading at each transmission. In regard to their approach to combating fading, channel-aware routing protocols are divided into two sub-categories: channel-adaptive routing and diversity-based routing. Some designs have exploited both aspects.

2.5.1 Channel-Adaptive Routing Protocols and Techniques

Channel-adaptive routing schemes use adaptive techniques to establish a new route or preemptively change a breaking connection based on instantaneous link quality. These schemes periodically monitor radio links to identify the best relays with the strongest CSI, such as signal strength [49], outage probability [50], power [51], bit transmission rate [52, 53], packet error rate [54], SNR [55, 56], bandwidth [57], or any combination of these measures [58, 59, 60]. Adaptive routing schemes can take advantage of short-term channel variations on a hop-by-hop basis [61, 62] or long-term channel variations on an end-to-end basis [58, 63]. However, these strategies work well only if the CSI remains up-to-date. Since CSI is valid for time scales similar to the channel coherence time ¹, channel-adaptive schemes require continuously evaluating the radio connections to keep link quality acceptable. Therefore, the gains achieved by channel adaptation may be traded off by channel probing overheads.

We now present some typical channel-adaptive routing techniques in details.

Channel-Adaptive Routing Metrics

The Expected Transmission count metric (ETX) [64] is proposed to favour high throughput links. “The ETX of a link is the predicted number of data transmissions required to send a packet over that link, including retransmissions” [64]. It takes advantage of the packet successful reception rates of a given link on both forward direction and reverse direction, and is given by

$$\text{ETX} = \frac{1}{d_f \times d_r}$$

where d_f is the forward delivery ratio, which represents the ratio of the number of received packets to the number of transmitted packets, and d_r is the reverse delivery ratio for acknowledgement (ACK) packets. The two parameters are measured periodically by using probe packets. ETX measures link performance at several aspects, taking into account interference, packet loss, and asymmetry in the packet loss ratios between the two directions of a link. However, it is shown that ETX is not able to react quickly to the changes of link quality [65].

The Medium Time Metric (MTM) [52] is proposed for MANETs with multiple data-rates. The traditional routing metrics, such as the minimum hop-count (MH)

¹The inverse of the coherence bandwidth (given in Section 1.2.3) gives a measure of the coherence time [7].

metric, tend to select routes comprised of longer links which inherently have low data-rate and inferior quality. MTM assigns each link with a weight that is proportional to the packet transmission time on that link. The weight of a path is the total medium time consumed when a packet traverses it. Therefore, MTM identifies paths that minimize the total transmission time. However, it does not consider packet losses at each link. This metric also prefers paths with a greater number of shorter distance links. When more links attend packet relaying, contention for the shared medium will increase.

The Route Outage Probability (ROP) [50] for a given route is defined as the probability of packet transmission failure in that route due to fading. The cost of a particular route is estimated from the outage probability of all the links in that route, and it is used to represent the route reliability. ROP prefers delivering data packets along the most reliable route rather than the shortest one, to minimize fading introduced packet loss. The feasibility of ROP is that a long route with a few more hops to deliver a packet to the destination with high probability of successful packet transmission is preferable to a short one with a high packet drop rate. ROP can be used to find the routes with the lowest probability of packet loss. The disadvantage of ROP is that more resources may be spent delivering a packet to its destination due to increased number of hops in a path.

Bandwidth Guarded Channel Adaptive Routing Protocol

The Bandwidth Guarded Channel Adaptive (BGCA) routing protocol [60] adaptively establishes and changes routes based on the CSI of those routes. BGCA continuously monitors each of its links. Based on the instantaneous CSI, adaptive channel coding and modulation schemes are used to change the data-rate of a link. In route discovery phase, all the links fall into four classes based on their data-rates. A class-based “hop”, which is a weighed hopcount, is assigned for each link. BGCA employs the weighted hopcount metric to select stable routes. In route maintenance phase, when the bandwidth of a link is lower than a specified threshold, the downstream node of that link sends a message to the upstream node. After receiving the message, the upstream node first will check whether the link bandwidth can meet the requirements. If not, the node initiates a locally performed route discovery process to find a bypass route to repair the original one. Because the local route discovery is initiated when the quality of a link is already lower than a particular threshold, route changing in BGCA is rather “passive” to channel variations.

2.5 Channel-Aware Routing Protocols and Techniques

Receiver-Initiated Channel Adaptive Routing Protocol

Instead of only changing a few fading links, as what happens in BGCA, the Receiver-Initiated Channel Adaptive (RICA) routing protocol [58] adaptively changes an entire route if an alternative path has a better instantaneous CSI than that route. To measure the CSI of each path, a destination node periodically broadcasts a CSI checking packet. When a source receives several CSI checking packets originating from the destination, it chooses the route with the best CSI as the new path, no matter whether the past one is in good channel conditions or not. RICA takes advantage of the time-varying properties of wireless channel to maintain high throughput connections. However, the channel adaptation scheme in RICA is on an end-to-end CSI measurement basis, which means that the protocol has limited adaptation ability. Moreover, the periodically probing mechanism can lead a high level of routing control overhead.

Adaptive Forwarding Techniques

Routing schemes can also be adaptive to channel variations on a hop-by-hop basis. Channel-adaptive forwarding techniques allow opportunistically selecting the next-hop relays which are experiencing good channel conditions [66]. Typical examples of adaptive forwarding algorithms include Selection Diversity Forwarding (SDF) [67] and Channel-Adaptive Relaying (CAR) [61].

SDF enhances the classical forwarding strategies of NFP (Nearest with Forward Progress) and MFR (Most Forward with fixed Radius R) [68]. It allows a node to multicast packets to multiple relays. In response to feedbacks from the relays, the node makes a forwarding decision based on positive forward progress [69]. The relay selection in SDF is based on location information rather than the knowledge of channel state. It is suitable in environments where CSI is unavailable.

In contrast, the Channel-Adaptive Relaying (CAR) [61] routing scheme jointly considers geographical information and channel fading. The protocol makes use of a cross-layer design to achieve adaptivity to both large-scale and small-scale channel fading. Firstly, at the network layer, a number of next-hop relays of a given node are selected as candidates based on the long-term CSI measurements in term of the average SNR. This strategy is used to combat large-scale fading. Then, the addresses of the candidates are passed to the MAC layer. When having packets to forward, at the MAC layer, the node will multicast a polling message to the candidates, then a relay is selected finally with respect to the maximum expected progress (MEP)

values of the candidates. In this way CAR overcomes small-scale channel variations. Therefore, CAR adapts well to channel fading.

Generally, the local channel-adaptive routing approaches on a hop-by-hop basis outperform those on an end-to-end basis to mitigate channel fading. However, they require geographical information or more resources (e.g., multicast in SDF).

Section Summary *Channel-adaptive routing schemes use adaptive techniques to establish a new route or preemptively change a breaking connection. They require periodically monitoring the network in order to identify relays with the strongest CSI (signal strength, outage probability, bit-rate, packet error rate, SNR, bandwidth, etc.). However, the periodical channel probing or adaptive route maintaining in a channel-adaptive routing protocol can result in a high level of routing overhead, which may partly counteract the gains achieved by channel adaptation.*

2.5.2 Diversity-Based Routing Protocols and Techniques

There are abundant diversity resources in MANETs, such as multi-user diversity (or spatial diversity), multiple path diversity and frequency diversity. A vast array of routing protocols has been proposed to take advantage of these network diversities. Some typical diversity-based routing techniques will be discussed in detail in the following sections.

Multi-user Diversity

Cooperative routing is widely used to achieve multi-user diversity gain in the network layer. Generally, at each transmission, this kind of schemes form a virtual antenna array via several single antenna nodes [70] to maintain transmission reliability. Several multi-user cooperative schemes can be found in [21, 71, 51]. Both [21, 71] develop cooperative transmission schemes on a hop-by-hop basis. It is proposed in [21] that, when a node transmits a packet, the relays that have successfully decoded that packet utilize an orthogonal space-time code to cooperatively relay the packet. The orthogonality constraint in [21] is relaxed in [71] by allowing a source node and relays to transmit simultaneously. It is shown that [71] can improve network performance while at a higher decoding complexity. However, these approaches require a large amount of coordination and are difficult in practice.

In [51], a virtual Multiple Input Multiple Output (MIMO) routing scheme is proposed to achieve multi-user diversity. The network is with a clustering hierarchy,

2.5 Channel-Aware Routing Protocols and Techniques

and a cluster head is elected for each cluster. The data transmission in each hop is divided into two steps. First, a cluster head broadcasts packets to the cluster members within its cluster. Then, the cluster members encode the packets using an orthogonal Space-Time Block Code (STBC), and forward them to the cluster head in the next-hop cluster. This cross-layer design can jointly improve energy efficiency, reliability, and end-to-end QoS provisioning. However, it requires nodes in each cluster locally synchronized. Moreover, each packet is relayed by multiple nodes, which can lead to high traffic load in a network.

Frequency Diversity

When multiple channels are available, such as in a system based on IEEE 802.11 wireless media standard or a system with multi-carriers, it is feasible to exploit frequency diversity. Examples of protocols to exploit frequency diversity include [72] and Multi-channel Opportunistic Auto Rate (MOAR) [73]. MOAR is proposed for multi-channel and multi-rate MANETs supported by IEEE 802.11. The protocol allows a receiver to measure the SNR value of a Request-To-Send (RTS) frame. If the measured SNR is lower than a given threshold, the receiver negotiates with the transmitter to skip to a new channel, to find a channel with better quality. This scheme is able to achieve frequency diversity gain in the MAC layer, while it requires a cost of resources spent in channel measurement. The work of [72] integrates channel assignment into routing protocol to exploit frequency diversity in the network layer. It employs a routing metric which indicates the cost of interface switching on a path, to select less interfering paths. However, the diversity gain achieved in an end-to-end implementation would be limited.

Clearly, most of these schemes intend to exploit diversity in a single carrier system. There is a lack of routing protocols to exploit diversity in multi-carrier systems. In contrast to single carrier systems, where typically only one channel is in use, multi-carriers systems, such as OFDMA and MC-CDMA, are in possession of multiple channels that can be used simultaneously. It is advisable to take advantage of the multiple channels in a multi-carriers system. This motivates our research on the work of MSCC.

Multiple path diversity

In MANETs, multiple paths that are experiencing independent fading are usually available between a source node and a destination node. Hence there is a high probability that some of them are in good channel conditions. There are a large number of works on multiple path routing schemes, such as Multipath Source Routing (MSR) [57], On-demand Multipath Distance Vector Routing (AOMDV) [31], Mobility Prediction Ad Hoc On-demand Multipath Distance Vector (MP-AOMDV) [59], and Split Multipath Routing (SMR) [47].

MSR is a multipath extension of the DSR routing protocol. In MSR, in order to establish multiple alternative paths, a destination node will feed a RREP back to the source for each RREQ that has reached the destination. In contrast, AOMDV extends the routing mechanism of AODV by adopting the notion of an *advertised hop count* to maintain multiple paths. However, the paths in AOMDV or MSR are pre-computed during route discovery, then prone to being stale. MPAOMDV enhances the routing scheme of AOMDV on this issue. It uses periodical packets to measure the channel state of each path, and chooses the one with the best quality for data transmission. Finally, instead of using link-state or distance vector algorithms, SMR establishes multiple maximally disjoint paths. A packet allocation scheme is then employed to distribute packets into the multiple paths. This scheme utilizes network resources efficiently, and it prevents routes from being congested in heavily loaded traffic situations.

Section Summary *Channel-aware routing schemes, including channel-adaptive routing and diversity-based routing, intent to address topology dynamics as well as channel fading. Channel-adaptive routing protocols give preference to relays with the strongest propagating parameters based upon the statistical channel characteristics. To keep the CSI up-to-date, channel-adaptive routing schemes require periodically monitoring radio links. Consequently, there is a trade-off between channel probing overhead and the gains achieved by channel adaptation. Diversity is another powerful technique to combat fading. MANETs possess abundant sources of diversity, such as multi-user (or spatial) diversity, multiple path diversity, and frequency diversity. However, this approach potentially increases traffic load in networks and requires a large amount of coordination in some cases.*

2.6 Mobile Radio Propagation

The section marks the beginning of the second part of this chapter. This part mainly describes the radio channel models which are commonly used to address mobile communications.

Radio propagation is mainly characterized by two nearly independent phenomena: small-scale fading and large-scale path loss [6, 27]. For each wireless connection, the obstacles in the environment can result in multiple propagating paths, and the received signals consist of several multipath components that with random amplitudes, angles of arrival, and Doppler shifts. Thus, even a relatively small movement of a receiving node on the order of carrier wavelength can cause instantaneous signal strength varying widely. This kind of channel fluctuations is characterized by small-scale multipath fading models. Whereas to predict how the mean signal strength attenuates with transmission distance, large-scale path loss models are utilized. In Figure 2.2 we give an example of the movements of, and the relative distance between, two nodes A and B in a mobile ad hoc network, and in Figure 2.3 the fluctuations of the received signal power for a radio connection is plotted, where both large-scale fading and small-scale fading are included.

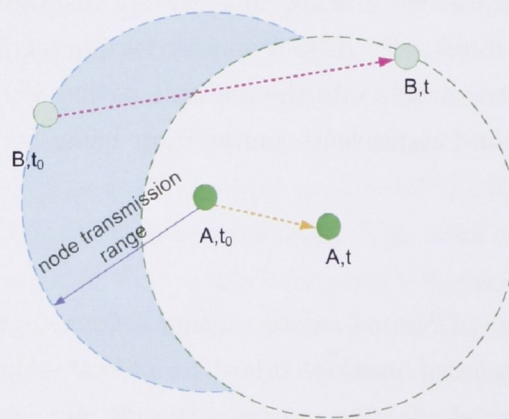


Figure 2.2: Example of movement of two nodes, A and B , and the relative distances between them at time t_0 and t .

Large-Scale Path Loss

Two of the most widely used large-scale path loss models are free space propagation and two-ray ground model. Typically the free space propagation model is used to characterize signal strength on line-of-sight paths, where signal power decays with

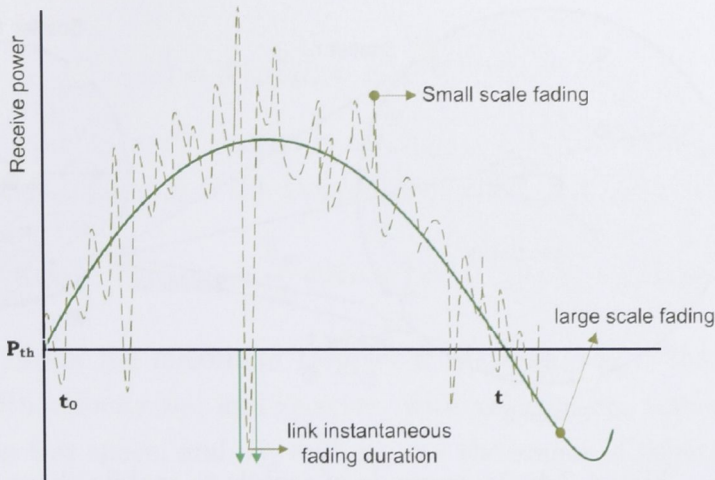


Figure 2.3: The fluctuations of the received signal power for a radio connection, where both large-scale path loss and small-scale fading are included.

the square of propagation distance. Specifically, the received strength is given by the Friis free space equation [27]. In contrast, in the two-ray ground model a mobile radio channel consists of a direct line-of-sight path and a ground reflected path. It has been proved reasonably accurate to characterize the mean signal strength over large distances of several kilometers for mobile systems with tall towers [27].

Small-Scale Fading

Small-scale fading describes the fast variations of instantaneous signal amplitude, phase, or multipath delay over a short distance or a short time interval [27]. The particular fading experienced by a signal is determined by the feature of both the transmitting signal and the propagated channel. Generally, time dispersion, which results from multipath delay spread, causes a radio signal undergoing flat fading or frequency selective fading.

Section Summary Assume a wireless channel model includes the effects of small-scale flat fading and large-scale path loss, for a transmission over a distance, d , the received signal power, P_r , is then exponentially distributed with mean $G_0 d^{-\alpha}$, given by

$$P_r = G_0 d^{-\alpha} \quad (2.6.1)$$

where P_r is the received power, G_0 is proportional to the transmit power, α is the propagation loss coefficient, typically between 2 and 4, and d is the signal propagating

2.7 Mobile-to-Mobile Channel

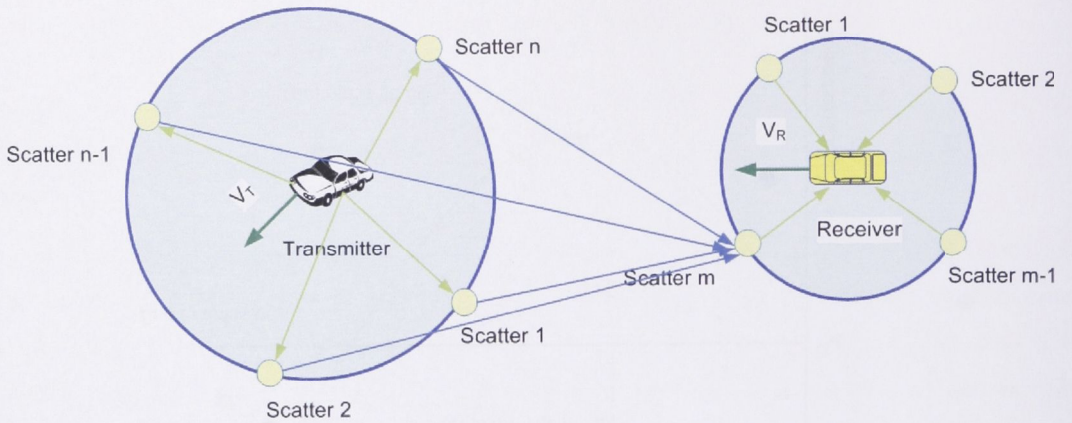


Figure 2.4: An example of mobile-to-mobile channel.

distance.

2.7 Mobile-to-Mobile Channel

In conventional cellular radio systems, base stations are mostly stationary and only with the terminals in motion. Whereas, in MANETs, potentially all of the nodes are moving. Though the signal envelope is still Rayleigh faded under non line-of-sight connections, the mobility of both the transmitter and the receiver results in different statistical properties of mobile-to-mobile wireless channels, as what have been proposed by Akki and Haber for mobile communication systems [74, 75]. The mobile-to-mobile channel model uses the speeds of both nodes engaged in a communication link, which makes it inherently suitable for MANETs. An example of a mobile-to-mobile environment is illustrated in Figure 2.4.

2.7.1 Channel Model

Let a modulated signal to be transmitted is

$$s_T(t) = \Re\{u(t) \exp(j2\pi f_0 t)\} \quad (2.7.1)$$

where $u(t)$ is the unit-power complex envelope and f_0 is the carrier frequency. Let there be L clusters of scatterers in the transmission environment, giving rise to L resolvable multipath components. The individual contribution of the ℓ^{th} multipath is

given by

$$s_{R_\ell}(t) = \Re\{\alpha_\ell u(t - \tau_\ell) e^{j(2\pi f_\ell t + \theta_\ell)} e^{j2\pi f_0 t}\} \quad (2.7.2)$$

where α_ℓ is the gain of the ℓ^{th} cluster, τ_ℓ is the path delay, θ_ℓ is the phase, uniformly distributed on $(-\pi, \pi]$ and f_ℓ is the Doppler frequency shift, given by

$$f_\ell = f_0 \left(\frac{v_T}{c} \cos \alpha_{T_\ell} + \frac{v_R}{c} \cos \alpha_{R_\ell} \right) = f_T \cos \alpha_{T_\ell} + f_R \cos \alpha_{R_\ell} \quad (2.7.3)$$

where f_T and f_R are the maximum Doppler frequencies due to the motions of the transmitter, with velocity v_T , and receiver, with velocity v_R , respectively, c is the speed of light in free space, and α_{T_ℓ} and α_{R_ℓ} are the angles of departure and arrival of the ℓ^{th} multipath component, measured with respect to the transmitter and the receiver velocity vectors. It can be found that the Doppler frequency experienced by each cluster is the sum of the Doppler induced by the movement of the transmitter and the receiver individually.

Then, the total received signal is given by the sum of the L contributions, $s_{R_\ell}(t)$, as follows

$$s_R(t) = \sum_{\ell=0}^{L-1} s_{R_\ell}(t). \quad (2.7.4)$$

Comparing the received signal with the transmitted one, from (2.7.1) and (2.7.4), we can get the complex envelope of the received signal, assuming an isotropic antenna at the receiver, which is given by

$$g(t) = \sum_{\ell=0}^{L-1} \alpha_\ell u(t - \tau_\ell) e^{j(2\pi f_\ell t + \theta_\ell)}. \quad (2.7.5)$$

The time-varying transfer function of the mobile radio channel is given by $H(f, t) = g(t)/u(t)$, where $u(t) = \exp(j2\pi ft)$ and f is the baseband frequency, such that

$$H(f, t) = \sum_{\ell=0}^{L-1} \alpha_\ell e^{-j(2\pi f \tau_\ell - \theta_\ell)} e^{j2\pi f_\ell t}. \quad (2.7.6)$$

2.7 Mobile-to-Mobile Channel

Time Correlation of the Mobile-to-Mobile Channel

With ominously directional antennas and under isotropic scattering environment, the time correlation function of the mobile-to-mobile channel is given by [76]

$$R_t(m) = \sigma_1^2 J_0(2\pi f_T m) J_0(2\pi f_R m) \quad (2.7.7)$$

where m is the discrete time delay, $\sigma_1 = R_{\text{rms}}/\sqrt{2}$, R_{rms} is the local root mean square (rms) amplitude of the fading envelope, J_0 is the 0th order Bessel function of the first kind, f_T and f_R are the maximum Doppler frequencies of the transmitter and receiver, respectively.

2.7.2 Statistical Characteristics of Mobile-to-Mobile Channel

Most properties of signal transmission over a mobile radio channel can be predicted from channel statistical characteristics which describe how often an acceptable signal level to be maintained during channel fading. With the capability to relate the rate of signal fluctuation to node mobility, channel statistical characteristics are useful for channel-adaptive and diversity design in mobile radio networks. Now we provide a brief review of the second order statistics of the mobile-to-mobile channel. The two most important parameters, Level Crossing Rate (LCR) and Average Fading duration (AFD), are described in the following sections.

Level Crossing Rate

The level crossing rate (LCR), N_ρ , describes how often the envelope crosses a certain threshold level, R_{th} , in the positive direction. Akki has presented the expressions of LCR and AFD for a mobile-to-mobile channel in [76]. The LCR is given by

$$N_\rho = f_T \sqrt{2\pi(1 + \mu^2)} \rho e^{-\rho^2} \quad (2.7.8)$$

where f_T is the maximum Doppler frequency of the transmitter, $\mu = v_R/v_T$ is the ratio of the receiver velocity, v_R , to that of the transmitter, v_T , and $\rho = R_{\text{th}}/R_{\text{rms}}$ is the ratio between the signal threshold, R_{th} , and the local root mean square (rms) amplitude of the fading envelope. The LCR, normalized with respect to the maximum transmitter Doppler frequency, is plotted in Figure 2.5 as a function of μ and ρ .

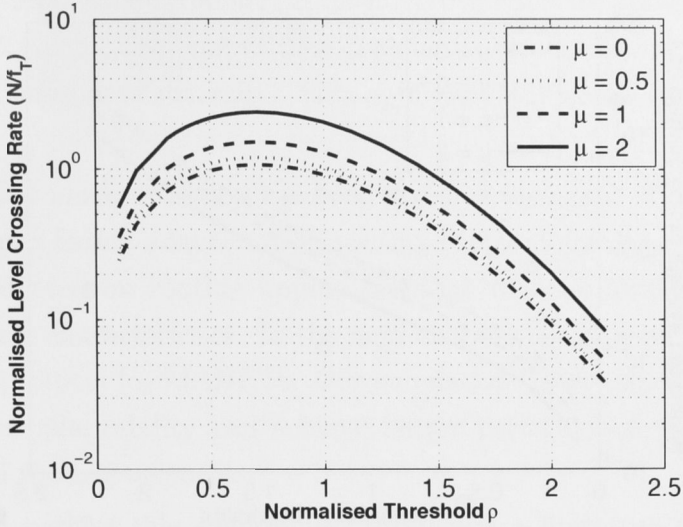


Figure 2.5: The relationship between normalized level crossing rate and the ratio of the signal threshold and the root mean square received signal amplitude, $\rho = R_{\text{th}}/R_{\text{rms}}$, for various $\mu = v_R/v_T$, for the mobile-to-mobile channel from (2.7.8).

Average Fading Duration

Another parameter of interest is the average fading duration (AFD). The AFD, $\bar{\chi}$, is the average amount of time that the signal envelope is lower than a given threshold, R_{th} . The AFD of mobile-to-mobile channel is given by [76]

$$\bar{\chi} = \frac{e^{\rho^2} - 1}{\rho f_T \sqrt{2\pi(1 + \mu^2)}}. \quad (2.7.9)$$

The AFD is plotted as a function of μ and ρ in Figure 2.6, normalized with respect to f_T . It can be seen that increasing μ decreases the AFD due to the corresponding increased rate of signal fluctuations.

Remark 2.7.1. In a mobile-to-mobile channel, from (2.7.8) and (2.7.9), it can be seen that the LCR and AFD are directly related to the mobility of both the transmitter (v_T) and the receiver (v_R), as the increasing node mobility will increase the rate of signal fluctuations.

2.8 Conclusion

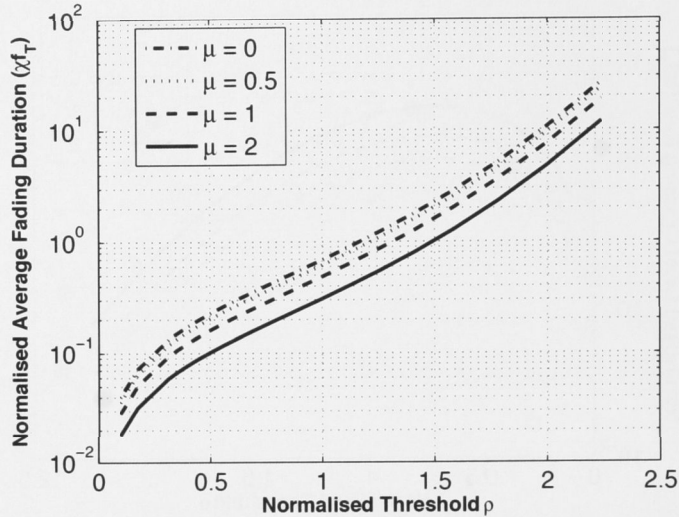


Figure 2.6: The relationship between normalized average fading duration and the ratio of the signal threshold and the root mean square received signal amplitude, $\rho = R_{\text{th}}/R_{\text{rms}}$, for various $\mu = v_R/v_T$, for the mobile-to-mobile channel from (2.7.9).

2.8 Conclusion

Background material for the thesis was briefly introduced in this chapter. We presented the routing protocols and techniques proposed for MANETs. We also investigated typical wireless channel models and their characteristics.

First, this chapter has presented an overview of existing routing protocols in MANETs. These protocols are briefly categorised as topology-based routing, congestion-aware routing, and channel-aware routing protocols. A large collection of routing protocols is proposed following the traditional topology-based routing approach. In this approach, dynamics of network topology is of major concern. Therefore, topology-based routing protocols lack adaptability to congestion or fading, and generally are unsuitable for networks with large-scale traffic or high mobility. In contrast, when large-scale traffic is present in networks, congestion-aware routing, which takes advantage of congestion avoidance, can greatly reduce packet losses. However, it requires an amount of overheads to introduce congestion awareness. Finally, channel-aware routing makes use of adaptation and diversity techniques to address topology dynamics as well as channel fading. It includes channel-adaptive routing and diversity-based routing. Channel-adaptive routing introduces an awareness of channel characteristics into routing protocols. However, it requires periodically monitoring radio links, thus

there is a trade-off between channel probing overhead and the gains achieved by adaptation. Diversity is another powerful technique to combat fading in MANETs that with abundant sources of diversity. This approach may result in a high traffic load in networks.

Generally, not much attention has been given to the issues of congestion management and channel fading adaptation in routing protocol designs. Therefore, research should be conducted on routing approaches that with an awareness of congestion status or channel characteristics. In the next chapter, we propose a new congestion-aware routing protocol for MANETs. Our simulation results show that the protocols with congestion adaptability can achieve better performance than the traditional topology-based routing protocols.

The second part of this chapter has conducted a literature survey on relevant mobile radio channels and their statistical characteristics. This provides groundwork for our research on the channel-aware routing protocols in the third part of the thesis.

Chapter 3

Congestion-Aware Routing Protocol for MANETs

This chapter is the second part of this thesis. It is to design a congestion-aware routing protocol for MANETs. We first propose a congestion-aware routing metric which employs packet transmission rate, channel access overhead, and buffer queuing delay to measure congestion level in multiple approaches. The proposed routing metric improves channel utilization with preference given to less congested high throughput links. By incorporating the proposed routing metric with particular routing schemes, we introduce the Congestion-Aware Routing protocol for Mobile ad hoc networks (CARM). CARM applies a link data-rate categorization approach to prevent routes with mismatched link data-rates. In this chapter, CARM is only discussed and simulated in relation IEEE 802.11b networks; however, it can be applied to any multi-rate ad hoc network.

The layout of this chapter is as follows. In Section 3.1, a literature survey of research work on congestion-aware routing in ad hoc networks is presented. Section 3.2 provides a brief review of the IEEE 802.11 medium access control (MAC) protocol. We investigate issues that potentially result in congestion in multi-rate ad hoc networks in Section 3.3. In Section 3.4 and Section 3.5 we describe the proposed congestion-aware routing metric and routing protocol, respectively. Simulation results are presented in Section 3.6. Finally, we draw our conclusions in Section 3.7.

3.1 Introduction

Congestion occurs in mobile ad hoc networks where/when network resources required by users are above what the networks can provide. Recently, there has been ever growing demand for support of applications such as new multimedia services and video on demand in MANETs. Multimedia applications generate large amounts of real-time traffic which is bandwidth intensive and tends to be in bursts, therefore, is liable to congestion [46]. Moreover, in MANETs, due to shared wireless channel and node mobility, packet transmissions frequently suffer from interference and time-varying channel fading, causing high transmission errors. Such transmission errors can significantly burden network load in severe environments. Congestion leads to packet losses and bandwidth degradation, and wastes time and energy on congestion recovery. A congestion-aware routing protocol can preempt congestion by bypassing the affected links.

Wireless standards, such as IEEE 802.11a and IEEE 802.11b, support adaptive data transmission in MANETs to accommodate time-varying channels. However, the authors in [77] point out that, when operating under heavy traffic conditions (where every node always has packets to transmit), the IEEE 802.11 distributed coordination function (DCF) provides long term per packet fairness in single-hop networks. This incurs a network performance anomaly: in a one-hop network, the active low data-rate links decrease the throughput of neighbouring high data-rate links. One of possible solutions to these throughput decrease in multi-rate networks is to use multiple channels [78]. Another solution, which is feasible in multi-hop networks, is to employ a routing protocol which gives priority to higher data-rate links to establish routing paths. Because low data-rate links have a lower probability of being utilised, the overall network throughput is then improved.

In single data-rate networks, the minimum hop-count routing metric is commonly used in conventional routing protocols, such as AODV [37] and DSR [29]. The main draw-back with such an approach is that using fewer links between a pair of nodes results in long links which, in a mobile network, are more likely to be almost at breaking point with respect to transmission range. If multiple data-rates are allowed in the network, these longer links will also, inherently, have the lowest data-rates, so that having a range of data-rates is not necessarily taken full advantage of. Choosing higher data-rate links, as suggested by the Medium Time Metric (MTM) in [52], will generally mean that links are short and more of them are included in any given

3.2 Review of IEEE 802.11 MAC

route. This is an advantage in that we have higher data rates while the packets are in transmission along these links. However, more links in a route also means more channel access contention, potentially increasing congestion in the network. In [53], the use of channel access delay was proposed as an enhancement to the MTM, providing awareness of congestion to help avoid routing through bottleneck regions. Meaningful measurement of link congestion levels should combine channel occupation, packet drop rate, and buffer load [8]. Examples of congestion measurement can be found in [8, 79].

A further issue in multi-rate ad hoc networks is that different data-rates will almost certainly lead to some routes having different links with quite different data-rates. If lower data-rate links follow higher data-rate links, packets will build up at the nodes heading the lower data-rate links, leading to long queueing delays. Finally, lack of reliability on radio links will exacerbate congestion build-up. If links break, congestion is increased due to packet retransmission. In short, it is necessary to take all of above issues into consideration to design an efficient congestion-aware routing protocol.

3.2 Review of IEEE 802.11 MAC

In this chapter we consider the IEEE 802.11b [80] mobile ad hoc networks. First we give a brief review of the IEEE 801.11 medium access control (MAC) protocol and its distributed coordination function (DCF).

3.2.1 IEEE 802.11 DCF

The DCF access method in IEEE 802.11 uses a carrier sense multiple access with collision avoidance (CSMA/CA) scheme to contend for wireless medium access. The virtual carrier sense mechanism can be achieved through the request-to-send (RTS)/clear-to-send (CTS) handshake [81]. When it has some packets to transmit, a node first needs to monitor the channel to ensure that it is idle for at least a time interval equivalent to the Distributed Inter Frame Space (DIFS). It then sends a RTS packet to the receiver. After successfully receiving the RTS, the receiver will feedback a CTS packet to the transmitter. All the neighbouring nodes overhearing the RTS-CTS handshake will update their Network Allocation Vector (NAV) to record the amount of time during which the channel is to be occupied for this data transmission.

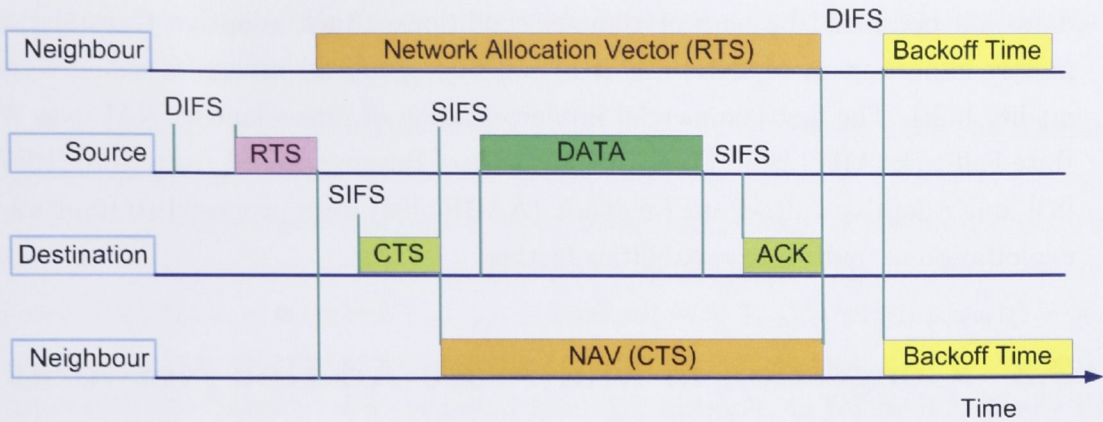


Figure 3.1: The standard transmission sequence in IEEE 802.11 DCF

When the transmitter receives the CTS, it will begin data transmission after a time period equivalent to the Short Inter Frame Space (SIFS). Once the data has been correctly transmitted, the receiver then will send an acknowledgement (ACK) packet after another fixed SIFS period of time. If an ACK is not received by the transmitter, it will attempt to retransmit the data packet.

If there are couples of nodes contending for the channel to transmit, a neighbouring node might sense a busy channel. The node then enters a collision avoidance phase by waiting for a random backoff interval before attempting a new channel contention. The time duration of backoff is random, chosen uniformly from the range $[0, CW] \times aSlotTime$. At the first transmission attempt, the congestion window CW is set to CW_{min} (minimum contention window). If a node does not correctly receive an ACK within a particular time, the node will assume a collision has occurred. Each time a node happens to collide, it executes a binary exponential backoff algorithm in which the value of CW is doubled, up to the maximum value $CW_{max} = 2N_R CW_{min}$, where N_R is the number of allowed retransmissions.

The standard IEEE 802.11 DCF transmission sequence is shown in Figure 3.1.

3.2.2 Multi-rate Transmission in IEEE 802.11 MAC

The widely used IEEE 802.11 standard, such as IEEE 802.11b and IEEE 802.11a, is typically designed to support multi-rate transmission. IEEE 802.11b supports four data-rates of 1, 2, 5.5 or 11 Mbps, and there are eight data-rates of 6, 9, 12, 18, 24, 36, 48 or 54 Mbps available in IEEE 802.11a and IEEE 802.11g. This multi-rate capability enables adaptive data-rate selection to transmit packets at the highest

data-rate permitted by current channel conditions. Such adaptive transmission is mostly important in MANETs as it allows taking full advantage of available good quality links. The first commercial implementation of rate adaptive MAC was Auto Rate Fallback (ARF) [82]. Then, the protocols of Receiver Based Auto Rate (RBAR) [83] and Adaptive Auto-Rate Feedback (AARF) [84] were proposed to improve the exploitation of multi-rate capabilities further.

3.3 Congestion in Multi-rate Ad Hoc Networks

As we discussed in Section 3.1, channel access contention, channel reliability, and mismatched link data-rate routes, are important issues which cause congestion in IEEE 802.11 ad hoc networks. Now we address these issues in detail.

3.3.1 MAC Control Overhead in Congestion

Channel Access Contention

First we consider the MAC control overhead generated during a data transmission. In IEEE 802.11, according to the description in Section 3.2, the minimum channel occupation due to MAC control overhead is

$$T_{\text{MACmin}} = T_{\text{RTS}} + T_{\text{CTS}} + 3T_{\text{SIFS}} \quad (3.3.1)$$

where T_{RTS} and T_{CTS} are the time consumed on RTS and CTS packet transmission, respectively, and T_{SIFS} is the SIFS period. Here we have not included the time consumed on ACK, as we are only considering time to get the data to the receiving node. If we include the time taken due to contention for the channel, the MAC control overhead is

$$T_{\text{MACall}} = T_{\text{MACmin}} + T_{\text{cgs}} \quad (3.3.2)$$

where T_{cgs} is the time taken due to channel access contention (including NAV waiting and back-off intervals).

Let the channel delay for a link, ℓ , be defined as the interval between the start of the RTS transmission at the transmitter and the time the data packet is correctly received at the receiver. Then the link channel delay for ℓ is given by

$$\mathfrak{T}_{\ell} = T_{\text{MACall}} + T_{\text{data}} \quad (3.3.3)$$

where $T_{\text{data}} = L_{\text{data}}/B_{\ell}$ is the data transmission time, L_{data} is the length of the data in bits, and B_{ℓ} is the data-rate of link ℓ in bits per second.

The amount of MAC control overhead, T_{MACcall} , is dependent upon the medium access contention and the number of packet collisions. That is, T_{MACcall} is strongly related to the congestion around a given node. With little or no contention, the channel delay is effectively a constant, given by $T_{\text{MACmin}} + T_{\text{data}}$. When channel access contention is included, T_{MACmin} is replaced with T_{MACcall} which is variable and can become relatively large if congestion is incurred and not controlled, dramatically decreasing the capacity of a congested link. For example, in Figure 3.2, if only the bit-rate is considered, the link in scenario II (11 Mbps) would be said to have a higher capacity than the link in scenario I (5.5 Mbps). However, when channel access contention is included, the links in the two scenarios turn out to have identical overall channel delays, giving them the same *real* channel capacities. Therefore, in the design of a congestion-aware metric for multi-rate ad hoc networks, the data-rate and the channel access contention should be jointly considered to more accurately indicate channel capacity.

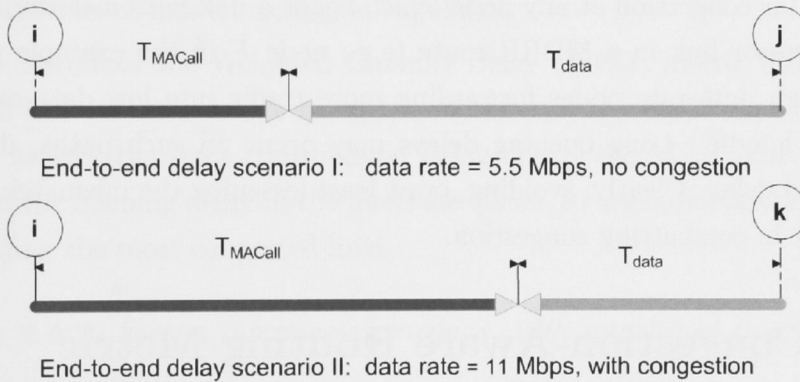


Figure 3.2: Two scenarios with the same overall delay but different MAC and transmission delays due to different data-rates and congestion levels.

Channel Reliability

Packet transmission in MANETs is also affected by channel reliability, with packet losses being incurred due to factors such as interference and fading in the channel. In IEEE 802.11 DCF, packets are dropped after several failed retransmissions. Not only will congestion deteriorate performance with respect to packet losses, but increased

3.4 Congestion-Aware Routing Metric

packet losses will lead to more congestion due to higher packet retransmissions. Unreliable links consume more time in MAC control overheads in order to successfully transmit a packet. Thus, the MAC control overhead is also an important indication of channel reliability.

3.3.2 Mismatched Link Data-Rate Routes

In multi-rate ad hoc networks, throughput via a given route is limited by the minimum data-rate over all of its constituent links.

Definition 3.3.1. *Consider a route with significantly different data-rates over each of its links (e.g., $A \rightarrow B \rightarrow D \rightarrow F \rightarrow H$ in Figure 3.3). Let us call such a route a Mismatched Data-Rate Route (MDRR).*

When large-scale traffic, such as with multimedia streams, is transmitted via a MDRR route, the benefits of having multi-rate links can be compromised. There is potential for congestion at any node which heads a link with a slower data-rate than its predecessor link in a MDRR route (e.g., node F in the example path). This is due to high data-rate nodes forwarding more traffic into low data-rate nodes than they can handle. Long queuing delays may occur on such paths, dominating the end-to-end delay. Clearly, avoiding, or at least lessening the mismatch in, MDRRs is important in combatting congestion.

3.4 Congestion-Aware Routing Metric

A congestion-aware routing metric for MANETs should incorporate the congestion level, channel reliability, and transmission capability of a link. In the previous section we saw that congestion is related to channel access contention and channel reliability. The MAC control overhead from (3.3.2) is a good measure of congestion, being a combination of these two factors. In addition to MAC control overhead, we contend that queuing delay in the interface queue is a useful measure of congestion, as discussed in Section 3.1. When a data-rate adaptation feature is included, a radio is able to select a suitable physical layer data-rate using the observed CSI, such as the signal strength or Signal-to-Noise Ratio (SNR) measurements of received packets. As the data-rate of each link changes with time and node movement, such adaptive data-rate

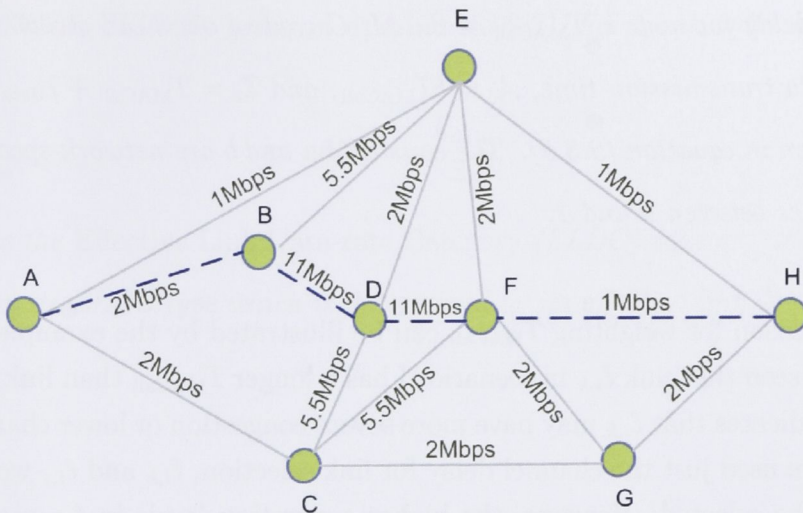


Figure 3.3: An example of an 802.11b multi-rate ad hoc network.

selection causes the data transmission time at a given link to vary more dynamically than when a single fixed data-rate is used. Consequently, it is of benefit to introduce data transmission time into the design of a routing metric, to take into account the dynamic variations of link transmission capability.

We now introduce the Weighted Channel Delay (WCD) metric which assigns a cost to each link in the network using the aforementioned MAC layer information. The WCD utilizes the data transmission delay, T_{data} , the MAC control overhead, T_{MACall} , and the queuing delay in the interface queue, to select maximum throughput paths, avoiding the most congested links.

Definition 3.4.1. For an intermediate node, i , with established transmission with several of its neighbours, the Weighted Channel Delay (WCD) for the link, ℓ , from node i to a particular neighbouring node is given by

$$\begin{aligned} \text{WCD}_\ell &= a \sum_{k \in \vartheta_i} \mathfrak{T}_{i,k} Q_{i,k} + (1 + b) T_{\text{MACall}} + T_{\text{data}} \\ &= Q_i + \mathcal{A}_\ell + \mathfrak{T}_\ell \end{aligned} \quad (3.4.1)$$

where ϑ_i is the set of all nodes neighbouring node i , $Q_{i,k}$ is the number of packets buffered in the node i queue bound for node k , $Q_i = a \sum_{k \in \vartheta_i} \mathfrak{T}_{i,k} Q_{i,k}$ is the total

3.5 Congestion-Aware Routing Protocol

queuing delay for node i , T_{MACall} is the MAC control overhead given in (3.3.2), T_{data} is the data transmission time, $\mathcal{A}_\ell = bT_{\text{MACall}}$, and $\mathfrak{T}_\ell = T_{\text{MACall}} + T_{\text{data}}$ is the channel delay given in equation (3.3.3). The constants a and b are network-specific parameters with values between 0 and 1.

The reason for weighting T_{MACall} can be illustrated by the example in Figure 3.2. It can be seen that link $\ell_{i,k}$ in scenario II has a longer T_{MACall} than link $\ell_{i,j}$ in scenario I. This indicates that $\ell_{i,k}$ may have more severe congestion or lower channel reliability. Now, if we used just the channel delay for link selection, $\ell_{i,k}$ and $\ell_{i,j}$ would be equally likely to be selected. However, the higher congestion levels in $\ell_{i,k}$ mean that it has greater potential for transmission failure, in terms of higher levels of collision or corruption. So, if we weight T_{MACall} in the metric we include some measure of the possible packet loss into link selection, reducing the chances of selecting a congested node. The WCD seeks to capture as many effects of congestion as possible, so that the network is aware of local congestion. A smaller WCD for a link is more favourable, meaning that the link is more likely to be selected in any given route.

3.5 Congestion-Aware Routing Protocol

The Congestion-Aware Routing protocol for Mobile ad hoc networks (CARM) is an on-demand routing protocol that aims to create congestion-free routes by making use of information gathered from the MAC layer. The CARM route discovery packet is similar to that in DSR [29] where every packet carries the entire route node sequence. CARM employs the WCD metric proposed in equation (3.4.1) to account for the congestion level. In addition, CARM adopts a route effective data-rate category scheme to combat the MDRR problem discussed in Section 3.3.2. The combination of these two mechanisms enables CARM to ameliorate the effects of congestion in multi-rate ad hoc networks. CARM uses the same route maintenance approach as that in DSR.

3.5.1 Addressing Mismatched Data-Rate Routes

Because the effective bandwidth of a link can be dramatically degraded by congestion, regardless of its specified physical bit rate, we introduce the following definitions.

Definition 3.5.1. With \mathfrak{T}_ℓ given in equation (3.3.3), for a link with effective link data-rate

$$\mathcal{LD}_\ell^{\text{eff}} = \frac{L_{\text{data}}}{\mathfrak{T}_\ell} \quad (3.5.1)$$

we introduce the Effective Link Data-rate Category (ELDC) scheme, where each link is marked by its ELDC type which is determined by its effective link data-rate range.

For example, in an IEEE 802.11b network with data-rates ranging from 1 Mbps to 11 Mbps, we might choose the following two categories:

$$\begin{aligned} \text{ELBC I} : \mathcal{LD}_\ell^{\text{eff}} &< 6\text{Mbps}; \\ \text{ELBC II} : \mathcal{LD}_\ell^{\text{eff}} &\geq 6\text{Mbps}. \end{aligned} \quad (3.5.2)$$

For a given route, the route ELDC is taken as that for the link directly connected to the source and is included in the route request (RREQ) packet. During route discovery, an intermediate node only forwards a RREQ if the ELDC type of the link preceding the current node is higher than or equal to that of the route. That is, for two ELDCs, if the route ELDC is I then all paths are possible. However, if the route ELDC is II, only links with ELDC II may be chosen, eliminating low data-rate links and lessening the chances of congestion. This lessens the occurrence of very slow initial links being teamed with very fast links in the same route.

While using the ELDC scheme helps to alleviate the MDRR problem, in extreme cases the limiting of choice of links in a route could lead to route discovery failure. To counter this situation, we include a field, ELDCF, in the RREQ packet to flag whether or not the ELDC scheme is in operation. It is utilised in the following way. On an initial route discovery attempt, the ELDCF field is set to 1, indicating that the ELDC scheme is in use, such that nodes should only forward the RREQ under the ELDC rules given above. If this route discovery process is unsuccessful, another is initiated, this time with the ELDCF field set to 0. In this way, all RREQs are forwarded as in DSR.

3.5.2 Route Discovery

RREQ Initiation

A source node wishing to transmit data to a given destination generates a RREQ and broadcasts it to the network. The RREQ packet from an intermediate node i contains the following fields: $\langle \text{source ID}, \text{source sequence number}, \text{destination ID}, \text{transmission start-time at } i, Q_i, B_\ell, \text{ELDC}, \text{ELDCF}, \text{record of route hop sequence} \rangle$, where Q_i is the total queuing delay for node i , and B_ℓ is the data-rate. The ELDC field is assigned appropriately at the first intermediate node. For the first route search cycle the ELDCF field is set to 1, indicating that the ELDC scheme is in use. If this route discovery is unsuccessful, ELDCF is set to 0 and a second cycle is initiated.

Processing a RREQ

Each intermediate node maintains a local forwarding list of the triples $\langle \text{source ID}, \text{source sequence number}, \text{ELDC} \rangle$ to record and keep track of the RREQs that it has received. Upon receiving a RREQ, an intermediate node compares the appropriate fields in the RREQ and its local list to avoid propagating duplicate RREQs. The ELDCF field is also checked. If $\text{ELDCF} = 1$, the ELDC of the preceding link is determined and compared with that in the RREQ. If the link ELDC is lower than the route ELDC, the RREQ is discarded.

Note that in DSR intermediate nodes drop any RREQ with the same source ID and lower or identical source sequence number to those in any RREQ they have already seen. So, in DSR each node only forwards a RREQ, during a given route discovery process, once. In CARM, as the ELDC is also taken into account, any node may forward a RREQ during a route discovery up to the number of ELDC types. This means that more routing information is required to establish feasible routes because more copies of the same RREQ are propagated around the network. This causes a slight increase in overhead during the route discovery phase of CARM over DSR.

Prioritizing RREQ with WCD

In the interface queue routing packets have higher priority over data packets, such that they are forwarded immediately, without queuing. Because of this, the congestion level information inherent in queuing delays is lost in DSR. This is addressed in CARM via the WCD described in Section 3.4.

Having determined that it will keep a RREQ from node i , node j calculates $(Q_i + \mathcal{A}_\ell)$ from the WCD_ℓ in (3.4.1) according to the information recorded in the RREQ. Then, node j delays forwarding of the RREQ by this amount, so that the total time that a RREQ is delayed, from the time it is sent by node i , to the time that node j is ready to forward it is equal to WCD_ℓ . This ensures that each node forwards RREQs on a priority basis related to congestion level, as encompassed by the WCD. So, RREQs for routes with higher throughput and lower congestion will reach the destination first and, because the intermediate nodes will drop later arriving duplicate RREQs, congested links are much less likely to be included in any established routes.

Route Reply

As part of CARM, intermediate nodes are prohibited from generating route reply (RREP) packets. That is, only the destination node may generate and send RREPs, to avoid stale information at intermediate nodes. The destination responds to RREQs by sending a RREP packet back to the source along the route via which it came. The first RREP to reach the source establishes the route. Routes indicated in any subsequent RREPs are cached at the source in case of failure of the established route.

3.6 Simulations

3.6.1 Simulation Setup

In the simulations, we compare the performance of DSR with two slightly different versions of CARM. In the first, only the WCD metric is taken into account in DSR, which we call CARMdelay. In the second, both the WCD and the ELDC scheme are taken into account, which we call CARM. The simulations were carried out using the network simulator, ns-2.29 [85] with adaptive auto-rate feedback [84] multi-rate extension. DSR works by building routes based on the shortest delay, lessening control overhead by allowing intermediate nodes to issue RREPs using cached routing information.

The simulations assumed an IEEE 802.11b network, configured with 80 nodes uniformly distributed over a 1500 m \times 1500 m area, moving according to a random waypoint model [86] with a maximum speed of 5 m/s and a pause time of 10 seconds. Ten nodes were randomly chosen to be constant bit rate (CBR) sources, generating 512 byte data packets to be sent to randomly chosen destinations. The network traffic

3.6 Simulations

Table 3.1: Simulation parameters

Data Rate	Receiving Threshold	Transmission Range
carrier sense	-101 dB	1071 m
1 Mbps	-91 dB	597 m
2 Mbps	-89 dB	532 m
5.5 Mbps	-87 dB	475 m
11 Mbps	-82 dB	356 m

was increased from 10 to 80 packets per second, with each simulation running for 300s. The MAC layer was based on IEEE 802.11 DCF with a control packet transmission rate of 1 Mbps. The interface queue at the MAC layer had a length of 50 packets while the routing buffer at the network layer had a length of 64 data packets. The transmission power was fixed at 13 dBm. The simulated receiving threshold powers for various data-rates and their respective transmission ranges (based on the two-ray ground propagation model) are shown in Table 3.1. Note that for calculating the WCD component in CARMdelay and CARM, from (3.4.1), we chose $a = 0.25$ and $b = 0.1$, based on a comparison of results for a range of values for a and b .

In developing the simulations, we considered the following properties to assess the performance of routing protocols:

1. **Packet delivery ratio (PDR)**: the ratio of the number of data packets successfully received at the destinations to the number of data packets generated by the sources;
2. **Average end-to-end delay**: the average time taken to transfer a data packet from a source to a destination;
3. **Normalized routing control overhead**: the ratio of the number of control packets to the number of delivered data packets.

3.6.2 Packet Delivery Ratio

Figure 3.4 illustrates the trend of PDR with increasing packet rate. It can be seen that CARM and CARMdelay outperform DSR, particularly for higher traffic loads. At higher traffic loads, in general, links face a higher probability of congestion, and the packet drop rate increases due to collisions or buffer overload. DSR uses cached routes to re-establish the connection when a route becomes unusable. The cached

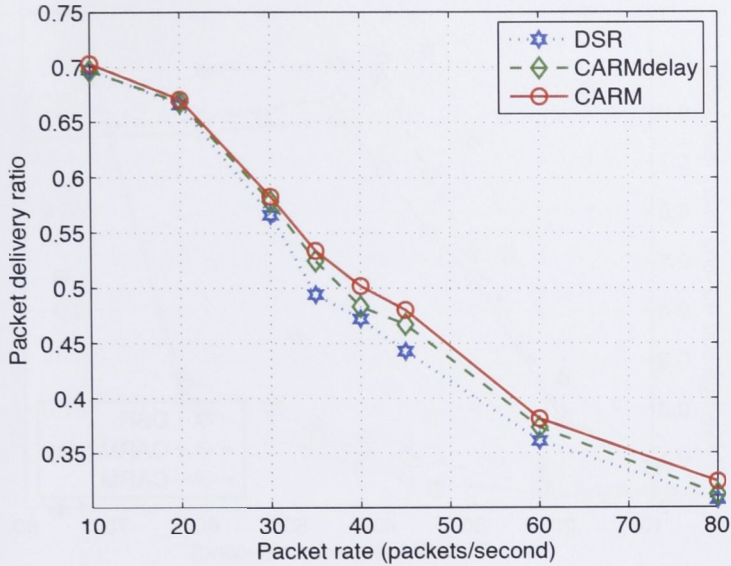


Figure 3.4: Comparison of packet delivery ratio (PDR) with increasing packet rates from 10 to 80 per second for CARM , CARMdelay and DSR.

routes may be stale and no longer optimal for the current topology, and high traffic levels make them more fragile. From the results, we can see that the use of the WCD can increase the number of packets delivered in DSR by up to 10%. The employment in CARM of the WCD, combined with the avoidance of mismatched link data-rate routes, aids in the selection of routes more robust to congestion. Through these mechanisms, CARM is able to deliver more packets than DSR.

3.6.3 Average End-to-End Delay

Figure 3.5 shows the average end-to-end delay for CARM, CARMdelay and DSR with an increase in the packet rate. It can be seen that both CARM and CARMdelay outperform DSR with respect to the effect of traffic level on end-to-end delay. In DSR, if a route becomes disconnected, the source then attempts to make use of cached routes in either the source node itself or intermediate nodes before initiating another route discovery. However, the DSR link error notification mechanism means that not all nodes necessarily find out about a breakage until they next use that link, so many cached routes may be stale. Unwittingly attempting to forward data through such routes uses up transmission time. The use of the WCD in effectively delaying RREQs which have come through congested links means that such links are unlikely

3.6 Simulations

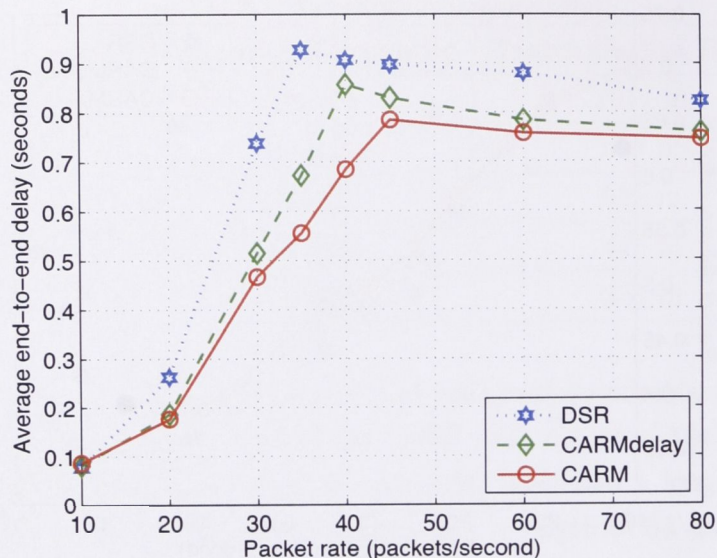


Figure 3.5: Comparison of end-to-end delay with increasing packet rates from 10 to 80 per second for CARM, CARMdelay and DSR.

to be included in established routes in CARMdelay and CARM. The additional use of the ELDC scheme in CARM further ameliorates congestion.

3.6.4 Normalized Routing Control Overhead

Finally, Figure 3.6 shows the trend of the normalized routing control overhead with increasing traffic, for CARM, CARMdelay and DSR. It can be seen that CARMdelay and CARM generally outperform DSR with respect to normalised control overhead, except under light traffic conditions where DSR outperforms CARM. When the traffic is light, route discovery packets dominate the routing control overhead. CARM requires more routing information because of its ELDC mechanism. However, CARM only allows RREQs to be broadcast if the ELDC is appropriate, thereby somewhat lessening the impact of RREQ propagation. At high traffic, the network is more prone to congestion, increasing the number of stale cached routes in DSR and the likelihood of the need for a new route discovery process. It has been noted [87] that in DSR the routing load is dominated by RREP packets. However, in CARM this is not the case, due to the suppression of RREPs at intermediate nodes. CARMdelay and CARM work to exclude congested links via the use of the WCD. In CARM, ELDCs also contribute to congestion control. So, while DSR yields lower overhead due to route

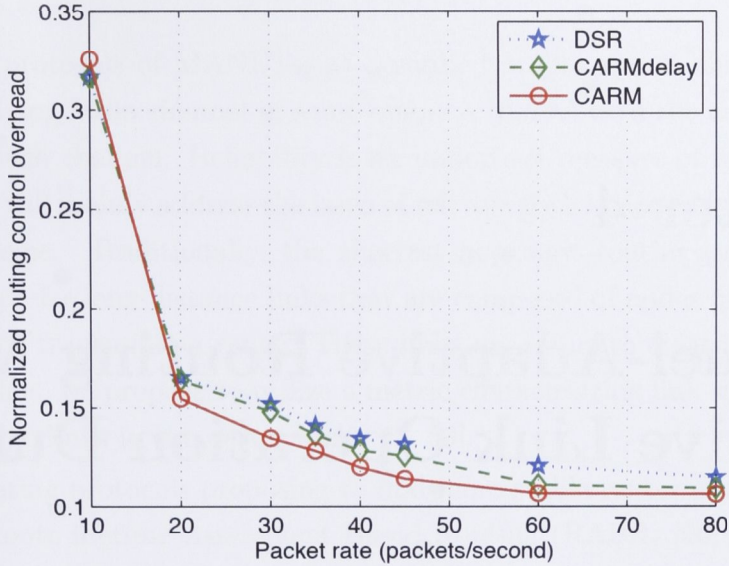


Figure 3.6: Comparison of normalized control overhead with increasing packet rates from 10 to 80 per second for CARM, CARMdelay and DSR.

discovery, it requires route discovery more often due to congestion. In CARMdelay and CARM, the reduced number of congested links in established routes contributes to better performance in high traffic loads.

3.7 Conclusion

Congestion in mobile ad hoc networks leads to transmission delays and packet losses, and causes wastage of time and energy on recovery. Routing protocols which are adaptive to the congestion status of a mobile ad hoc network can greatly improve network performance. In this chapter, we have proposed a congestion-aware routing protocol for mobile ad hoc networks (CARM). CARM utilizes two mechanisms to improve the routing protocol adaptability to congestion. Firstly, the weighted channel delay (WCD) is used to select high throughput routes with low congestion. The second mechanism that CARM employs is the avoidance of mismatched link data-rate routes via the use of effective link data-rate categories (ELDCs). In short, the protocol tackles congestion via several approaches, taking into account causes, indicators and effects. The decisions made by CARM are performed locally. Our simulation results demonstrate that CARM outperforms DSR due to its adaptability to congestion.

Chapter 4

Channel-Adaptive Routing Metric: Effective Link Operation Duration

This chapter begins the third part of this thesis. Based on our observations of channel characteristics in the second part of Chapter 2, several channel-aware routing protocols will be developed in this part. In particular, two channel-adaptive routing mechanisms are proposed in Chapter 4 and Chapter 5, and in Chapter 6 we present the proposed diversity-based routing protocol.

In this chapter, we first present a novel channel-adaptive routing metric, Effective Link Operation Duration (ELOD). ELOD is defined as the duration in which the nodes are within each other's transmission range with no fading. To estimate the ELOD, first, the proposed scheme makes use of node mobility to predict link lifetime; then it combines the link lifetime with channel fading statistics to obtain the ELOD. Therefore, applying ELOD as a routing metric addresses issues caused by node mobility as well as those caused by channel fading. The ELOD is then incorporated into AODV (AODV-ELOD) to promote channel-adaptive routing decisions. AODV-ELOD is shown to reduce routing overheads and cope well with the channel unreliability.

The layout of this chapter is as follows. Section 4.1 provides a brief review of reliable path selection in MANETs. In Section 4.2 we define the proposed channel-aware routing metric, ELOD. In Section 4.3 we describe the calculation of ELOD. The improved channel aware routing protocol, AODV-ELOD, is presented in Section 4.4. Simulation results are presented in Section 4.5 and in Section 4.6 we draw our conclusions.

4.1 Introduction

The routing protocols of MANETs, as described in Chapter 1, should be adaptive to the underlying radio channel in some manner, to deal with the adverse conditions common to such channel. Reliability is an important measure of radio link quality. This chapter will mainly address the issue of reliable path selection based on a channel adaptive scheme. Traditionally, the shortest hopcount routing protocols, such as AODV [37], prefer long-distance links that are composed of nodes placed at the edge of each other's transmission range. These links are prone to error and may not last very long. Thus, we propose to utilize a metric characterizing link stability to choose the most stable links in the network [49, 88, 89].

Many routing protocols proposing to find more stable routes can be found in the literature. Route lifetime Assessment Based Routing (RABR) [90] predicts the link lifetime using the measured value of average change in received signal strength over the last few samples. The Flow Oriented Routing Protocol (FORP) [91] makes use of node movement to predict the link expiration time and discover routes. The authors in [89] propose a probabilistic link availability model, where link availability is defined as the probability that there will be an active link between two mobile nodes at time $T + t$ given that this link is available at time T and, in [92], an improved model using a path reliability metric is illustrated. Two link stability metrics are proposed to categorize stable links in [93] based on empirical distributions of link duration and residual link lifetime.

While most of the existing schemes mainly focus on the impact of node mobility on link reliability, they have ignored channel fading. When a link suffers from a fade:

1. if the fade is shallow, or lasts only for a short time, it can be combated via physical layer (PHY) techniques, such as adaptive transmission and error control coding, or by adopting retransmission schemes in the medium access control protocol in the data link layer, allowing link connection to continue;
2. if the fade is deep and lasts for a long time, which might incur a number of continuous packet losses, the link will be disconnected.

In both cases, the channel fading incurs extra network overhead in the PHY, MAC, or network layer. We propose to measure the stability of a link by the duration for which the nodes at the ends of the link are within each other's transmission range with no fading. We call this new metric *Effective Link Operation Duration* (ELOD).

4.2 Effective Link Operation Duration

Any measure of link reliability should include an indication of how stable the link is in terms of longevity. When channel fading is taken into consideration, the stability of a link should be represented by the time for which the link is up, which is not simply the duration in which the nodes are within each other's transmission range, but the one in which the nodes are within each other's transmission range with no fading. The former is defined as link lifetime, T_f , and the latter as Effective Link Operation Duration (ELOD), \mathcal{O}_ℓ .

Definition 4.2.1. *The lifetime, T_f , is defined as the amount of time two nodes remain within each other's transmission range, given a non-fading path loss only channel.*

Definition 4.2.2. *The effective link operation duration (ELOD), \mathcal{O}_ℓ , is defined as the amount of time two nodes are able to continuously directly communicate in a fading plus path loss channel.*

The relationship between link lifetime and ELOD is

$$\mathcal{O}_\ell = T_f \Pr\{\text{link } \ell \text{ in connection during } T_f\}. \quad (4.2.1)$$

The ELOD is actually the total time duration within the link lifetime in which the received signal power is above a certain predefined threshold. The introduction of ELOD has particular benefits for mobile ad hoc networks. For example, a link composed of nodes with long pause times that are located at the edge of each other's transmission range, will have a relatively long lifetime which, at first glance, seems to indicate a stable link. However, when channel fading is incorporated, the ELOD for such a link may be relatively low, reflecting the true effectiveness of the link.

4.3 Calculation the ELOD

4.3.1 Channel Model

In this chapter we assume that the channel for each link is subject to flat fading [27]. The wireless channel model includes the effects of small-scale fading and large-scale

path-loss. We assume that the transmit power is fixed and the same for each node. For a transmission over a distance, d , in the presence of Rayleigh fading, the received signal power, P_r , is exponentially distributed with mean, $G_0 d^{-\alpha}$, given by (2.6.1). The probability, Θ , that the received signal power above a specified threshold, P_{th} , is

$$\Theta = \Pr\{P_r \geq P_{th}\} = e^{-\frac{P_{th}}{G_0 d^{-\alpha}}}. \quad (4.3.1)$$

4.3.2 Effective Link Operation Duration Estimation

In this section, we describe how to predict the link operation duration (ELOD) for a link in a mobile ad hoc network. We assume that all of the nodes in the network are equipped with a Global Positioning System (GPS) to enable them to determine their current positions and velocities. We also assume that all of the nodes in the network have equal transmission range, R , and that the movements of all nodes in the network is according to a random waypoint model [86], where each node travels with a fixed speed for a given period of time and then pauses, before moving to the next point. In Figure 4.1 we give an example of the movements of, and the relative distance between, two nodes A and B in a mobile ad hoc network. For the two nodes

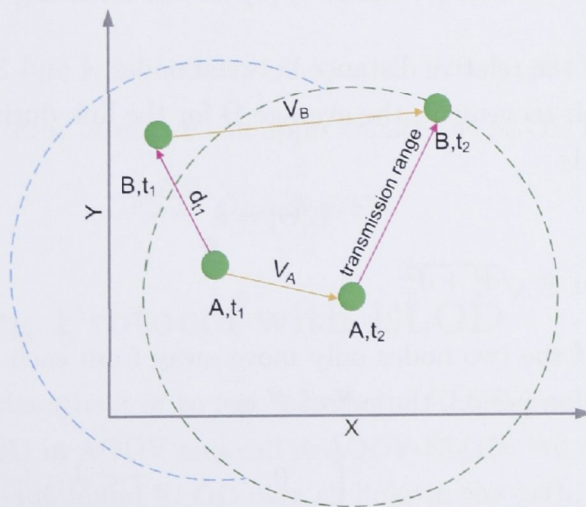


Figure 4.1: Example of movement, V_A and V_B , and the relative distances between nodes A and node B at times t_1 and t_2 .

A and B in Figure 4.1, with respect to a stationary Cartesian coordinate system, let (x_i, y_i) be the x - y position for mobile node i , and $(v_{i,x}, v_{i,y})$ be its speed components.

4.3 Calculation the ELOD

We can predict the link lifetime T_f from [91]:

$$T_f = \frac{-(d_x v_x + d_y v_y) + \sqrt{R^2(v_x^2 + v_y^2) - (d_y v_x - d_x v_y)^2}}{v_x^2 + v_y^2} \quad (4.3.2)$$

where $d_x = x_B - x_A$, $d_y = y_B - y_A$, $v_x = v_{B,x} - v_{A,x}$, and $v_y = v_{B,y} - v_{A,y}$.

Using the statistics of the channel fading from (4.3.1), which is the probability that a link is not in a fade, we can estimate the ELOD, \mathcal{O}_ℓ . However, because of the movement of the nodes, the relative distance between them is time-varying, which makes Θ vary with node movement. To account for this random topology, we replace d in (4.3.1) with a random variable, Z , representing the distance between the transmitter and the receiver. Therefore, the expected value of the probability, $E[\Theta]$, can be written as

$$E[\Theta] = \int_{d_{\min}}^R e^{-\frac{P_{\text{th}}}{G_0 Z^{-\alpha}}} f_Z(z) dz \quad (4.3.3)$$

where d_{\min} is the minimum distance between the two nodes at the ends of a link during the prediction period, and $f_Z(z)$ is the probability density function (PDF) of the random variable Z . Because we assume that the speed of a node is constant during the prediction period, the distance between two nodes should have a uniform distribution. Then, we can determine $f_Z(z)$ for the following distinct cases:

Case 1: if the relative distance between nodes A and B stays fixed during their movement, the average Θ for the link during the prediction period is

$$E[\Theta] = e^{-\frac{P_{\text{th}}}{G_0 d_{t1}^{-\alpha}}} \quad (4.3.4)$$

with $d_{t1} = \sqrt{d_x^2 + d_y^2}$,

Case 2: if the two nodes only move away from each other during the prediction period, the pdf of Z is

$$f_Z\{z\} = \begin{cases} 0, & z < d_{t1}; \\ \frac{1}{R-d_{t1}}, & d_{t1} \leq z \leq R; \\ 0, & z > R. \end{cases} \quad (4.3.5)$$

The average Θ for the link during connection is

$$E[\Theta] = \int_{d_{t1}}^R \frac{1}{R-d_{t1}} e^{-\frac{P_{\text{th}}}{G_0 z^{-\alpha}}} dz. \quad (4.3.6)$$

For example, when $\alpha = 2$,

$$E[\Theta] = \frac{\sqrt{\pi}}{2m(R - d_{t1})} [\Phi(mR) - \Phi(md_{t1})] \quad (4.3.7)$$

where $m = \sqrt{\frac{P_{th}}{G_0}}$, and $\Phi(x) = \frac{2}{\sqrt{\pi}} \int_0^x e^{-t^2} dt$;

Case 3: if the two nodes first move toward each other, then apart some time later, the pdf of Z is

$$f_Z\{z\} = \begin{cases} \frac{2}{d_{t1}+R}, & z < d_{t1}; \\ \frac{1}{d_{t1}+R}, & d_{t1} \leq z \leq R; \\ 0, & z > R. \end{cases} \quad (4.3.8)$$

The average Θ for the link during connection is

$$E[\Theta] = \int_0^{d_{t1}} \frac{2}{d_{t1}+R} e^{-\frac{P_{th}}{G_0 Z^{-\alpha}}} dZ + \int_{d_{t1}}^R \frac{1}{d_{t1}+R} e^{-\frac{P_{th}}{G_0 Z^{-\alpha}}} dZ. \quad (4.3.9)$$

For $\alpha = 2$,

$$E[\Theta] = \frac{\sqrt{\pi}}{m(d_{t1}+R)} \Phi(md_{t1}) + \frac{\sqrt{\pi}}{2m(d_{t1}+R)} (\Phi(mR) - \Phi(md_{t1})). \quad (4.3.10)$$

Then, for these three cases, we can approximate the ELOD for a link ℓ as

$$\mathcal{O}_\ell = T_f E[\Theta]. \quad (4.3.11)$$

4.4 Routing Protocol with ELOD

In this section, we describe how to incorporate the ELOD into the routing protocol. We implement ELOD in AODV and call it AODV-ELOD. We define \mathcal{O}_r , the ELOD for a path, r , as the minimum ELOD over all links in the path, such that

$$\mathcal{O}_r = \min_{\ell \in r} [\mathcal{O}_\ell]. \quad (4.4.1)$$

Using ELOD as the routing metric, we will obtain paths composed of links with longer fade-free periods. However, such a path may have many more hops than the shortest one. When packet relaying involves more hops, since the radio channel is shared

4.4 Routing Protocol with ELOD

among neighbouring nodes in the network, it will increase medium access contention, interference, congestion, and packet collisions. Therefore, path length should also be considered when selecting a suitable path based on stability. In this section we describe how to combine link signal quality and path length to choose stable paths.

4.4.1 Routing Metric

First, we illustrate the impact of path length on network performance. Assume that there are N nodes in an ad hoc network which are independently and uniformly distributed in a rectangular area with length $2S$ on each edge. The node spatial intensity, ε , is equal to $N/(2S)^2$. With a fixed node transmission range, R , the average number of neighbouring nodes within a circle with radius R is $n = \varepsilon\pi R^2$. Assume C is the number of source-destination connections on transmission in the network. The expected distance between source and destination for each connection is $\frac{S}{3}(\sqrt{2} + \ln(1 + \sqrt{2}))$ [94]. The expected number of hops, $\hat{\mathcal{H}}$, required to deliver a packet can be approximated as

$$\hat{\mathcal{H}} = \frac{(\sqrt{2} + \ln(1 + \sqrt{2}))S}{3R}. \quad (4.4.2)$$

Thus, the maximum number of nodes in the network which might be involved in packet deliveries, N_a , is

$$N_a = \begin{cases} \hat{\mathcal{H}}C, & \hat{\mathcal{H}}C < N; \\ N, & \hat{\mathcal{H}}C \geq N. \end{cases} \quad (4.4.3)$$

Then, the probability that a node has packets to transmit is N_a/N . In networks using the IEEE 802.11 distributed coordination function (DCF), nodes within each other's transmission ranges cannot transmit at the same time. When operating under heavy traffic conditions (every node always has packets to transmit), 802.11 DCF provides long term per packet fairness in single-hop networks [77]. Thus each node in the shared radio has a probability of $1/n$ of occupying the channel. Combining the probability that a node has packets to transmit, the average node transmission probability is $N_a/(nN)$. For a transmitting node on an active path, the probability that it can occupy the channel, or the probability that the channel won't be occupied by any of the $n - 1$ neighbours, q_o , is

$$q_o = 1 - \frac{N_a(n - 1)}{nN}. \quad (4.4.4)$$

For transmission over one-hop, q_o is the average achievable throughput due to channel access contention. Assume a path is composed of h hops. The average achievable path throughput, Γ , is

$$\Gamma = \mathcal{O}_r q_o^h = \mathcal{O}_r \left(1 - \frac{N_a(n-1)}{nN} \right)^h. \quad (4.4.5)$$

The throughput, Γ , combines the impacts of ELOD and path length. In AODV-ELOD, we use Γ as the routing metric to select stable paths with higher throughput.

4.4.2 The Proposed Routing Protocol

We incorporate the proposed routing metric, Γ , into AODV [37] to achieve channel adaptability and we call the new channel-adaptive routing protocol AODV-ELOD. The routing path establishment and maintenance procedure of AODV-ELOD is similar to that of AODV.

During the route discovery phase, before broadcasting a route request (RREQ) packet to its neighbours, a node will insert its current location and speed in the RREQ packet header for the receivers to calculate the \mathcal{O}_ℓ s using (4.3.11). The ELOD for the propagating path, \mathcal{O}_r , is also recorded in the RREQ. By using the information recorded in the RREQ packets, the intermediate nodes and the destination then determine the Γ given in (4.4.5) for the route.

An intermediate node will broadcast a RREQ into the network immediately if it didn't see the RREQ before. Or if it has received a RREQ advertised for the same source-destination pair before, the node also will forward the broadcasting packet further if the RREQ has a higher sequence number than the previously received ones, or if the RREQ has the same sequence number as previously received ones, but with a higher Γ . After the destination receives a RREQ, it delays for a short while, in order to obtain as many as possible, then selects the path with the highest Γ and feeds a route reply (RREP) packet back to the source.

4.5 Simulations

The performance of the proposed AODV-ELOD is compared with that of AODV [37], and Flow Oriented Routing Protocol (FORP) [91] using the network simulator ns-2.30 [85] with Rayleigh fading channel extension [95], where the handoff scheme in FORP is omitted to focus on the comparison of the routing metrics. Physical layer parameters of the Lucent WaveLAN wireless network card [85] are adopted in

4.5 Simulations

the simulations. The radio transmission range is 250 m. The Random waypoint [86] model with a pause time of 5 s is used for node mobility. The medium access control protocol is IEEE 802.11 DCF. All mobile nodes have the same channel bandwidth of 2 Mb/s. Scenarios for the simulation were configured with an 80-node 10-connection network in a 1500 m \times 1500 m terrain, where the nodes are uniformly distributed in the network and randomly move with maximum speed. Each simulation was run for 300 s.

4.5.1 Varying Node Mobility

First, we compare the performance of the routing protocols in time varying mobile multihop networks. The node maximum speed is increased from 2 m/s to 40 m/s to increase node mobility. Constant Bit Rate (CBR) sources are used at a rate of 4 packets per second with a size of 512 bytes and transmit to randomly chosen destinations.

Throughput is defined as the number of data packets transmitted through the network during the simulation. The simulation results for throughput is shown in Figure 4.2. It can be seen that while the throughput for all three routing protocols

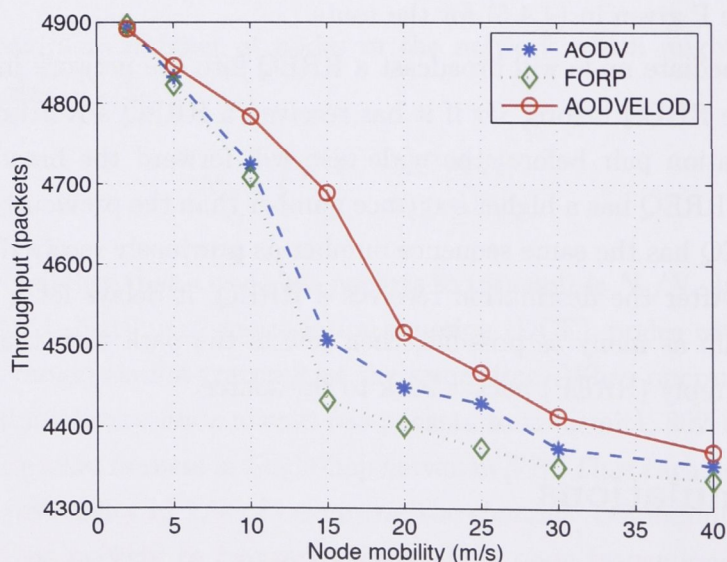


Figure 4.2: Throughput comparison under increasing node mobility.

decreased with increasing node mobility, the AODV-ELOD always outperforms the other two routing protocols. FORP has the worst performance in particular every

case. This is because FORP chooses paths composed of links with longer lifetimes but, consequently, greater number of hops. The increased number of hops increases interference, contention, and packet collisions in the network. Under a highly mobile environment, long paths are fragile because any movement of a node on the path might cause the path to fail. AODV uses a shortest hop-count metric, which makes it tend to select links composed of nodes that are located at the edge of each other's transmission ranges. Compared with the other two routing protocols, AODV-ELOD takes account of both link reliability and hop-count. Moreover, the criterion for link reliability in AODV-ELOD combines node movement with channel fading statistics. Thus, AODV-ELOD tends to select paths with shorter lengths and more stable links, improving network performance. However, AODV-ELOD assumes the nodes do not move during the interval in which the channel statistics are predicted, which might introduce some prediction errors and reduce the network performance, especially when the node movement is high (over 25 m/s).

Routing Control Overhead

Normalized routing control overhead is defined as the ratio of the number of routing control packets to the total number of delivered data packets. The normalized routing control overhead results for AODV-ELOD, AODV, and FORP are plotted in Figure 4.3. It can be seen that the routing control overhead for all three routing protocols increases with the increasing node mobility. This is because that higher node mobility leads to more dynamic network topology and more route failure. The AODV-ELOD has the lowest routing overhead compared with AODV and FORP, with a maximum 9% reduction than AODV and 10% decrease than FORP at $v = 15$ m /s.

Average end-to-end delay

Figure 4.4 illustrates the simulation results for the average packet transmission delay of the three routing protocols. From Figure 4.4, it can be seen that AODV-ELOD maintains the lowest average end-to-end delay compared with AODV and FORP. Neither AODV nor FORP considers link stability, therefore, it may utilise fragile paths to direct packet transmission. The breaking paths will incur long re-establishment delay once they are disconnected. By incorporating the channel adaptive metric ELOD into its path selection, AODV-ELOD takes into account the path stability as well as path length to improve network performance.

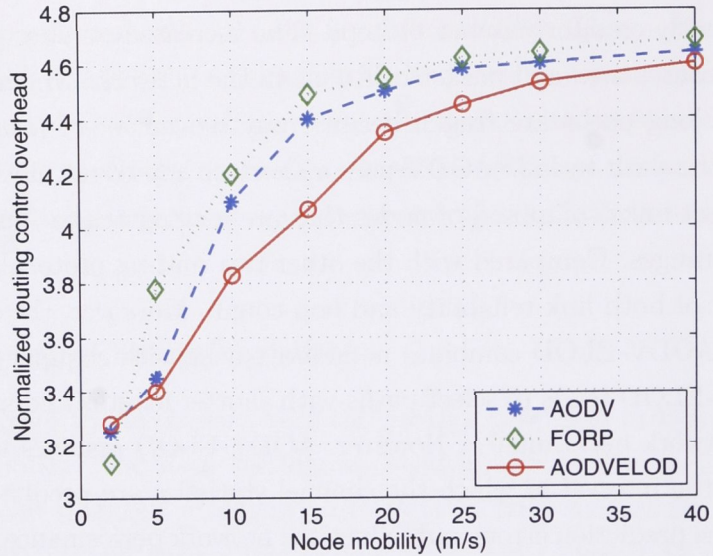


Figure 4.3: Normalized routing control overhead comparison under increasing node mobility.

Route Discovery Frequency

The simulation results for the route discovery frequency of AODV-ELOD, AODV, and FORP as a function of node mobility are shown in Figure 4.5. The results indicate that a more quickly changing network topology accelerates the route updating in all the three routing protocols. The figure also shows a decrease in the route discovery frequency of AODV-ELOD compared with those of AODV and FORP, specifically, with a maximum 30% reduction than FORP at $v = 5$ m/s, and a 15% reduction than AODV at $v = 10$ m/s.

Note that for each of these performance measures, the performances tend to be indistinguishable at low mobility (1-2 m/s), move apart as mobility increases and then start to converge again at high mobility (40 m/s). This is because at high mobility both the channel conditions and hop lengths are changing so rapidly that any advantage of taking into account either or both is lost.

4.5.2 Varying Traffic Load

Next, we fixed the node maximum speed at $v = 5$ m/s while varying the packet rate at each source from 1 to 30 packets/second, to evaluate the performance of the routing

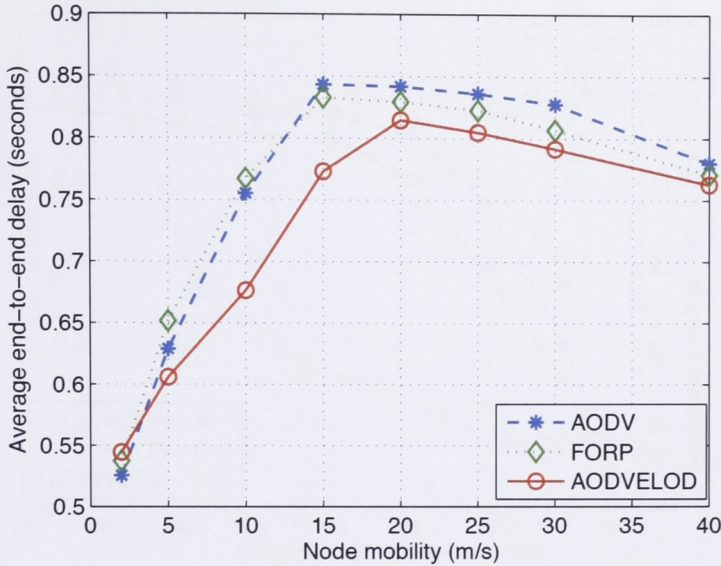


Figure 4.4: Average end-to-end delay comparison under increasing node mobility.

protocols with increasing network traffic load.

Packet Delivery Ratio

Figure 4.6 illustrates the packet delivery ratio (PDR) for the routing protocols with varying packet rate. For all of the routing protocols, the packet delivery ratio decreases with increasing traffic load. The performance degradation is due to the increased interference and congestion when the network traffic load is increased. We can see that AODV-ELOD has better performance in terms of PDR than AODV and FORP. This is due to the channel-aware metric in AODV-ELOD which makes the routing protocol choose long-lasting, high throughput links to reduce path failure then increase network throughput.

Average End-to-end Delay

Figure 4.7 shows the average end-to-end delay for the routing protocols with increasing traffic load. As the traffic load increases, the packet transmission delays in all of the three routing protocols increase dramatically at first, but then decrease once the traffic load in the network is over a particular point (5 packets/second for AODV and FORP, and 10 packets/second for AODV-ELOD). This is because very low packet rate means packets tend to go straightly through as the transmission medium is

4.6 Conclusion

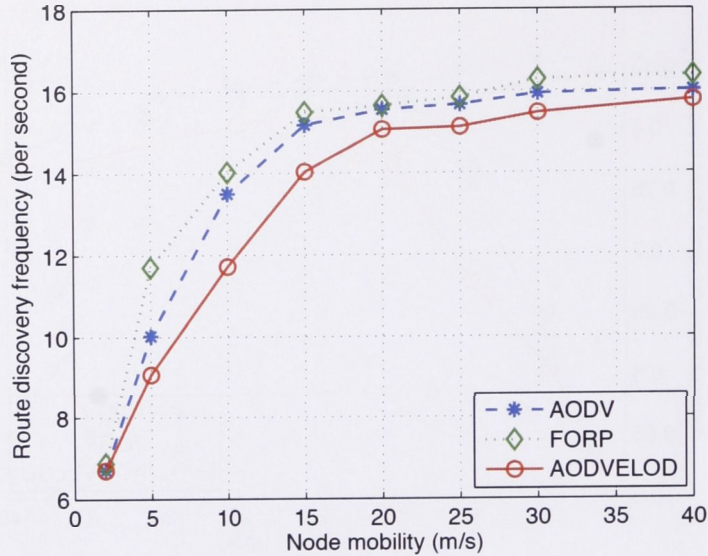


Figure 4.5: Average route discovery frequency comparison under different node mobility.

practically always available. As the packet rate increases there is more contention for the channel and so the delay goes up. However, as the packet rate increases further the delay goes down, because by the time the network is in congestion and only the packets via shorter paths can reach their destinations. For all the scenarios, AODV-ELOD has the lowest average end-to-end delay than AODV and FORP, because it is able to choose more stable routes.

4.6 Conclusion

In summary, this chapter has presented a channel-adaptive routing metric which takes account of link reliability. Link reliability is often measured by the estimated lifetime and the stability of a link, and is represented by node movement as well as channel fading statistics. We have proposed that the stability of a link can be represented by the time duration in which the two nodes at each end of a link are within each other's transmission ranges as well as the time during which channel fading is above an acceptable threshold. Based on a consideration of link reliability, innovative channel adaptive routing metric called effective link operation duration (ELOD) has been proposed. The ELOD is incorporated into AODV (AODV-ELOD), taking into account path length, interference, and medium access contention. Simulation results

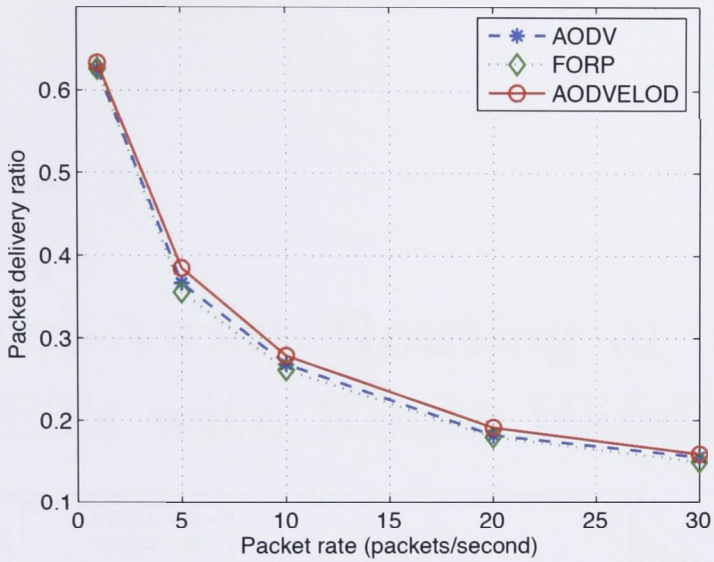


Figure 4.6: Packet delivery ratio comparison under increasing traffic load.

show that the proposed AODV-ELOD outperforms AODV and FORP in terms of packet delivery ratio, routing control overhead, and end-to-end packet delay.

4.6 Conclusion

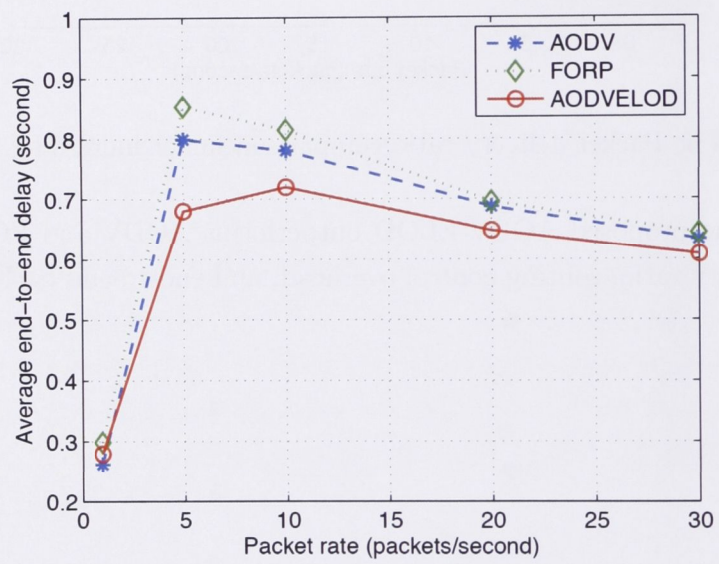


Figure 4.7: Average end-to-end delay comparison under increasing traffic load.

Chapter 5

Channel-Aware Routing in MANETs with Route Handoff

5.1 Introduction

In the previous chapter we have proposed a channel-adaptive routing metric, the Effective Link Operation Duration (ELOD). This chapter presents a channel-adaptive routing protocol which extends the Ad-hoc On-Demand Multipath Distance Vector routing protocol (AOMDV) [31] with several channel adaptation schemes to accommodate channel fading.

Firstly, the proposed routing protocol, Channel-Aware AOMDV (CA-AOMDV), uses the channel average non-fading duration (ANFD) as a new routing metric. During route discovery phase, the ANFD, which represents the quality of a fading link, is combined with the hopcount metric to select the path which is optimal in terms of both stability and length. Then, during route maintenance phase, the predicted signal power and the channel average fading duration (AFD) are combined with a preemptive handoff strategy to identify and avoid fragile paths. Thus, CA-AOMDV exploits channel state information in the network layer to fully maintain reliable connections. Simulation results show that the channel adaptability of CA-AOMDV leads to improved routing decisions.

In comparison with ELOD, which seeks an approach of adaptation by employing a channel-adaptive routing metric, CA-AOMDV takes advantage of several channel adaptation schemes to ameliorate fading. It uses the CSI in both route discovery and route maintenance phases. With better knowledge of channel states, CA-AOMDV can more accurately choose the best links to build a path, or adaptively switch a failing

5.2 Review of AOMDV

connection to a new one with more favourable channel conditions. However, CA-AOMDV requires continually monitoring instantaneous link conditions to trigger a handoff once a fade occurs. The channel probing would be rather high and counteract adaptation gains in a highly mobile environment.

The layout of this chapter is as follows. In Section 5.2 we review the AOMDV routing protocol, from which the proposed channel-aware routing protocol is derived. Statistical properties of the mobile-to-mobile channel model are discussed in Section 5.3. The CA-AOMDV routing protocol is presented in Section 5.4. Theoretical analysis is developed in Section 5.5, and simulation results are discussed in Section 5.6. Finally, conclusions are drawn in Section 5.7.

5.2 Review of AOMDV

AOMDV [31] uses a *sequence number* to ensure loop-free paths. That is, each node maintains one or more paths to a destination corresponding to only the highest known sequence number for that destination. Moreover, AOMDV adopts the notion of an *advertised hop count* to maintain multiple paths with the same sequence number. An intermediate node, i , will maintain an advertised hop count and a sequence number for a particular destination node. The advertised hop count of node i to destination node d represents the “maximum” hop count of the multiple paths for d through node i . The protocol only allows for acceptance of alternate paths with lower hop counts. Whenever i receives a path advertisement to the destination d from a neighbour j , j will be the next hop from i to d if the path advertisement has a higher sequence number than the existing routes stored at node i , or the path advertisement has a sequence number equal to the existing routes at node i but with a shorter hop-count.

The multiple paths in AOMDV are link-disjoint. To get multiple link-disjoint paths, the destination can reply to multiple copies of a given RREQ, as long as these RREQs arrived via different neighbours. An example of multiple link-disjoint paths is given in Figure 5.1.

5.3 Mobile-to-Mobile Channel Model

In MANETs, potentially all of the nodes are in motion, thus, it is appropriate to use the mobile-to-mobile channel model to characterize the channel between any two nodes [76]. Moreover, it is practically difficult to find the *relative speeds* between

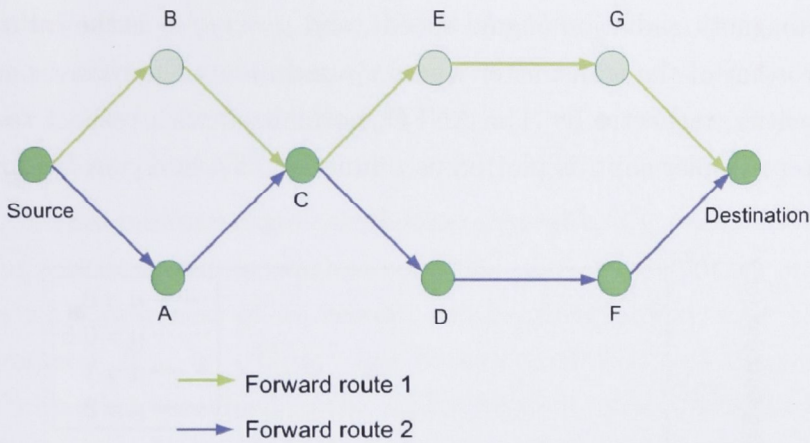


Figure 5.1: Two link-disjoint paths in AOMDV from Source to Destination via nodes BCEG and ACDF, respectively.

mobile nodes in the network and the time varying mobile-to-mobile channel model has the advantage of only using the individual speeds of the nodes.

The mobile-to-mobile channel model used in this chapter incorporates large scale path loss and small-scale flat fading. For transmission over a distance, d , in the presence of flat fading, the received signal power is exponentially distributed with mean $G_0 d^{-\alpha}$, as given in (2.6.1), where G_0 is proportional to the transmit power and α is the propagation loss coefficient, typically between 2 and 4 [96].

5.3.1 Average Non-Fading Duration

The average non-fading duration (ANFD) is a second-order statistic of the mobile-to-mobile channel model. It is affected by both the physical propagation environment (e.g., obstacles such as trees and buildings) and the velocities of the mobile nodes. The ANFD, $\bar{\vartheta}$, is the average length of time that the signal envelope, x , spends above a network specific threshold, R_{th} , and is given by

$$\begin{aligned}
 \bar{\vartheta} &= \frac{1}{N_\rho} \Pr\{x > R_{th}\} = \frac{1}{\rho f_T \sqrt{2\pi(1 + \mu^2)}} \\
 &= \frac{1}{\frac{R_{th}}{c\sqrt{G_0}} d^{\frac{\alpha}{2}} f_0 \sqrt{2\pi(v_T^2 + v_R^2)}}
 \end{aligned} \tag{5.3.1}$$

where $\rho = R_{th}/R_{rms}$, ($R_{rms} = \sqrt{G_0 d^{-\alpha}}$) is the ratio between the signal threshold and the local rms amplitude of the fading envelope, $f_T = f_0 v_T/c$ is the maximum Doppler shift of the transmitter, f_0 is the signal carrier frequency, $c \approx 3 \times 10^8 \text{ ms}^{-1}$ is the speed

5.3 Mobile-to-Mobile Channel Model

of electromagnetic radiation (signal speed), and $\mu = v_R/v_T$ is the ratio of the receiver velocity to that of the transmitter where v_R and v_T are the receiver and transmitter node velocities, respectively. The ANFD, normalized with respect to the maximum transmitter Doppler shift, is plotted as a function of μ and ρ in Figure 5.2.

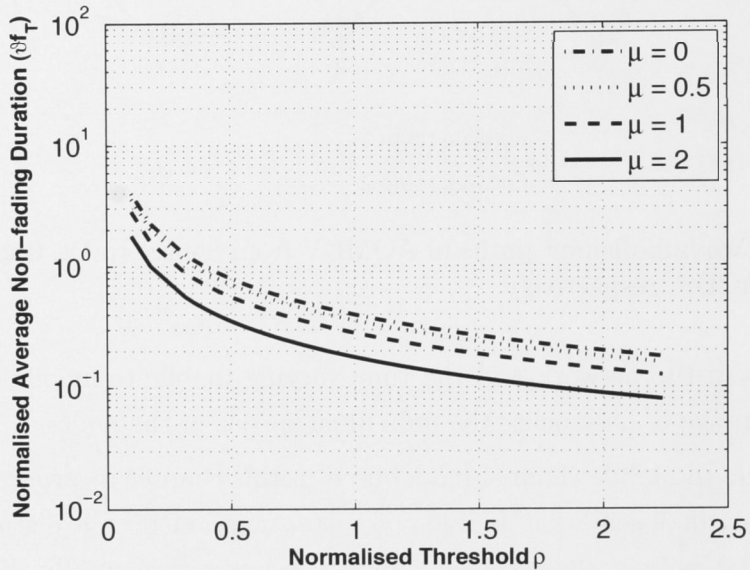


Figure 5.2: The relationship between normalized average non-fading duration and the ratio of the signal threshold and the root mean square received signal amplitude, $\rho = R_{th}/R_{rms}$, for various $\mu = v_R/v_T$, for the mobile-to-mobile channel from (5.3.1).

It can be seen from Figure 5.2 that the value of the ANFD is, as expected, high for low transmission threshold ρ , and decreases with an increase of μ or ρ . It can also be surmised from (5.3.1) that increased node mobility (captured by v_R and v_T) would cause a corresponding decrease in the ANFD due to the increased rate of signal fluctuations and that an increased link distance (via d) would cause a decrease in ANFD due to a greater path-loss influence.

In MANETs, it is necessary to choose the most stable links for route establishment to ensure reliable packet transmission. The stability of a link can be represented by the relative distance between the nodes forming that link, and the nodes' mobilities. Any measure of how stable a link is should include an indication of both of these factors.

It can be surmised, from the discussion above, that the ANFD is a good measure for link stability. The ANFD of a link is inversely proportional to the link length, d ,

and the node velocities v_T and v_R . The ANFD of a link between two highly mobile or separated nodes will tend to be shorter than that of a link between two slow moving and/or close nodes. In short, a link with a high ANFD will have a relatively long lifetime. Thus, using the ANFD as a metric will result in choosing more stable links.

Further, there is minimal extra calculation required by the nodes to determine the ANFDs if each node in the network is equipped with a Global Positioning System (GPS) then with awareness of its current geographical location and velocity. The channel parameter $R_{\text{rms}} = \sqrt{G_0 d^{-\alpha}}$ can be approximated by a receiver using the transmitter's location contained in the packet headers. The maximum Doppler frequency shift can be calculated via $f_T = f_0 v_T / c$, and, for the calculation of μ , nodes simply need to include their speeds in the headers of the data packets, for active links, or the "hello" packets for inactive links.

Therefore, we introduce the ANFD into the routing protocol, using it as a metric to represent the quality of the transmission links to find the most reliable paths.

5.3.2 Average Fading Duration

Similarly to the ANFD and more widely used as a metric in the communications literature, the average fading duration (AFD), $\bar{\chi}$, is the average length of time that the signal envelope spends below the specified threshold R_{th} . It is considered that transmission is not possible across a link while the signal envelope for that link is below the threshold. The AFD for the mobile-to-mobile channel is given in (2.7.9) with

$$\bar{\chi} = \frac{e^{\rho^2} - 1}{\rho f_T \sqrt{2\pi(1 + \mu^2)}}.$$

The AFD metric is used in CA-AOMDV to determine how long a faded link will be unavailable for. This value is recorded in the routing cache and is used to indicate the expected length of time for which a faded link will be unavailable. This will be discussed in detail in Section 5.4.2.

5.3.3 Channel Prediction Using Time Correlation

One of the features of CA-AOMDV is the use of channel prediction to instigate a handoff between paths, when the active path is predicted to be about to go into a fade on one of its links, as described in Section 5.4.2. We have chosen the linear minimum mean square error (LMMSE) algorithm [97] as our channel prediction method. We

5.3 Mobile-to-Mobile Channel Model

assume a slow fading channel such that it is constant for the duration of a symbol.

Let M be the number of previously received signal strength samples used to predict at discrete time interval n (each discrete time interval with a time space of Δt). If $\hat{x}(n + \psi)$ is the LMMSE prediction for the received signal strength, x , with prediction length ψ , we have

$$\hat{x}(n + \psi) = \mathbf{R}_{\hat{x}x} \mathbf{R}_{xx}^{-1} \mathbf{x} \quad (5.3.2)$$

where $\mathbf{R}_{\hat{x}x}$ is the cross-correlation vector of \hat{x} and \mathbf{x} , \mathbf{R}_{xx} is the auto-correlation matrix of $\mathbf{x} = [x(n - 1), x(n - 2), \dots, x(n - M)]^T$. The auto-correlation matrix \mathbf{R}_{xx} is given by

$$\mathbf{R}_{xx} = \begin{bmatrix} R_{xx}(1, 1) & R_{xx}(1, 2) & \cdots & R_{xx}(1, M) \\ R_{xx}(2, 1) & R_{xx}(2, 2) & \cdots & R_{xx}(2, M) \\ \vdots & \vdots & \cdots & \vdots \\ R_{xx}(M, 1) & R_{xx}(M, 2) & \cdots & R_{xx}(M, M) \end{bmatrix} \quad (5.3.3)$$

where element $R_{xx}(\ell, m)$ is given by (2.7.7)

$$\begin{aligned} R_{xx}(\ell, m) &= E\{x(n - \ell)x^H(n - m)\} \\ &= \sigma_1^2 J_0(2\pi f_T(m - \ell))J_0(2\pi f_R(m - \ell)) \end{aligned} \quad (5.3.4)$$

where $(\cdot)^H$ denotes Hermitian transpose, $\sigma_1 = R_{\text{rms}}/\sqrt{2}$ and J_0 is the 0th order Bessel function of the first kind. Finally,

$$\mathbf{R}_{\hat{x}x} = [R_{\hat{x}x}(1), R_{\hat{x}x}(2), \dots, R_{\hat{x}x}(M)]$$

where

$$\begin{aligned} R_{\hat{x}x}(m) &= E\{\hat{x}(n + \psi)x^H(n + \psi - m)\} \\ &= \sigma_1^2 J_0(2\pi f_T m)J_0(2\pi f_R m). \end{aligned} \quad (5.3.5)$$

Clearly, with the presence of Bessel functions, the LMMSE algorithm is quite computationally intensive. So, to enhance its amenability to application to channel

prediction in MANETs, (5.3.2) can be reduced as follows.

$$\begin{aligned}
 \hat{x}(n + \psi) &= (\mathbf{R}_{\hat{x}x} \mathbf{R}_{xx}^{-1}) \mathbf{x} \\
 &= \mathbf{W} \mathbf{x} \\
 &= [w(1), \dots, w(M)] [r(n-1), \dots, r(n-M)]^T \\
 &= \sum_{i=1}^M w(i) r(n-i)
 \end{aligned} \tag{5.3.6}$$

where $\mathbf{W} = (\mathbf{R}_{\hat{x}x} \mathbf{R}_{xx}^{-1})$ with elements $w(i) \{i = 1, \dots, M\}$. The values of $w(i)$ can be calculated off-line and stored in a lookup table indexed by the Doppler frequency shift and the discrete time shift. The use of this low-complexity LMMSE prediction in CA-AOMDV handoff is discussed in Section 5.4.2.

5.4 Channel-Aware AOMDV Protocol

Transmissions via unreliable wireless connections can suffer from large packet losses [98, 99]. Thus, it makes sense to consider routing protocols which adapt to variations in the channel. To this end, we have devised a channel-aware routing protocol which extends AOMDV. We call it CA-AOMDV.

As mentioned in Section 5.2, route discovery in AOMDV results in the selection of multiple loop-free and link-disjoint paths between the source and the destination, with alternative paths only being utilized if the selected path becomes unserviceable. However, one of the main shortcomings of AOMDV is that the only characteristic that is considered when choosing a path is the number of hops it has. The stability or quality of the path is completely ignored. Thus, selected paths tend to have a small number of long hops meaning that nodes are already relatively close to the maximum possible communication distance apart, which potentially results in frequent link disconnections. Further, channel conditions are idealised to the path-loss (or transmission range) model, ignoring the fading characteristics inherent in practically all wireless communication environments.

In CA-AOMDV, we address this deficiency in two ways. In the route discovery phase we utilise the ANFD, defined in Section 5.3.1, of each link as a measure of its stability. In the route maintenance phase, instead of waiting for the active path to fail, we pre-empt a failure by using channel prediction on path links, allowing a handover to one of the remaining selected paths. This results in saved packets and

5.4 Channel-Aware AOMDV Protocol

consequently smaller delays. We now consider route discovery and route maintenance in CA-AOMDV in detail.

5.4.1 Route Discovery in CA-AOMDV

Route discovery in CA-AOMDV is an enhanced version of route discovery in AOMDV, incorporating channel properties for choosing more reliable paths. We assume all the nodes in the network are equipped with a Global Positioning System (GPS) thus with awareness of their current positions and velocities. We also assume that all nodes in the network have identical transmission ranges, and that the nodes all move according to a random waypoint model [86]. In the random waypoint mobility model each node chooses a destination point and travels in a straight line at a fixed speed until it reaches that point, pausing for a scenario-specific, possibly variable, amount of time, before moving on to the next chosen point.

In Section 5.3.1, we defined the ANFD for one link of a path, according to the mobile-to-mobile channel model. CA-AOMDV uses the ANFD as a measure of link lifetime.

Definition 5.4.1. *The duration, \mathcal{D} , of a path is defined as the minimum ANFD over all of its links,*

$$\mathcal{D} \triangleq \min_{1 \leq h \leq \mathcal{H}} \text{ANFD}_h \quad (5.4.1)$$

where h is the link number, and \mathcal{H} is the number of links (or hops) in the path.

Before forwarding a RREQ to its neighbours, a node inserts its current location and speed into the RREQ header so that its neighbours can calculate the link ANFD using (5.3.1). The path duration, \mathcal{D} , is also recorded in the RREQ, updated, as necessary, at each intermediate node. Thus, all information required for calculating the ANFD is available via the RREQ packets, minimizing added complexity.

Similarly to the way of path advertisement in AOMDV, to allow for the worst case at each node, in CA-AOMDV the advertised path duration, \mathcal{D}_{ap} , is also used as part of the cost function in path selection. It is defined as follows.

Definition 5.4.2. *The advertised path duration, $\mathcal{D}_{\text{ap}}^{i,u}$, is defined as the minimum \mathcal{D}*

Table 5.1: Comparison of routing table entry structures in AOMDV and CA-AOMDV.

AOMDV routing table	CA-AOMDV routing table
destination	destination
sequence number	sequence number
advertised_hopcount	advertised_hopcount
path_list	\mathcal{D}_{ap}
{(nexthop ₁ ,hopcount ₁), (nexthop ₂ ,hopcount ₂),...}	path_list {(nexthop ₁ ,hopcount ₁ , \mathcal{D}_1), (nexthop ₂ ,hopcount ₂ , \mathcal{D}_2),...}
expiration_timeout	expiration_timeout
	handoff_dormant_time

over all paths between a given node, i , and a destination node, u . That is,

$$\mathcal{D}_{ap}^{i,u} \triangleq \min_{\zeta \in \text{path_list}_i^u} \mathcal{D}_{\zeta} \quad (5.4.2)$$

where path_list_i^u is the list of all saved paths between nodes i and u .

The route discovery update algorithm in CA-AOMDV is a slight modification of that of AOMDV. If a received path advertisement for destination u at node i from a neighbour node, j , has a higher sequence number or shorter hop-count than the existing route for destination u at node i , the route update criterion in CA-AOMDV is the same as that in AOMDV. However, if the received path advertisement has a sequence number and hop-count equal to the existing route at node i but with a greater $\mathcal{D}_{ap}^{i,u}$, the list of paths to u in node i 's routing table is updated.

So, in CA-AOMDV, path selection is based on $\mathcal{D}_{ap}^{i,u}$ as well as sequence number and advertised hop-count. The routing table structures for each path entry in AOMDV and CA-AOMDV are shown in Table 5.1. The “handoff_dormant_time” field in the routing table for CA-AOMDV is the amount of time for which the path should be made dormant due to channel fading. It is set to the maximum value of the AFDs over all links in the path. This use of the “handoff_dormant_time” field will be described in more detail in the next section.

5.4.2 Path Maintenance in CA-AOMDV

In mobile environments, it is necessary to find computationally and energy efficient ways of addressing path failure. Using prediction and handoff to preempt fading on a link on the active path, disconnections can be minimized, reducing transmission latency and packet drop rate [91, 55]. An example of handoff in CA-AOMDV is shown in Figure 5.3. The handoff process is implemented via a handoff request (HREQ) packet. The CA-AOMDV handoff scheme is described below.

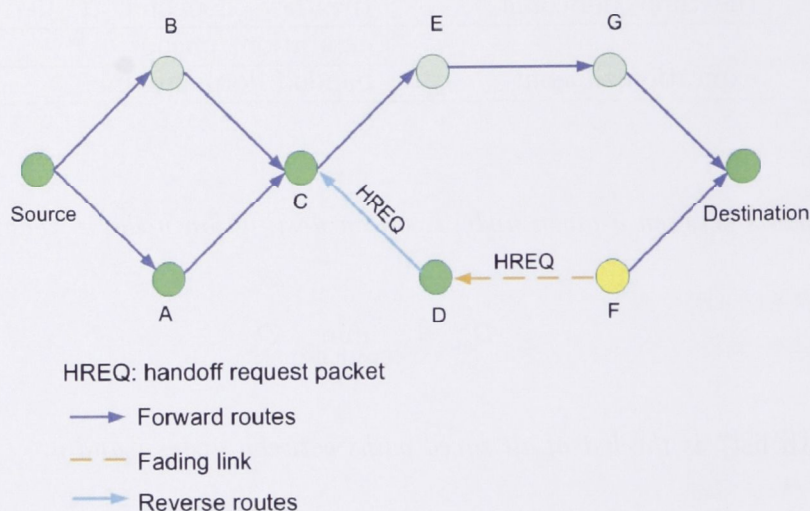


Figure 5.3: Handoff in CA-AOMDV. Node F has predicted a forthcoming fade for its link with node D and has generated a HREQ. Having no alternative paths to choose from, node D forwards the HREQ to node C which may then be able to handoff to the path with node E as the next node.

Handoff Trigger

Path handoff is triggered when a node predicts that the signal strength on the active link is about to go into a fade. Signal strength prediction is carried out via the low-complexity table-lookup version of the LMMSE algorithm detailed in Section 5.3.3. To assist in the prediction process, all nodes maintain a table of past signal strengths, recording the following information for each received packet: `previous_hop`, `signal_power`, `arrival_time`. Information is stored for packets back to the time required for prediction in the LMMSE algorithm. (Ideally there will be M packets where M is the required number of past samples from (5.3.2). However, this will depend on the packet receipt times compared with the specified discrete time

interval, Δt . If packets are received at time intervals greater than Δt , sample signal strengths for the missed time interval can be approximated by the signal strength of the packet closest in time to the one missed. If packets are received at intervals of shorter duration than Δt , some may be skipped.)

As previously mentioned, in CA-AOMDV the speed of each transmitter is recorded in the packet (data and hello) header for the receivers to calculate the link AFD from (2.7.9). If the predicted signal strength moves below a network specific threshold, the node at the receiving end of the fading link triggers a handoff. This node is called the *handoff initiator*. A HREQ packet is generated by the handoff initiator and propagated back to the data source. The AFD for the breaking link is recorded in the HREQ, so that the channel may be again utilized once it comes out of the fade. The HREQ also includes the following fields: source ID, destination ID, and source_sequence_number [37].

Avoidance of Duplicate HREQs Using Handoff Table

In addition to the routing table described in Table 5.1, each node in CA-AOMDV also maintains a local handoff table. Each entry in the handoff table includes: source ID, source sequence number, destination ID and expiration timeout. The expiration timeout indicates when a path is expected to be available again (will be out of the fade) and is set to the maximum AFD of all currently faded links with paths through that node to a particular source. Note that this is similar to the way the advertised hopcount is set to the maximum number of hops for any path going through a node for a particular source ID, in AOMDV. Whenever a node receives a HREQ targeting a particular source node, it checks its handoff table for an entry relating to that source. The handoff table is updated if no entry exists for that source, if the new HREQ has a longer AFD or if the existing entry is stale due to the expiration timeout having expired. If any unexpired entry is found for that source ID with the same or higher source sequence number, the HREQ is dropped.

Forwarding the HREQ:

Any node which receives a non-duplicate HREQ will check whether it has alternative paths to the destination node. If it does not, as for the case of node *D* in Figure 5.3, it will propagate the HREQ. Otherwise, if it has one or more “good” alternative paths to the destination, it will mark the fading path indicated in the HREQ as dormant,

5.4 Channel-Aware AOMDV Protocol

by setting the handoff dormant time in its routing table entry for that path to the AFD recorded in the HREQ. The HREQ is then dropped.

If a fade is predicted on the active path, a nondormant alternative path to the destination is then adopted prior to the onset of link failure. For example, if node C in Figure 5.3 receives a HREQ from node D , it will mark the path with $\text{NextHop} = D$ as dormant, and adopt the path with $\text{NextHop} = E$. The dormant path is retained for use when the fading is over, reducing path discovery overhead.

5.4.3 Choosing Prediction Length

For a nonstationary channel, the LMMSE prediction algorithm performs quite poorly if not matched to the current channel conditions. Therefore, the prediction length should not be too long. Moreover, in CA-AOMDV a given node might have multiple paths, each with different nexthop nodes to the destination. If an intermediate node has multiple paths to the destination, upon receiving an HREQ it can immediately switch from the active path to a good alternative one, without further propagating the HREQ. Therefore, the time needed to implement a handoff in CA-AOMDV is the duration, in terms of the discrete time interval Δt , for the HREQ to be propagated to the node on the other end of the fading link, which is a one-hop neighbour of the HREQ initiator. For example, if i and j are neighbours in a given path and j predicts a fade on link $\ell_{i,j}$, it will generate a HREQ and forward it to i . Thus, a suitable prediction length ψ in (5.3.2) corresponds to the number of discrete time intervals, Δt , for transmission of a HREQ between nodes j and i , which can be approximated by using the data propagation time T_j^i from node j to node i . Therefore, the prediction length in CA-AOMDV is chosen to be

$$\psi = \text{round}\left(\frac{T_j^i}{\Delta t}\right). \quad (5.4.3)$$

where “round” is the integer rounding function.

Section Summary *In CA-AOMDV, we make use of CSI in both the route discovery and path maintenance phases, to improve path stability.*

- *Route discovery: In CA-AOMDV, the ANFD is combined with the hop-count criterion from AOMDV to serve as a metric with which to select short but stable paths instead of simply choosing the shortest path, as in AOMDV. Therefore,*

CA-AOMDV targets paths taking into account both the stability and the length, to improve overall path quality.

- *Route maintenance: Assuming independently time-varying path characteristics, CA-AOMDV uses predicted signal strength to trigger a handoff before a fade occurs, reducing the source-destination connection failure rate. The AFD for the breaking link is also recorded, so that the channel may be utilised again once it comes out of the fade.*

In this section, we have presented the mechanisms involved in CA-AOMDV. In the next section we present a theoretical analysis and comparison of the performances of CA-AOMDV and AOMDV.

5.5 Theoretical Analysis

A framework is now presented to analyse the performances of the AOMDV and CA-AOMDV routing protocols. First, we introduce the network parameters, both fixed and random, governing all internode communication. Then, the probability density functions of the lifetimes of a single path and multiple paths are derived. Finally, the performance in terms of routing control overhead and network throughput of both AOMDV and CA-AOMDV based on the link lifetime distributions are analysed. A list of parameters used in the analysis is presented in Table 5.2.

5.5.1 Network Model

Assume that in our network there are N nodes uniformly distributed over a square area with length $2S$ on each side. The node density is $\varepsilon = N/(2S)^2$ nodes per m^2 . The number of traffic flows (connections) in the network is C . With a fixed node transmission range, R , the average number of neighbouring nodes within a circle with radius R is $n = \varepsilon\pi R^2$. The expected number of hops $\hat{\mathcal{H}}$ required to deliver a packet is given in the equation of (4.4.2) with

$$\hat{\mathcal{H}} = \frac{S(\sqrt{2} + \ln(1 + \sqrt{2}))}{3R}.$$

Assume that each link in a path has equal likelihood of being broken at any point in time. Then, on average, the number of hops into a connection (path) before encountering a broken link is $(\hat{\mathcal{H}} + 1)/2$. Moreover, because the average number of

5.5 Theoretical Analysis

Table 5.2: Parameters used in the analysis

C	number of connections in the network
ε	node spatial intensity
Y	random variable for link, path or multiple path system downtime
Z	random variable for link, path or multiple path system lifetime
f	probability density function (PDF)
F	cumulative distribution function (CDF)
N	number of nodes in the network
$\hat{\mathcal{H}}$	expected number of hops to deliver a packet
T	total connection operation time
Ω	route discovery frequency
n	average number of neighbouring nodes within a circle with radius R
I	expected number of hops to deliver a HREQ
t_Q	one-hop propagation time for RREQ
t_P	one-hop propagation time for RREP
t_R	one-hop propagation time for RRER
Υ	control overhead
Ψ	packet delivery ratio
λ	parameter of link lifetime PDF (under fading)
γ	parameter of link downtime PDF (under fading)
B	average number of connected paths over a link
N_p	number of saved paths
L	length of a single path, in hops

links being used at any given time is $C\hat{\mathcal{H}}$, and the total number of links in the network is approximately $nN/2$, the average number of connections, B , over a given link is

$$B = \frac{2C\hat{\mathcal{H}}}{nN}. \quad (5.5.1)$$

5.5.2 Single Path Lifetime Statistics

The link lifetime indicates the length of time for which a link is “active”. It is affected by the movements of the pair of linked nodes and the channel fading characteristics. If only free-space propagation is considered, the link lifetime is simply the amount of time for which the two nodes are within each other’s transmission ranges. If channel fading is also taken into consideration the relationship between link lifetime and distance is not so straightforward, as the fading component is independent of distance. In the analysis for the active times for links, paths and the AOMDV multiple path system, we utilise the mathematical development in [100] using slightly modified notation more suited to our theoretical development.

We use the random variable Z_ℓ to represent the lifetime of a fading link. The link lifetime Z_ℓ is equal to the non-fading duration of the link, from (5.3.1). In [101], the authors have illustrated that the link lifetime distribution of Rayleigh fading channel can be approximated by an exponential distribution. We therefore assume that the lifetime for link ℓ has PDF, $f_{Z_\ell}(t) = \lambda_\ell e^{-\lambda_\ell t}$.

As discussed in Section 5.2, the multiple cached paths at a given source node for a given destination node are link-disjoint in AOMDV. Thus, we assume that the lifetimes of the links composing the multiple cached paths are independent. While this is not strictly the case, here we are seeking general trends, and this approximation is, therefore, appropriate. For a path composed of L fading links, the path lifetime can be represented by $Z_p = \min[Z_1, \dots, Z_L]$, where $Z_\ell, \{\ell = 1, \dots, L\}$, represents the exponentially distributed random variable for the lifetime of link ℓ with parameter λ_ℓ . The probability that the path lifetime is greater than t is the probability that the

5.5 Theoretical Analysis

minimum of the lifetimes of all of the links in the path is greater than t , given by

$$\begin{aligned}
 \Pr\{Z_p > t\} &= \Pr\{\min[Z_1, \dots, Z_L] > t\} \\
 &= \Pr\{(Z_1 > t) \cap (Z_2 > t) \cap \dots \cap (Z_L > t)\} \\
 &= \prod_{\ell=1}^L \Pr\{Z_\ell > t\} \\
 &= \prod_{\ell=1}^L [1 - F_{Z_\ell}(t)] = \prod_{\ell=1}^L e^{-\lambda_\ell t}
 \end{aligned} \tag{5.5.2}$$

where the step from line 2 to line 3 is because of the assumption of independent links and $F_{Z_\ell}(t)$ is the CDF of Z_ℓ . Using $F_{Z_p}(t)$ to represent the CDF of Z_p ,

$$\begin{aligned}
 F_{Z_p}(t) &= 1 - \Pr\{Z_p > t\} \\
 &= 1 - \prod_{\ell=1}^L e^{-\lambda_\ell t} = 1 - e^{-(t \sum_{\ell=1}^L \lambda_\ell)}.
 \end{aligned} \tag{5.5.3}$$

Taking the derivative of (5.5.3) with respect to t gives the PDF of Z_p ,

$$f_{Z_p}(t) = e^{-t \sum_{k=1}^L \lambda_k} \sum_{\ell=1}^L \lambda_\ell = \lambda_p e^{-\lambda_p t} \tag{5.5.4}$$

where $\lambda_p = \sum_{\ell=1}^L \lambda_\ell$. If all L links are independent and identically distributed (i.i.d.) with parameter λ , then (5.5.4) becomes

$$f_{Z_p}(t) = L\lambda e^{-L\lambda t}. \tag{5.5.5}$$

Using (5.5.4), the expected path lifetime is, then

$$E\{Z_p\} = \int_0^\infty t \lambda_p e^{-\lambda_p t} dt = \frac{1}{\lambda_p} = \frac{1}{\sum_{\ell=1}^L \lambda_\ell} \tag{5.5.6}$$

and $1/\lambda_p = 1/L\lambda$ for L i.i.d. links in a path. So, a path with L i.i.d. links has a lifetime L times less than any individual link, on average.

5.5.3 Multiple Path Lifetime in AOMDV

To determine the distributions of the active lifetimes of the multiple path systems in AOMDV and CA-AOMDV, we assume that N_p paths are established during the route

discovery stage for both routing protocols. In order to enable meaningful comparisons between the two schemes, we also assume that the each path has exactly L links and that the individual link lifetimes are exponentially i.i.d. with parameter λ for $Z_\ell, \{\ell = 1, \dots, L\}$.

Assume that at time t path p_1 is the active path in a network utilising AOMDV. When p_1 fails, the source attempts to adopt one of the alternative paths, and p_1 is discarded from the cache. Communication between the source and destination nodes is broken only when all N_p paths have subsequently failed. Let Z_A be the random variable representing the lifetime of the multiple path system in AOMDV and let Z_{p_i} be the random variable which represents the lifetime of path p_i with parameter $\lambda_p = L\lambda$, and $Z_A = \max(Z_{p_1}, \dots, Z_{p_{N_p}})$. Using (5.5.3) and (5.5.4), the probability that all paths have failed at time t is given by

$$\begin{aligned}
 \Pr\{Z_A < t\} &= \Pr\{\max(Z_{p_1}, \dots, Z_{p_{N_p}}) < t\} \\
 &= \Pr\{(Z_{p_1} < t) \cap (Z_{p_2} < t) \cap \dots \cap (Z_{p_{N_p}} < t)\} \\
 &= \prod_{i=1}^{N_p} \Pr\{Z_{p_i} < t\} = \prod_{i=1}^{N_p} F_{Z_{p_i}}(t) \\
 &= (1 - e^{-\lambda_p t})^{N_p}.
 \end{aligned} \tag{5.5.7}$$

Equation (5.5.7) is the CDF of Z_A . Taking the derivative of (5.5.7) with respect to t , the PDF of Z_A is given by

$$\begin{aligned}
 f_{Z_A}(t) &= N_p \lambda_p e^{-\lambda_p t} (1 - e^{-\lambda_p t})^{N_p - 1} \\
 &= N_p \lambda_p \sum_{k=0}^{N_p - 1} (-1)^{N_p - k - 1} \binom{N_p - 1}{k} e^{-(N_p - k)\lambda_p t}.
 \end{aligned} \tag{5.5.8}$$

where the second line of (5.5.8) is from (1.111) of [102]. And the expected value of Z_A is given by

$$\begin{aligned}
 E\{Z_A\} &= \int_0^\infty t f_{Z_A}(t) dt \\
 &= \frac{N_p}{\lambda_p} \sum_{k=0}^{N_p - 1} (-1)^{N_p - k - 1} \binom{N_p - 1}{k} \frac{1}{(N_p - k)^2}.
 \end{aligned} \tag{5.5.9}$$

Thus we have shown the average multiple path system active lifetime for AOMDV with N_p paths each with L i.i.d. links.

5.5.4 Multiple Path Downtime in CA-AOMDV

Let us now consider the multiple path system in CA-AOMDV. A handoff scheme is adopted in CA-AOMDV to enable swapping between the alternative paths when a fade is predicted on the active path. At time t , again let path p_1 be the active path. When p_1 fails, it is marked as dormant for the predicted period of its fade and p_2 is put into operation, and so on. The difference from AOMDV is that once any path p_i comes out of its fade, it can again be considered for active use. In AOMDV, once a path goes into a fade, it is discarded and can no longer be considered. So, with CA-AOMDV, a new route discovery process is only required when all N_p paths are *simultaneously* in a fade. So, we need to know how often this happens, or how long the multiple path system "downtime" is for multiple reselectable paths.

Now, because, in CA-AOMDV, the system is active if any one path is active at any time, but "disconnected" only if all paths are "down" (or in a fade) simultaneously, it is simpler to start with expressions for the system downtime and then determine the system lifetime in terms of the system downtime. We start at the link level. Similarly to the link lifetime (or non-fading duration), the link downtime (or fading duration) also has an exponential distribution. Remembering that all links are i.i.d., let the random variable Y_ℓ represent the downtime of link ℓ , with parameter γ , with CDF $F_{Y_\ell}(t) = 1 - e^{-\gamma t}$. Also let the random variable Y_p represent the downtime of path p , with parameter γ_p , with CDF $F_{Y_p}(t)$. Further, let the random variable Y_C represent the multiple path system downtime for CA-AOMDV, with CDF $F_{Y_C}(t)$. The CA-AOMDV system is down only when all paths are down, which occurs when at least one link in each path is down. So, the probability that the CA-AOMDV system is down at time t is

$$\begin{aligned}
 \Pr\{Y_C > t\} &= \prod_{i=1}^{N_p} \Pr\{Y_{p_i} > t\} \\
 &= \prod_{i=1}^{N_p} \left(1 - \prod_{k=1}^L \Pr\{Y_{\ell_k} < t\} \right) \\
 &= \prod_{i=1}^{N_p} \left(1 - \prod_{k=1}^L F_{Y_{\ell_k}}(t) \right) \\
 &= \left[1 - (1 - e^{-\gamma t})^L \right]^{N_p}.
 \end{aligned} \tag{5.5.10}$$

$$\begin{aligned}
 f_{Y_C}(t) &= \gamma N_p L e^{-\gamma t} (1 - e^{-\gamma t})^{L-1} \left[1 - (1 - e^{-\gamma t})^L \right]^{N_p-1} \\
 &= \gamma N_p L \sum_{k=0}^{N_p-1} (-1)^{N_p-k-1} \binom{N_p-1}{k} \\
 &\quad \times \sum_{i=0}^{L(N_p-k)-1} (-1)^{L(N_p-k)-1-i} \binom{L(N_p-k)-1}{i} e^{-[L(N_p-k)-i]\gamma t} \quad (5.5.12)
 \end{aligned}$$

$$\begin{aligned}
 E\{Y_C\} &= \int_0^{\infty} t \gamma N_p L e^{-\gamma t} (1 - e^{-\gamma t})^{L-1} \left[1 - (1 - e^{-\gamma t})^L \right]^{N_p-1} dt \\
 &= \frac{N_p L}{\gamma} \sum_{k=0}^{N_p-1} (-1)^{N_p-k-1} \binom{N_p-1}{k} \\
 &\quad \times \sum_{i=0}^{L(N_p-k)-1} (-1)^{L(N_p-k)-1-i} \binom{L(N_p-k)-1}{i} \frac{1}{(L[N_p-k]-i)^2}. \quad (5.5.13)
 \end{aligned}$$

Then the CDF of the CA-AOMDV multiple path system downtime, Y_C , is given by

$$F_{Y_C}(t) = 1 - \left[1 - (1 - e^{-\gamma t})^L \right]^{N_p}. \quad (5.5.11)$$

Then, taking the derivative of (5.5.11), the PDF of the CA-AOMDV multiple path system downtime, Y_C , with i.i.d. links is given by (5.5.12) and, subsequently, the expected downtime of the CA-AOMDV multiple path system is given by (5.5.13).

Now, let the random variable Z_C represent the multiple path system lifetime in CA-AOMDV.

5.5.5 Multiple Path Lifetime in CA-AOMDV

When we consider a fading channel, the AFD is given by the quotient of the probability of a fade and the level crossing rate (LCR), where the LCR is the rate in times per second that the signal amplitude in the channel crosses a given threshold in the positive going direction. Similarly, the ANFD is given by the quotient of the probability of not being in a fade and the LCR. To determine the ANFD in terms of

5.5 Theoretical Analysis

the AFD, we proceed as follows.

$$\begin{aligned} \text{ANFD} &= \frac{\Pr(\text{channel is not in a fade})}{\text{LCR}} \\ &= \frac{1 - \Pr(\text{channel is in a fade})}{\Pr(\text{channel is in a fade})} \text{AFD} \end{aligned} \quad (5.5.14)$$

For a multiple path system, the AFD is analogous to the system downtime and the ANFD is analogous to the system lifetime. So, for CA-AOMDV, we substitute (5.5.13) for the AFD. We need to determine an expression for the probability that the CA-AOMDV system is “in a fade”, or ”down”. Now, the probability that the CA-AOMDV multiple path system is down is the probability that all paths are down. The probability that any particular path is down is the probability that at least one link in the path is undergoing a fade. In [74] it was shown that the signal envelope of a mobile-to-mobile signal has a Rayleigh distribution. Recall the Rayleigh parameter, ρ , from Section 5.3.1. The probability that the CA-AOMDV system is in a fade is given by

$$\Pr(\text{system in fade}) = \prod_{i=1}^{N_p} \left(1 - \prod_{\ell=1}^L e^{-\rho^2} \right) = \left(1 - e^{-L\rho^2} \right)^{N_p}. \quad (5.5.15)$$

Then, letting Z_C be the random variable representing the CA-AOMDV system lifetime and combining (5.5.13), (5.5.14) and (5.5.15), the average system lifetime for CA-AOMDV is given by

$$E\{Z_C\} = \frac{1 - \left(1 - e^{-L\rho^2} \right)^{N_p}}{\left(1 - e^{-L\rho^2} \right)^{N_p}} E\{Y_C\}. \quad (5.5.16)$$

5.5.6 Comparison of Multiple Path System Lifetimes of AOMDV and CA-AOMDV

In Figure 5.4, Figure 5.5, Figure 5.7 and Figure 5.6, we show the ratio of the multiple path system lifetime of a CA-AOMDV system to an AOMDV system with varying numbers of paths and links per path, as it varies with link Rayleigh fading threshold parameter ρ . The cases shown attempt to cover “worst case” and “best case” scenarios. Figure 5.4 is a best case in terms of minimal number of links for different numbers of paths in the system, while Figure 5.5 is a worst case with six links per path. Similarly, Figure 5.6 is a best case in terms of maximal number of paths for

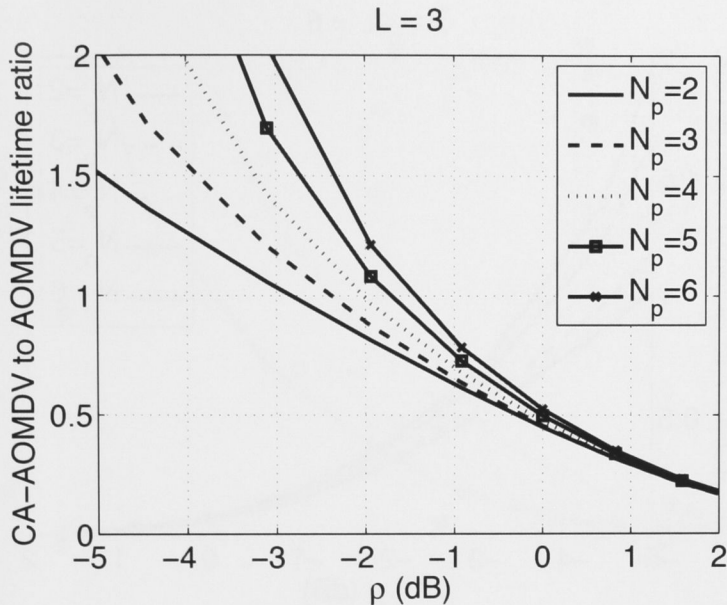


Figure 5.4: Ratio of multiple path system lifetime for CA-AOMDV to AOMDV for increasing values of link fading threshold parameter ρ , for $L = 3$ links per path, for $N_p = 2, 3, 4, 5, 6$ paths.

varying numbers of links per path, while Figure 5.7 is a worst case with only two paths in the system.

It can be seen that the ratio of system lifetime for CA-AOMDV versus AOMDV increases exponentially in all cases as the fading threshold ρ decreases. Recall that ρ is the ratio of the signal strength threshold at which the link is said to be in a fade, to the link RMS signal strength. So, the higher the value of ρ , the higher the signal strength must be for the link to be considered *not* in a fade. The ratio improves with an increase in number of paths and a decrease in number of links per path. The multiple path system lifetime becomes greater (ratio < 1) for AOMDV as ρ approaches 1. That is, AOMDV only begins to have a better system lifetime when the likelihood of all paths in the CA-AOMDV system being down becomes too large. Specifically, CA-AOMDV outperforms AOMDV, in terms of system lifetime as long as the fading channel parameter, $\rho < -5$ dB. So, CA-AOMDV outperforms AOMDV in more typical channel fading conditions, whereas AOMDV will outperform CA-AOMDV, in terms of system lifetime, in adverse fading conditions.

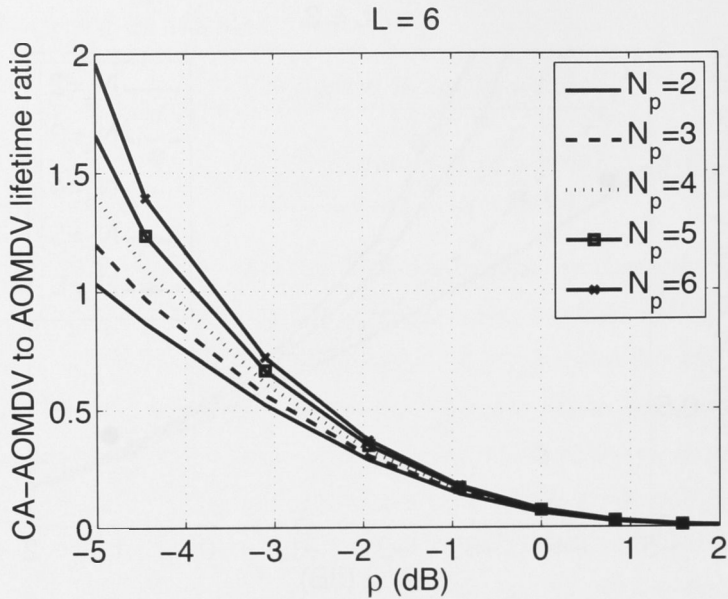


Figure 5.5: Ratio of multiple path system lifetime for CA-AOMDV to AOMDV for increasing values of link fading threshold parameter ρ , for $L = 6$ links per path, for $N_p = 2, 3, 4, 5, 6$ paths.

5.5.7 Performance Analysis of AOMDV and CA-AOMDV

We now determine expressions for network performance in terms of routing control overhead and packet delivery ratio, in AOMDV and CA-AOMDV. If Φ^d is the average delay for each route discovery and $E\{Z\}$ is the average lifetime of a connection pair in AOMDV or CA-AOMDV, from (5.5.9) or (5.5.16), then $(E\{Z\} + \Phi^d)$ represents the average duration between two successive route discoveries [100]. We introduce Ω , the number of route discoveries per second per pair, or route discovery frequency, as

$$\Omega = \frac{1}{E\{Z\} + \Phi^d}. \quad (5.5.17)$$

In CA-AOMDV and AOMDV, when a source wants to find a path to a destination, it broadcasts a RREQ into the network. The destination, or any intermediate node which has a fresh enough path to the destination, feeds a RREP back to the source to establish the path. We can approximate Φ^d as

$$\Phi^d = \hat{\mathcal{H}}(t_Q + t_P) \quad (5.5.18)$$

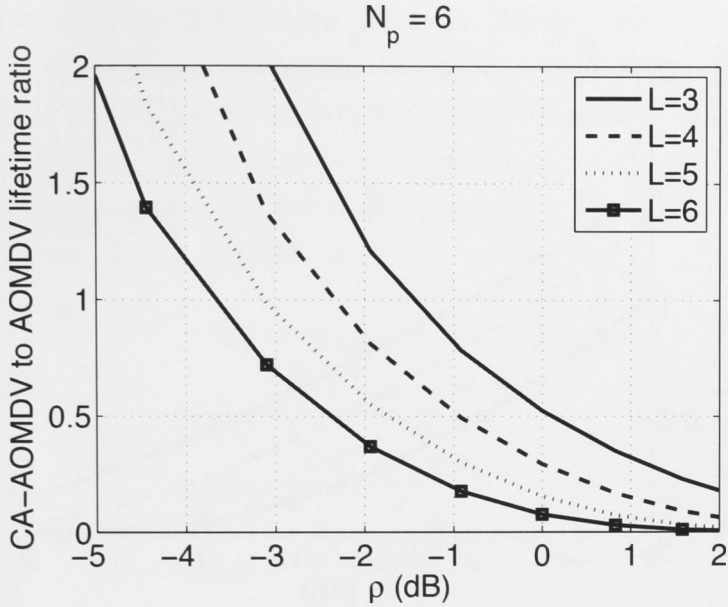


Figure 5.6: Ratio of multiple path system lifetime for CA-AOMDV to AOMDV for increasing values of link fading threshold parameter ρ , for $N_p = 6$ paths, for $L = 3, 4, 5, 6$ links per path.

where t_Q is the one-hop propagation time of a RREQ, and t_P is the one-hop propagation time of a RREP. Because there are a total of C connections in the network, each lasting an average of T seconds, the average number of route discovery processes in the network during interval T is equal to $N_{rd} = CT\Omega$.

Routing Control Overhead (Υ)

In a multiple path system, the routing control overhead Υ includes overhead to replace the failed path with an active alternative path, Υ^r , and the route discovery overhead, Υ^d , introduced when all alternative paths are broken.

First we consider the routing control overhead introduced by route discovery due to the disconnection of each communicating pair. For both AOMDV and CA-AOMDV, the RREQs are flooded into the N -node network, and N_p RREPs are unicast from the destination to the source, where N_p is the number of multiple paths established during route discovery. The total routing control overhead introduced by route discovery over a time T is given by

$$\Upsilon^d = n_{\text{RREQ}} + n_{\text{RREP}} = CT\Omega(N + N_p\hat{\mathcal{H}}) \quad (5.5.19)$$

5.5 Theoretical Analysis

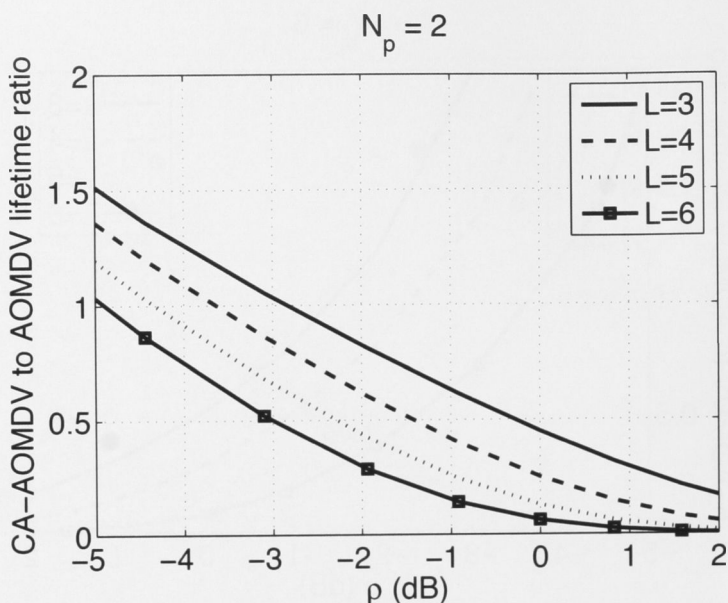


Figure 5.7: Ratio of multiple path system lifetime for CA-AOMDV to AOMDV for increasing values of link fading threshold parameter ρ , for $N_p = 2$ paths, for $L = 3, 4, 5, 6$ links per path.

where n_{RREQ} is the number of RREQs, and n_{RREP} is the number of RREPs, generated during the route discovery.

Now we consider the control overhead for path replacement, Υ^r . In each source-destination pair, there are N_p alternative paths, so, there can be at most N_p path repairs. In AOMDV, an intermediate node can have a single or multiple paths to a destination. In the event of a path disconnection, the upstream node of the broken link will initiate a RERR to notify the source of the link failure. If the upstream node has no alternative paths to the destination, and it is located closer to the destination than it is to the source, it will broadcast a RREQ to the destination to salvage the data packets. (In AOMDV, if the broken link is closer to the source than it is to the destination, any enroute packets are discarded.) Assuming that the link failure is equally likely to happen in any link of the path, the maximum number of path replacements is, therefore, $CT\Omega_A N_p/2$, where Ω_A is the route discovery frequency in AOMDV.

So, the routing control overhead due to path failure includes the RERRs triggered by the failed link, the path repair RREQs flooded from the fading link to the destination, and the RREP packets from the destination to the RREQ generator. Because only link breaks in the latter half of a path are atoned for, RREQs are flooded into the

network over an average of $\hat{\mathcal{H}}/4$ hops, with the average number of flooded RREQs during each path repair approximately being $N_{\text{rq}} = \pi(\hat{\mathcal{H}}R/4)^2\sigma$. The RREPs are unicast from the destination to the RREQ broadcasting node, while the RERRs are unicast from the fading link to the source. In each path failure, the average number of connected paths over a breaking link is B from (5.5.1). The routing control overhead due to path failure, Υ_A^r , in AOMDV is

$$\Upsilon_A^r = n_{\text{RERR}} + n_{\text{RREQ}} + n_{\text{RREP}} \quad (5.5.20)$$

$$n_{\text{RERR}} = \frac{CTN_p\Omega_A B(\hat{\mathcal{H}} + 1)}{2} \quad (5.5.21)$$

$$n_{\text{RREQ}} = \frac{CTN_p\Omega_A BN_{\text{rq}}}{2} \quad (5.5.22)$$

$$n_{\text{RREP}} = \frac{CTN_p\Omega_A B\hat{\mathcal{H}}}{4} \quad (5.5.23)$$

where n_{RERR} is the number of RERRs due to path failure, and Ω_A is the average route discovery frequency in AOMDV. The total routing control overhead in AOMDV due to alternative path failure during the interval T is, from (5.5.20), (5.5.21), (5.5.22), and (5.5.23)

$$\Upsilon_A^r = CTN_p\Omega_A B \left(\frac{3\hat{\mathcal{H}} + 2}{4} + \frac{N_{\text{rq}}}{2} \right). \quad (5.5.24)$$

However, if the upstream node of the broken link has multiple paths to the destination, during a path failure, it can use an alternative path to salvage the data packets, without propagation of RREQs and RREPs. Under these circumstances, (5.5.20) can be simplified to $\Upsilon_A^r = n_{\text{RERR}} = CTN_p\Omega_A B(\hat{\mathcal{H}} + 1)/2$.

In CA-AOMDV, for each path repair, routing control overhead involves the HREQs which are terminated at the nearest intermediate nodes which have multiple paths to the destinations. The number of handoffs between two successive route discoveries is determined by the channel fading status. However, we can approximate it by N_p . Assume that the expected number of hops to deliver a HREQ is $\hat{\mathcal{I}}$ with $\hat{\mathcal{I}} \leq \hat{\mathcal{H}}$, then the routing control overhead in CA-AOMDV due to path failure is

$$\Upsilon_C^r = n_{\text{HREQ}} = CTN_p\Omega_C B\hat{\mathcal{I}} \quad (5.5.25)$$

where Ω_C is the average route discovery frequency in CA-AOMDV. For the special case where multiple paths exist in the upstream nodes of the broken links, in each path failure, the routing control overhead of CA-AOMDV is just one-hop HREQ

5.5 Theoretical Analysis

propagation over the fading link with $\hat{\mathcal{I}} = 1$, that is, $\Upsilon_C^r = CTN_p\Omega_C B$.

Then, the total routing control overhead is $\Upsilon = \Upsilon^d + \Upsilon^r$, with

$$\Upsilon_A = CT\Omega_A(N + N_p\hat{\mathcal{H}}) + CTN_p\Omega_A B \left(\frac{3\hat{\mathcal{H}} + 2}{4} + \frac{N_{\text{rq}}}{2} \right) \quad (5.5.26)$$

$$\Upsilon_C = CT\Omega_C(N + N_p\hat{\mathcal{H}}) + CTN_p\Omega_C B\hat{\mathcal{I}} \quad (5.5.27)$$

where Ω_A and Ω_C are the route discovery frequency for AOMDV and CA-AOMDV, respectively.

We showed in the previous section that the multiple path system lifetime for CA-AOMDV was longer than that for AOMDV, for most practical cases, so the number of route discoveries per second for CA-AOMDV, Ω is smaller for CA-AOMDV than AOMDV. If we also compare the differentiating terms in (5.5.26) and (5.5.27), it can be shown that $3(\hat{\mathcal{H}} + 2)/4 + N_{\text{rq}}/2 > \hat{\mathcal{I}}$. Thus, the routing overhead for AOMDV is greater than that for CA-AOMDV for most practical cases.

Packet Delivery Ratio (Ψ)

In this section we consider packet delivery ratio. The packet delivery ratio is the ratio of the number of generated packets to the number of successfully received packets. The total simulation time T for a source-destination connection can be approximately divided into two parts, the data transmission duration, $\mathcal{S}_{\text{data}}$, which is used for data transmission, and the connection delay, which is the time used to contend for channel access and to reconnect the disconnected paths. In a network with constant bit rate (CBR) sources and constant data transmission rate, we can model the data as being delivered uniformly over time, such that the packets delivered within $\mathcal{S}_{\text{data}}$ are correctly received, and those delivered during the time of connection delay are incorrectly received. Then, the ratio between the data transmission time $\mathcal{S}_{\text{data}}$ and the total operation time T can be used to model packet delivery ratio.

First we consider path connection delay. The path connection delay Ψ includes the delay Φ^r due to activation of an alternative path, and the delay Φ^d , from (5.5.18), due to route discovery when all alternative paths are broken. In AOMDV, the delay due to alternative path activation is the time to propagate the RERRs back to the source. Assume that the one-hop propagation time of a RERR is t_r . The total delay due to switching between the alternative paths during an interval of length T is, from

(5.5.21)

$$\Phi_A^r = t_r \times n_{\text{REERR}} = \frac{TN_p\Omega_A t_r(\hat{\mathcal{H}} + 1)}{2}. \quad (5.5.28)$$

However, in CA-AOMDV, the connection delay is the handoff packet propagation duration $t_h\hat{\mathcal{I}}$. The total connection delay is $\Phi = \Phi^d + \Phi^r$. Thus, the time that can be used for data transmission is $T - \Phi$. For 802.11 DCF, there are also delays incurred for MAC overhead and retransmission. For each data transmission, the minimum channel occupation due to MAC overhead is $T_{\text{MAC}} = T_{\text{RTS}} + T_{\text{CTS}} + 3T_{\text{SIFS}}$, where T_{RTS} and T_{CTS} are the time consumed on RTS and CTS, respectively, and T_{SIFS} is the SIFS period. And, for each path failure, the delay due to packet retransmission is $N_R(t_d + T_{\text{MAC}})$, where N_R is the MAC retransmission count, and t_d is the time for each data packet transmission. Combining the time consumed on both the MAC and routing layers, the delay introduced by path failure can be written as

$$\begin{aligned} \Phi_A = \Phi^d\Omega_A T + \frac{TN_p\Omega_A(t_r + T_{\text{MAC}})(\hat{\mathcal{H}} + 1)}{2} \\ + TN_p\Omega_A N_R(t_d + T_{\text{MAC}}) + T\Omega_A T_{\text{MAC}}\hat{\mathcal{H}} \end{aligned} \quad (5.5.29)$$

$$\begin{aligned} \Phi_C = \Phi^d\Omega_C T + TN_p\Omega_C(t_h + T_{\text{MAC}})\hat{\mathcal{I}} \\ + T\Omega_C N_R(t_d + T_{\text{MAC}}) + T\Omega_C T_{\text{MAC}}\hat{\mathcal{H}}. \end{aligned} \quad (5.5.30)$$

A comparison of the terms in (5.5.29) and (5.5.30) reveals that, whenever $\Omega_C < \Omega_A$, terms 1, 3 and 4 are less for CA-AOMDV than for AOMDV. Term 3 is also advantaged in CA-AOMDV because it does not have the multiplicative N_p term. In the second term, however, the relative values depend on the actual value of $\hat{\mathcal{I}}$, which has been defined as $\hat{\mathcal{I}} < \hat{\mathcal{H}}$, the relative values of t_r and t_h and the relative values of Ω_C and Ω_A . Generally, however, AOMDV spends time on repairing path failure, which is preempted by adopting a handoff scheme in CA-AOMDV. The absence of handoff in AOMDV also increases the MAC delay due to packet retransmission in the event of path failure.

When IEEE 802.11 DCF is employed, we should also consider the throughput degradation due to channel access contention. Based on our random network traffic model, the maximum number of nodes in the network which might be involved in packet relaying is given in (4.4.3) with

$$N_a = \begin{cases} \hat{\mathcal{H}}C, & \hat{\mathcal{H}}C < N \\ N, & \hat{\mathcal{H}}C \geq N. \end{cases}$$

5.6 Simulation Results

Then for a transmitting node on an active path, the probability that it can occupy the channel, or the probability that the channel won't be occupied by any of the $n - 1$ neighbours, is given in (4.4.4) with

$$q_o = 1 - \frac{N_a(n-1)}{nN}.$$

Because each node on a path suffers the same average throughput degradation due to channel access contention, the time available for data transmission in a path is $(T - \Phi)q_o$. The achievable packet delivery ratio is $\Psi = (T - \Phi)q_o/T$. For AOMDV and CA-AOMDV respectively, the packet delivery ratio in the network is

$$\Psi_A = \frac{(T - \Phi_A)q_o}{T} \quad (5.5.31)$$

$$\Psi_C = \frac{(T - \Phi_C)q_o}{T} \quad (5.5.32)$$

where Φ_A and Φ_C are given in (5.5.29) and (5.5.30), respectively. Therefore, whenever $\Phi_A > \Phi_C$ the packet delivery ratio of AOMDV will be lower than that of CA-AOMDV.

5.6 Simulation Results

The performance of the proposed CA-AOMDV protocol is compared with that of AOMDV using the network simulator ns-2 [85]. We implemented the mobile-to-mobile channel as in [95, 103], and the Doppler frequency of a link is controlled by both the movement of the transmitter and the receiver. Physical layer parameters of the Lucent WaveLAN wireless network card [85] are adopted in the simulations. The radio transmission range is 250 m. We use the random waypoint [86] model as the mobility model. Constant Bit Rate (CBR) sources are used and each CBR source transmits to randomly chosen destinations. The medium access control (MAC) protocol is IEEE 802.11 DCF. The performances of the routing protocols are evaluated using throughput, average end-to-end delay, routing control overhead, and packet delivery ratio in the simulations.

5.6.1 Scenario to Evaluate the use of the ANFD in Routing

First, we evaluate the performance of a single link under different ANFDs by comparing the effect of the ANFD metric on the link throughput. Scenarios for the

simulation were configured with a 1000 m × 1000 m terrain. All mobile nodes have the same channel bandwidth of 2 Mb/s. Two nodes A and B are initially placed 70 m apart. Nodes A and B move in parallel directions. Node A moves with a fixed speed of $v_A = 1$ m/s, while node B moves with speeds of 1 m/s, 1.5 m/s, 2 m/s, 2.5 m/s, and 3m/s respectively, with $\mu = 1, 1.5, 2, 2.5, 3$ accordingly. By changing the speed of node B, we change the ratio of their speeds, thus varying the ANFD value for the link. The data packets are 512 bytes, transmitted at a rate of 40 packets per second. The simulation time is 50 s.

Throughput is the number of data packets transmitted through the network during the simulation. The network throughput versus μ is shown in Figure 5.8. It can be

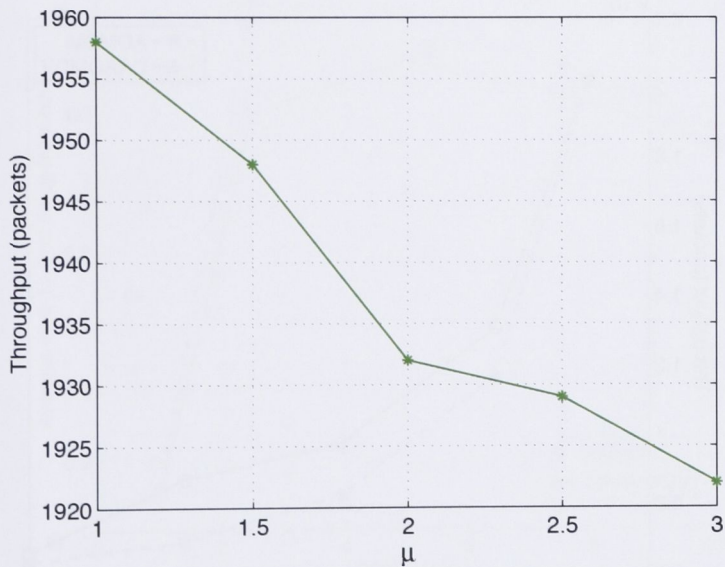


Figure 5.8: Link throughput vs. μ , $\mu = v_B/v_A$, v_A is fixed at 1 m/s, for communicating nodes, A and B, moving in parallel directions, separated by 70 m, initially.

seen that the link throughput is inversely proportional to μ . With increased μ , we increase the node mobility, thereby decreasing the ANFD for the link. As expected, lower mobility achieves higher network throughput, so utilising the ANFD in the routing metric can help to improve network throughput.

5.6.2 Varying Node Mobility

We now compare the performance of AOMDV and CA-AOMDV for different mobility scenarios. The simulations were configured with a 100-node 25-connection network

5.6 Simulation Results

in a $2200 \text{ m} \times 600 \text{ m}$ terrain, where the nodes were uniformly distributed in the network area and were moving at the maximum speed in random directions. The channel bandwidth was 2 Mb/s. The node maximum speed was increased from 1 m/s to 10 m/s to increase node mobility. The CBR sources were fixed at a rate of 4 packets per second with a size of 512 bytes. The simulation time was 500 seconds.

Throughput

First, we measure the relationship between the network throughput and node mobility. The simulation results for the network throughput of both routing protocols are shown in Figure 5.9. It can be seen that while the throughput for both routing protocols

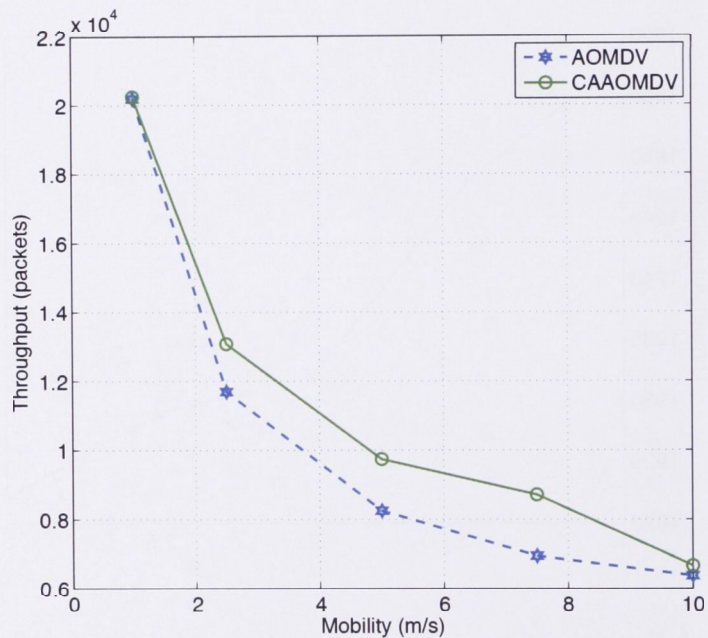


Figure 5.9: Network throughput comparison between CA-AOMDV and AOMDV with increasing node mobility.

decreases with increased node mobility, the CA-AOMDV throughput is always higher than that of AOMDV. For a speed of 7 m/s, there is about a 29% improvement for CA-AOMDV over AOMDV. The improvement in CA-AOMDV can be attributed to the introduction of the channel-aware metric and handoff scheme. The ANFD metric causes low-mobility or low outage probability links to be chosen to establish the paths, and the handoff scheme maintains the source-destination connectivity by reducing the probability of path failure. Note that at low and high mobilities the schemes

vary very little in throughput performance. At low mobilities, path characteristics do not vary very quickly and so that advantages of handoff in CA-AOMDV are lost. At high mobilities channel and path characteristics change very rapidly, again somewhat negating the advantages gained via the CA-AOMDV handoff scheme, as well as increasing the difficulties of signal strength prediction.

Average End-to-End Delay

Average end-to-end delay is the average time taken to transfer a data packet from a source to the destination. Figure 5.10 illustrates the simulation results for the

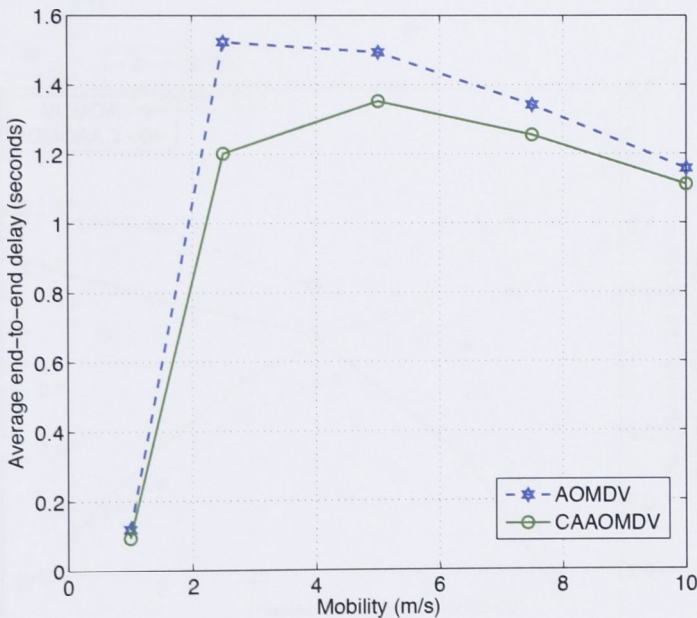


Figure 5.10: Average end-to-end delay comparison between CA-AOMDV and AOMDV with increasing node mobility.

average packet transmission delay for the two protocols. We can see that average end-to-end delay of CA-AOMDV outperforms that of AOMDV, with a maximum 25% improvement at $v = 2.5$ m /s. AOMDV does not consider the link stability or node mobility. Therefore, it may establish paths utilizing fragile links, incurring greater end-to-end delay costs to re-establish new paths. By utilising the ANFD in the path selection metric, CA-AOMDV takes into account the path stability as well as path length to combat fading links. The handoff scheme in CA-AOMDV preemptively switches off the breaking path reducing delays from packet retransmission and timeout

5.6 Simulation Results

from link failures. Again, at both low and high mobilities the advantages of CA-AOMDV are minimized. Further, the initial sharp increase in end-to-end delay for both protocols with increasing mobility is almost certainly due to the more frequently changing link statuses.

Normalized Routing Control Overhead

Normalized routing control overhead is defined as the ratio of the number of routing control packets to the total number of delivered data packets. The overhead results for both routing protocols are plotted in Figure 5.11. It can be seen that the control

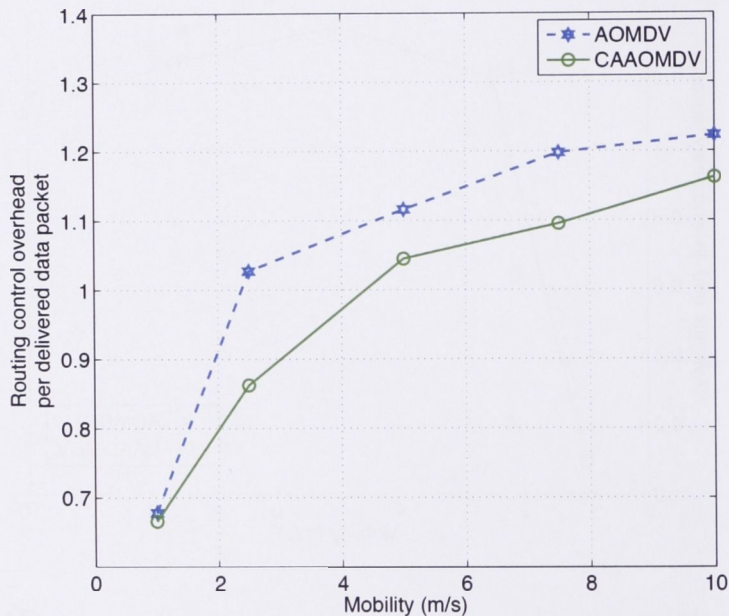


Figure 5.11: Normalized routing control overhead comparison between CA-AOMDV and AOMDV with increasing node mobility. Overhead is normalized with respect to delivered data packets.

overhead for both CA-AOMDV and AOMDV increases with increasing node mobility. This is because the more quickly changing network topology increases the routing update frequency. It can also be seen that CA-AOMDV maintains a lower routing overhead compared with AOMDV. Again, CA-AOMDV has greater performance advantage over AOMDV in the medium mobility range.

5.6.3 Varying Traffic Load

To evaluate the performance of both routing protocols with increasing network traffic load we fixed the maximum node speed at $v = 5$ m/s while varying the packet rate at each source from 1 to 8 packets/second, with a packet size of 512 bytes. Scenarios for the simulation were configured with a 100-node, 25-connection network in a $2200 \text{ m} \times 600 \text{ m}$ terrain. The channel bandwidth is 2 Mb/s. The simulation time is 500 seconds. Figure 5.12 illustrates the network throughput performance for both routing protocols with varying packet rate, while Figure 5.13 shows the normalized routing control overhead for both routing protocols with increasing packet rate. Both routing

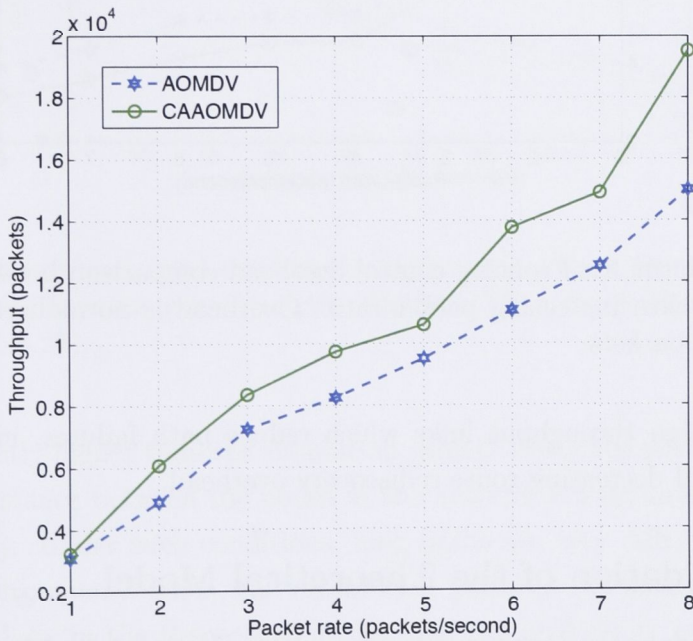


Figure 5.12: Throughput comparison between CA-AOMDV and AOMDV with increasing packet rate.

protocols have increased throughput and decreased control overhead with increasing packet rate. The decrease of control overhead in Figure 5.13 is because, at the same overhead cost to establish a connection, more packets can be transmitted with a higher packet rate. For both network throughput and control overhead, we can see that CA-AOMDV outperforms AOMDV, particularly when the network traffic load is higher. For a packet rate of 8 packets/second, there is over 30% improvement of network throughput and 25% improvement of the normalized routing control overhead. This is due to the channel adaptive mechanism in CA-AOMDV, which causes it to choose

5.6 Simulation Results

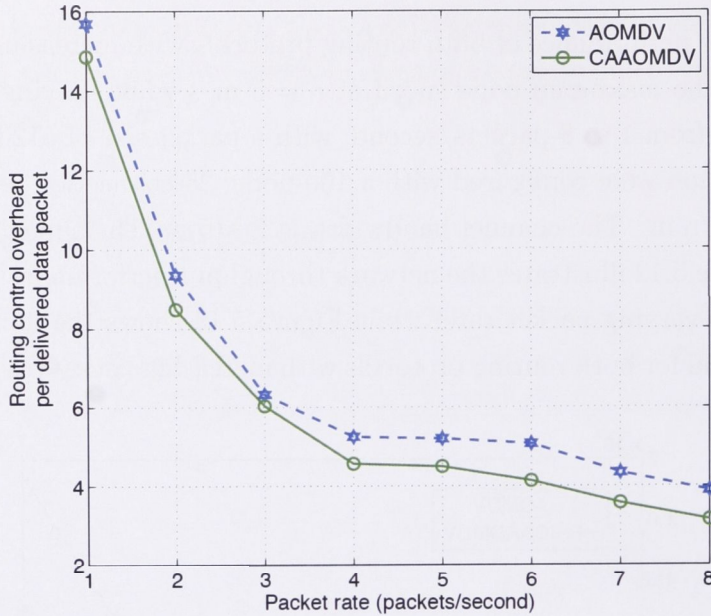


Figure 5.13: Normalized routing control overhead comparison between CA-AOMDV and AOMDV with increasing packet rate. Overhead is normalized with respect to delivered data packets.

long-lasting, high throughput links which reduce path failures, increasing network throughput and decreasing route rediscovery overhead.

5.6.4 Validation of the Theoretical Model

Lastly, we validate the theoretical analysis from Section 5.5 with simulations. Scenarios for the simulation were configured with an 80-node 10-connection random network. The channel bandwidth was 1 Mb/s. The packet rate at each source was 4 packets/second with a size of 1000 bytes. The simulation time was 300 seconds. We varied the network size to change the average node initial distance between two nearest neighbours. With fixed node transmission range, we then varied the velocity of nodes to change the average link lifetime. The average path lifetimes are given by (5.5.9) and (5.5.16). In the simulation, the average path lifetime is increased from 8s to 50s. The theoretical and simulated routing control overhead results for both routing protocols are shown in Figure 5.14. It can be seen that the simulated routing control overhead for both routing protocols match reasonably well with the theoretical results. However, when the path lifetime is very short, the theoretical throughput

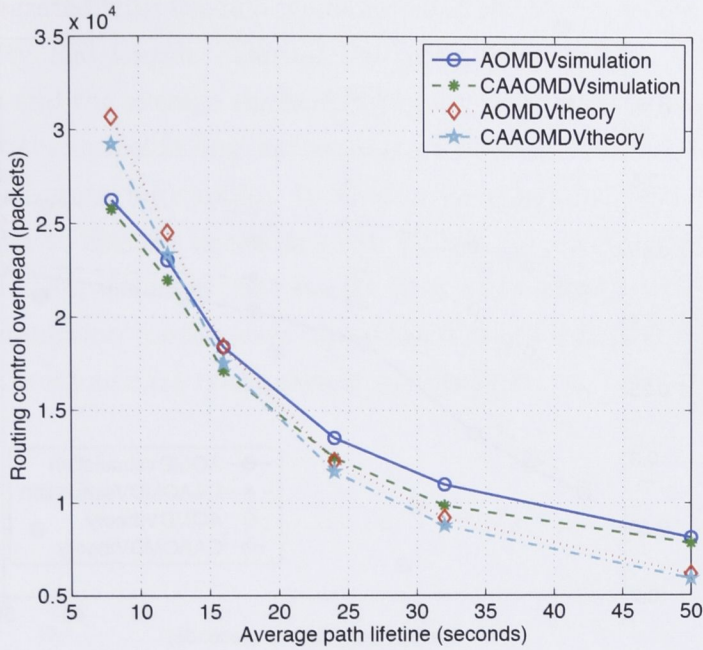


Figure 5.14: Routing control overhead comparison between theoretical and simulated results with increasing average path lifetime. Theoretical values evaluated from (5.5.26) and (5.5.27).

values are slightly higher than the simulation values. When the path lifetime is short, the average distance between the nodes in the network is long and/or the nodes are moving quickly. Under such conditions, long paths are very difficult to establish in a realistic environment. Thus, the established paths in the simulated network are shorter than those in the theoretical model, and the probability of a path breaking in the simulated network is lower than the theoretical value. When the path lifetime is long, we can see that the theoretical throughput values are lower than the simulation values, which may be due to the overhead introduced by interference and packet collisions in the network. CA-AOMDV performs better than AOMDV for both the simulated and theoretical results, as expected.

The results for theoretical and simulated packet delivery ratio for both routing protocols are illustrated in Figure 5.15. Again, CA-AOMDV outperforms AOMDV for both the simulated and theoretical results, as expected. We can see that, although the theoretical results follow the same trend as the simulated results, the former are always higher than the latter, especially when the average path lifetime is lower. The difference between the theoretical and simulated results is due to network inference

5.7 Conclusion

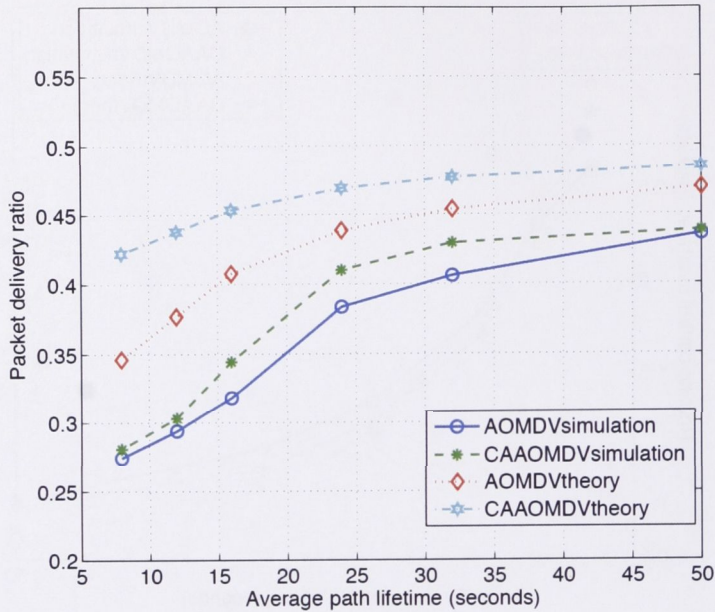


Figure 5.15: Packet delivery ratio comparison between theoretical and simulated results with increasing average path lifetime. Theoretical values evaluated from (5.5.31) and (5.5.32).

and packet collisions. In an adverse environment, with high frequency of broken paths, the packet drop rate and the number of packet retransmissions are relatively high, raising the amount of interference and the number of collisions, incurring greater congestion in the network. The packet drop rate can increase dramatically during congestion. As for previous results with respect to low and high mobility, the PDR performance of AOMDV and CA-AOMDV converge for low and high average path lifetimes.

5.7 Conclusion

Multipath fading in a wireless channel can significantly degrade performance in a wireless MANET. In this chapter, we first propose a channel adaptive routing metric which utilizes the average non-fading duration and aims to select stable links in a mobile wireless environment. Then, based on the proposed routing metric, a channel adaptive routing protocol, Channel Adaptive AOMDV (CA-AOMDV), is proposed. In CA-AOMDV, during the path discovery phase, the average channel non-fading

duration is integrated with the hop-count to select the path which is optimal in terms of both stability and length. During the path maintenance phase, the predicted signal strength and the average channel fading duration are combined with a handoff scheme to combat channel fading and improve radio channel utilization. CA-AOMDV employs channel state information to form a cross-layer architecture, making the network adaptive to changes in the channel. Utilizing channel state information leads to improved routing decisions and results in a more robust network. Theoretical analysis and simulation results show that CA-AOMDV achieves better performance than AOMDV in an adverse transmission environment.

Chapter 6

Multiple Shared Channels Cooperative Routing

The descriptions of two channel-adaptive routing schemes have been presented in Chapter 4 and Chapter 5, respectively. In this chapter, the approach of adopting diversity techniques to resist fading is under investigation. We propose a new diversity-based routing protocol, Multiple Shared Channels Cooperative Routing (MSCC) for Orthogonal Frequency Division Multiplex (OFDM) ad hoc networks. The proposed MSCC protocol has a clustering hierarchy. A bandwidth reuse scheme is applied among the clusters to reduce inter-cluster Co-Channel Interference (CCI). Moreover, within each cluster, a set of subchannels are distributed to cluster members in a non-colliding way, therefore, intra-cluster CCI can be eliminated. At each hop, packets are transmitted cooperatively via selected relays. Generally, MSCC takes advantage of diversity in a multiple shared channel environment, while reducing the CCI. Next, we derive theoretical expressions to analyse the performance of this protocol. The simulation results indicate that the exploitation of diversity leads an increase in throughput. The theoretical analysis is consistent with the simulation results.

The layout of this chapter is as follows. Section 6.1 provides background and motivation of this work. In Section 6.2 we present the system model and network architecture. The proposed routing protocol MSCC is described in Section 6.3. Section 6.4 illustrates the performance analysis of the cooperative system, and simulation results are presented in Section 6.5. In Section 6.6 we draw our conclusions.

6.1 Introduction

Radio transmission is impaired by channel fading which results from multipath propagation. In wireless ad hoc networks, the communication links can vary widely from directly line-of-sight to severely obstructed [27], with each of them fluctuating with the movement of the nodes at the ends of the links or in the surrounding environment. Mostly the links experience independent channel fading [73]. It is of benefit to adopt cooperative transmission [23], in which a packet is forwarded by a number of relays at each hop, to exploit network diversities. A large collection of distributed cooperative transmission schemes has been proposed [21, 104, 51]. In [21], all the nodes that have successfully decoded a packet utilize an orthogonal Space-Time Code (STC) to cooperatively relay that packet. In contrast, the work of [104] proposes a non-orthogonal cooperation scheme. A virtual Multiple Input Multiple Output (MIMO) cooperative routing scheme is proposed in [51]. It turns out that cooperative transmission is able to provide diversity gains on the order of the number of relaying nodes [22].

For cooperative transmission in wireless multihop ad hoc networks, routing and medium access are two problems of significant importance. Absent a central administrator, the networks require a distributed algorithm to select cooperative relays locally. On the other hand, in each cooperative transmission, a number of relays will transmit a packet concurrently, with which contention-based medium access schemes might not be able to cope efficiently. Orthogonal Frequency Division Multiple Access (OFDMA) [105] is based on Orthogonal Frequency Division Multiplexing (OFDM) [24] multicarrier system. It divides a frequency band into multiple orthogonal subcarriers, and then groups them into subchannels. Each user is allocated a particular set of subchannels. Consequently, several users are able to transmit simultaneously using orthogonal multiple shared channels. Thus, OFDMA is inherently suitable for cooperative networks. OFDMA has been widely adopted in many wireless standards, such as IEEE 802.16 [106]. New OFDMA systems have been investigated for wireless local area networks (WLANs) to enhance network performance [107, 108]. Therefore, developing cooperative routing scheme for OFDMA system has practical significance.

6.2 System Model and Network Architecture

6.2.1 System Model

Consider a wireless ad hoc network in which nodes are communicating by using OFDM. The frequency band is divided into K mutually orthogonal subchannels, each with b subcarriers. The subchannel bandwidth is chosen to be smaller than the channel coherence bandwidth, such that each subchannel is subject to flat fading. The fading is assumed to be independently distributed. The transmitted power of each node is fixed and equally distributed to each subcarrier. Thus, for transmission over a distance, r , the received signal power at a given subchannel is exponentially distributed with mean $\bar{\mathcal{P}} = G_0 r^{-\alpha}$ [96], where G_0 is proportional to the transmit power at the subchannel, and α is the path loss coefficient, typically between 2 and 4.

The system runs with fixed-length slots, and each slot consists of three short sub-slots and one long sub-slot. In each slot, a node will generate a data packet with probability q_d to a randomly chosen destination. Each node has a single antenna thus cannot transmit and receive simultaneously. We assume that nodes are effectively stationary during any particular slot, while changing their motion randomly between two slots.

6.2.2 Network Architecture

The proposed routing protocol makes use of geographical information. Similarly to other geographic routing protocols, it assumes that each node is equipped with a Global Positioning System (GPS) [109], such that a node is aware of its geographical location. A node is also able to determine the location of a given node with the aid of a location lookup service [42]. Each node has a unique identity (ID). The clustering architecture of MSCC is developed from that of GRID [110]. As shown in Figure 6.1, the geographical area of the network is divided into a number of two dimensional hexagons, each with a radius of ℓ and representing a cluster. A cluster is uniquely identified by a triple of (a, b, E_j) which means that the cluster centre is located at (a, b) with respect to a given coordinate system, and E_j will be given in Section 6.2.3. Specifically, any given geographical location in the network falls into a particular cluster by following a pre-defined mapping [110]. Each node in the network is equipped with that map. The pre-mapping scheme has practical applications, for

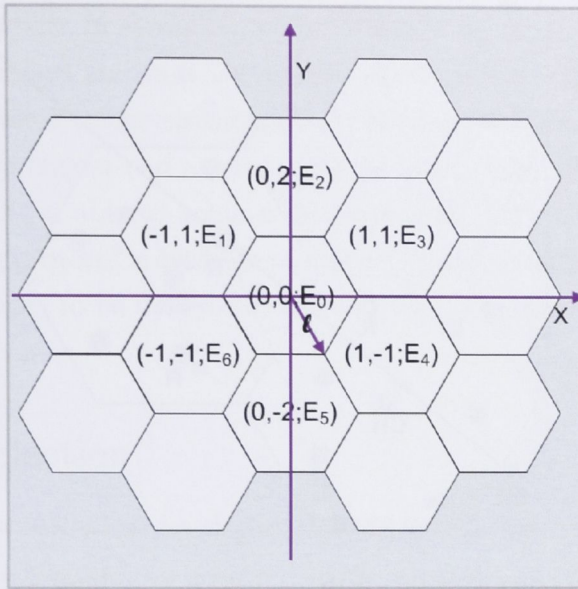


Figure 6.1: OFDMA ad hoc network with clustering architecture. Each hexagon is with a radius of ℓ and represents a cluster. A triple of $(a, b; E_j)$ uniquely identifies a cluster, which means that the cluster centre is located at (a, b) , and the subchannel set allocated to that cluster is E_j , ($j = 0, \dots, 6$).

example, in a disaster recovery which mostly takes place in a fixed site.

6.2.3 Frequency Reuse

Due to the wireless channel is shared by nodes that are within each other's transmission range, adjacent nodes should operate on different subchannels, otherwise co-channel interference (CCI) arises. As the number of nodes increases in an OFDM ad hoc network, CCI will increase and dominates network performance. To reduce inter-cluster CCI, a feasible solution is to apply appropriate bandwidth reuse among the clusters. Adopting a higher reuse factor generates a lower level of CCI; however, it will result in a lower channel usage. We take account of the cluster-by-cluster routing scheme of MSCC to devise a desirable reuse factor. As illustrated by the example in Figure 6.1, cluster $(-1, 1; E_1)$ should not use the same set of subchannels as that of cluster $(1, 1; E_3)$, as nodes in the two clusters might simultaneously forward packets to cluster $(0, 0; E_0)$. Therefore, we adopt a frequency reuse-7 [111] scheme. That is, the shared K subchannels are grouped into seven sets E_j ($j = 0, \dots, 6$), each with $K/7$ subchannels of $[j \times \frac{K}{7}, \dots, (j+1) \times \frac{K}{7} - 1]$. Because the frequency resources

6.3 Multiple Shared Channels Cooperative Routing

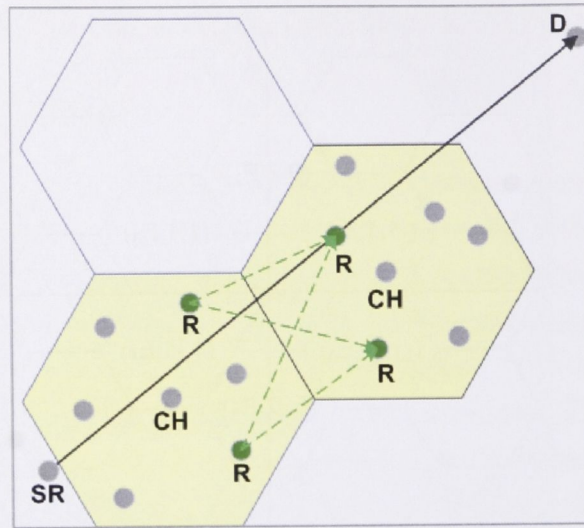


Figure 6.2: Cooperative routing strategy in MSCC, where SR is the source, D is the destination, CHs are cluster heads, R s are relay nodes, and each green line represents a communicating link.

are divided into a group of 7 cells, inter-cluster CCI is avoided in that group. Moreover, within each cluster, intra-cluster CCI is eliminated in the proposed protocol by allocating different subchannels to nodes located in that cluster.

6.3 Multiple Shared Channels Cooperative Routing

As described in Section 6.2, the proposed Multiple Shared Channels Cooperative (MSCC) routing protocol has a clustering architecture. Each cluster has one cluster head (CH) which is responsible for relay selection and subchannel assignment. The CH of a cluster is the node nearest to the cluster's geographical centre, and other nodes that are located in the cluster are cluster members (CMs).

The cooperative transmission in each hop is shown in Figure 6.2, where SR is the source node, D is the destination node, CH is the cluster head, and R is a relay. When a packet is delivered to a cluster that doesn't contain the destination node, the CMs that have received the packet will advertise themselves as candidate relays by sending their channel state information (CSI) to the local CH. Based on the CSIs, the CH will choose several nodes as relays and allocate subchannels to them. The subchannels allocated to each of the relays can be the same to resist time-offset (by

containing a cyclic prefix in symbols), or be different to exploit frequency diversity. Then, the selected relays transmit the packet simultaneously to nodes in the next-hop cluster. As several relays simultaneously forward the packet, consequently, a node at the next-hop cluster can receive multiple independently faded copies of that packet. Thus, MSCC is able to achieve diversity gain. The cooperation capability provides the routing protocol robustness; however, it may lead the total transmission rate between two nodes to be decreased, as two frequencies are now used to transmit redundant information.

6.3.1 Path Selection

A data packet is forwarded to its destination along a pre-selected path by making use of geographical information. When having a packet to deliver, a source node will identify the clusters (e.g., the yellow clusters in Figure 6.2) that compose the path with minimum geometry distance from the source to the destination node by looking up the clustering map. These clusters (including the source cluster) will be selected as routing clusters and contained in the packet header. The packet header will also include the source ID, the destination ID, the transmitting cluster ID, and the transmitting node ID. The packet is routed to the destination along the pre-selected clusters following the order recorded on its header.

6.3.2 Relay Selection Algorithm

We assume that the proposed cooperative routing is regenerative, where each relay decodes, encodes, and forwards a received packet. The relays at each cluster are locally selected by the CH based on the link quality of the relays in term of packet reception rate (or outage probability). Because radio links exhibit threshold effect [7], a constraint is required on the packet reception rate of candidate relays. That is, for a packet delivered from the previous-routing-cluster, only the receivers with packet reception rate, δ_p , exceeding a given threshold, δ_0 , are able to advertise themselves as potential relays.

Moreover, for a candidate relay, i , relay selection criteria should include not only the successful reception rate of a packet at i , but also the probability to successfully transmit the packet from i to next-hop relays. The next-hop packet success probability, δ_n , is given by the probability that instantaneous signal-to-noise-ratio is above a certain threshold γ_{th} , with $\delta_n = \Pr[\frac{\bar{P}}{\mathcal{G}_n} > \gamma_{th}]$, where \mathcal{G}_n denotes the power of AWGN

6.3 Multiple Shared Channels Cooperative Routing

(additive white Gaussian noise) with covariance σ^2 , and $\bar{\mathcal{P}}$ is the average received signal power. Here we ignore the interference. As nodes are uniformly distributed in the network, δ_n can be approximated as the probability to successfully transmit a packet from i to the geographical centre of the next-hop cluster. If the distance from i to the centre of the next-hop cluster is r_i , in the presence of Rayleigh fading, δ_n is given by

$$\delta_n = \exp\left(-\frac{\mathcal{G}_n \gamma_{th}}{G_0 r_i^{-\alpha}}\right) \quad (6.3.1)$$

where \mathcal{G}_n can be estimated by σ^2 . The overall packet reception rate, δ , of the two-hop transmission over i , is

$$\delta = \delta_p \delta_n. \quad (6.3.2)$$

A CH will select, at most, M relays based on their δ values to forward a packet.

6.3.3 Routing Protocol Design

The operation of MSCC consists of two states: cluster head election state, in which CHs are elected; and data transmission state, in which data packets are routed. At the beginning of a slot, if there are no CHs in a cluster, or if there are multiple CHs, the cluster enters cluster head election state. Once a unique CH is elected, the cluster is ready for data transmission and stays in data transmission state.

Cluster Head Election

A node uses Head Advertisement (HA) packet to elect itself as the CH of local cluster. The HA contains the cluster ID and the advertising node ID. In a cluster, if there are no CHs (the CMs don't receive any HA in the first sub-slot of a slot), or if there are multiple CHs (the CMs receive multiple HAs in that sub-slot), from the second sub-slot, each node in the cluster starts to broadcast HAs with a random delay of T_{BD} , with $0 \leq T_{BD} \leq T_{BS} - T_{HA}$, where T_{HA} is the transmission duration of HA, and T_{BS} is the remaining time of that slot. In case there are multiple CHs, only the nodes with a closer location to the cluster centre than that of the CHs participate in cluster head election. HA broadcasting will be lasted until a unique CH is elected. It may occupy several consecutive slots.

Similar to [51], the nodes are assumed to be locally time synchronized in each cluster at the end of this stage. To achieve this, it is proposed that each CH transmits a reference carrier and its CMs lock to this reference carrier using a phase locked loop

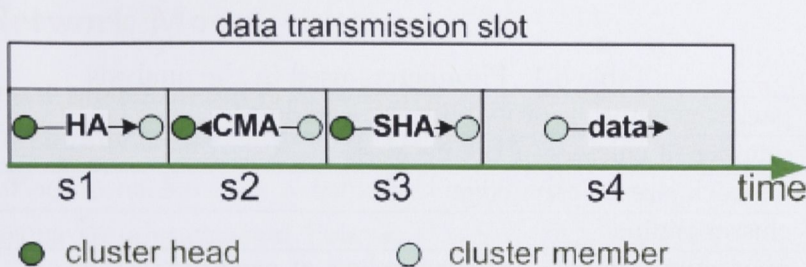


Figure 6.3: The frame of a slot in data transmission state, where s_i $\{i = 1, \dots, 4\}$ represents the i th sub-slot, HA is the head advertisement packet, CMA is cluster member advertisement packet, and SHA is the second head advertisement packet.

[51]. In MSCC, an accurate synchronization can also be conveniently achieved as every node is equipped with a GPS receiver [112]. However, even though a packet is transmitted by cooperating relays synchronously, copies of the packet might arrive at a receiver asynchronously, due to each copy via a different propagation path. It is feasible to mitigate this delay spread by insert a cyclic prefix in OFDM symbols. Another important issue of the cooperative scheme is frequency synchronization. The algorithm presented in [113] can be used to estimate frequency offset in the proposed cooperative system.

Data Transmission

A cluster steady in data transmission state uses the short sub-slots to exchange control messages between the CH and CMs to allow subchannel allocation and relay selection, and transmits data packets in the long sub-slots. The frame of a slot in data transmission state is shown in in Figure 6.3. In particular, at the beginning of the first sub-slot, each CH broadcasts a HA to the CMs in local cluster. A CH will allocate a specific number of subchannels to each of the CMs that it learned previously within a given period of time, and contain the subchannels allocation, the cluster ID, and its own ID in the HA.

Upon overhearing the HA, in the second sub-slot, the CMs will send a Cluster Member Advertisement (CMA) packet to the CH by using the subchannels allocated to them (if allocated) or using randomly selected subchannels that haven't been allocated in the HA. The CMA includes the node ID, the packet ID, the destination node ID, δ_p , the previous-hop cluster (the cluster from which the packet is arriving) head ID, and the next-hop cluster ID. Once the CH gets the CSIs contained in the CMAs, it chooses relays for each packet.

6.4 Protocol Analysis

Table 6.1: Parameters used in the analysis

q_d	packet generation probability at a node
N_c	number of clusters in the network
$2S$	network size on each edge
ℓ	cluster radius
M	maximum number of allowed relays at each hop
N	number of nodes in the network
q_c	collision probability for a given subchannel
K	number of subchannels
δ_h^i	average packet reception rate at the i th selected relay node on hop h
$\delta_{\mathcal{H}}$	average end-to-end packet reception rate
ε	node intensity in the network

Then, at the beginning of the third sub-slot, the CH broadcasts a Second Head Advertisement (SHA). SHA includes the cluster ID, the selected relays, and the subchannels allocated to each of them. As nodes are able to determine the location of a given node with the aid of location lookup service, if the CH identify that there is a CM nearer to the cluster centre than itself, it will change the cluster head to that node, and inform the local nodes in the SHA. Finally, the relays transmit data in the long sub-slot.

Route Maintenance

It is possible that there are no nodes available in a pre-selected routing cluster, resulting in route failure. To repair this failure, after having selected relays for a packet, a CH will send an acknowledgment (ACK) message back to its previous-hop cluster. If an ACK is not received within a particular period of time, the CH of the previous-hop cluster will allow the relays to retransmit that packet. After a given number of unsuccessful retransmissions, the CH will choose a new path in which the broken cluster is removed, to deliver the packet.

6.4 Protocol Analysis

In this section, we present a theoretical performance analysis of the MSCC routing protocol. We list the parameters used in the analysis in Table 6.1.

6.4.1 Network Model

The considered random multiple-hop ad hoc network consists of N nodes independently and uniformly located over a rectangular area \mathcal{L} with length $2S$ on each edge, with the surface considered as a torus. Node distribution in the network is that of homogeneous two-dimensional Poisson Point Process [114] with constant spatial intensity $\varepsilon = N/(2S)^2$. The number of clusters in the network is approximately $N_c = 8S^2/3\sqrt{3}\ell^2$. Thus, each subchannel set, E_j , is applied to a number of $n_c = N_c/7$ clusters. We call a group of clusters that operate on the same E_j subchannel set as co-channel clusters.

6.4.2 Subchannel Collision Probability

First, we calculate the collision probability, q_c , for a given subchannel which will be simultaneously used in two co-channel clusters. Assume the average number of hops that a packet will be propagated to reach its destination is \mathcal{H} . In the proposed network, the maximum number of concurrent traffic flows is about $q_d N M \mathcal{H}$, where q_d is the packet generation probability at each node and M is the number of allowed relays in each hop. In a long term view, these traffic flows will be divided equally into each cluster. Given by the Poisson distribution, the probability of finding at least one node in a cluster with an area V is $1 - e^{-\varepsilon V}$, where ε is the node intensity in the network, given in Section 6.4.1. Thus, for a subchannel k being used in a given cluster, the probability that it is used in a co-channel cluster is

$$q_c = \begin{cases} \frac{(1-e^{-\varepsilon V})^7 q_d N M \mathcal{H}}{N_c K}, & u < K/7 \\ 1 - e^{-\varepsilon V}, & u \geq K/7 \end{cases} \quad (6.4.1)$$

where u is the average number of traffic flows in each cluster, with $u = q_d N M \mathcal{H} / N_c$, and N_c is the number of clusters in the network.

The average path length is the average Euclidean distance between the randomly chosen sources and destinations on the torus. In a network where the nodes are uniformly distributed, it can be shown that the average distance between a randomly chosen source and a destination node is $\frac{S}{3}[\sqrt{2} + \ln(1 + \sqrt{2})]$ [94]. With regard to the proposed clustering network architecture, the average number of hops between a source and a destination node is approximate $\mathcal{H} = \frac{S}{3\sqrt{3}\ell}[\sqrt{2} + \ln(1 + \sqrt{2})]$, in which the average transmission distance of each hop is approximated as the distance between the geographically central points of two neighbouring clusters, which is $\sqrt{3}\ell$.

6.4.3 Location Distribution of the Co-channel Transmitters

Given Poisson point process assumption, the location of a node in the network is independent and identically distributed (i.i.d.) on \mathcal{L} . Due to the spatial invariance on a torus [114], we can assume that the desired receiver, Rx, is located at the centre of the network, say, the point of $(0,0)$ with respect to the coordinate system. The potential desired transmitter, Tx, can be located at the same cluster as Rx, or at any one-hop adjacent cluster. Considering the cluster-to-cluster routing scheme, we assume that Tx is located at a neighbouring cluster.

Assume the centre of cluster \mathcal{C}_t , $\{t = 1, \dots, N_c\}$ (N_c is the number of clusters in the network), is (ρ_t, θ_t) (in an angular coordinate system), where ρ_t is the distance from the centre of \mathcal{C}_t to the centre of the torus $(0,0)$. Each $\mathcal{C}_t \subset \mathcal{L}$ is approximated as a circle with radius ℓ . In case Tx is located in \mathcal{C}_t , its location is uniformly distributed within \mathcal{C}_t . Using random variable Z denotes the distance between Rx and Tx, the CDF of Z can be written as

$$\begin{aligned} F_Z(z) &= \underbrace{\int \int}_{\mathcal{C}_t, \rho \leq z} \frac{1}{V} d\rho d\theta \\ &= \frac{\Lambda(z)}{V}, \quad |z - \rho_t| \leq \ell, \quad z \leq \sqrt{2}S \end{aligned} \quad (6.4.2)$$

where V is the area of a cluster, ℓ is cluster radius, and S is the half length of a network size. In case that the whole circle of \mathcal{C}_t is located within \mathcal{L} , we can get $V = \pi\ell^2$, and $\Lambda(z) = z^2 \cos^{-1} \left(\frac{\rho_t^2 + z^2 - \ell^2}{2\rho_t z} \right) - \frac{1}{2} \sqrt{(-\rho_t + \ell + z)(\rho_t + \ell - z)(\rho_t - \ell + z)(\rho_t + \ell + z)} + \ell^2 \cos^{-1} \left(\frac{\rho_t^2 + \ell^2 - z^2}{2\rho_t \ell} \right)$, with $0 \leq r \leq \sqrt{2}S$. Taking the derivative of $F_Z(z)$ with respect to z , it can be shown that the PDF of z is

$$f_Z(z) = \frac{\Lambda'(z)}{V}, \quad |z - \rho_t| \leq \ell, \quad z \leq \sqrt{2}S \quad (6.4.3)$$

with $\Lambda'(z) = \frac{\sec \left[\frac{-\ell^2 + \rho_t^2 + z^2}{2\rho_t z} \right] \left(4\rho_t z + (\ell^2 - \rho_t^2 + z^2) \tan \left[\frac{-\ell^2 + \rho_t^2 + z^2}{2\rho_t z} \right] \right)}{2\rho_t} + \frac{\ell z \sec \left[\frac{\ell^2 + \rho_t^2 - z^2}{2\ell\rho_t} \right] \tan \left[\frac{\ell^2 + \rho_t^2 - z^2}{2\ell\rho_t} \right]}{\rho_t} - \frac{z(\ell^2 + \rho_t^2 - z^2)}{\sqrt{(\ell + \rho_t - z)(\ell - \rho_t + z)(-\ell + \rho_t + z)(\ell + \rho_t + z)}}$. If a cluster is only with partial of the circle in the network, $f_Z(z)$ can be obtained by taking the derivative from the $\Lambda(z)$ of that cluster.

6.4.4 Average Packet Reception Rate on a Subchannel

Now we calculate the average packet reception rate on a given subchannel in each single link. Packet transmission is impaired by the accumulated CCI from all the simultaneously transmitting co-channel interferers. In the proposed cooperative system, intra-cluster CCI is eliminated. The independently distributed fading assumption and fair channel allocation imply that each subchannel experiences equal average interference. Based on the frequency reuse scheme described in Section 6.2.3, for a given transmitting subchannel k , there should be at most one co-channel interferer in each co-channel cluster, and at most n_I co-channel interferers $\{h_1, h_2, \dots, h_{n_I}\}$ in the network, where $n_I = n_c - 1$, and n_c is the number of co-channel clusters for each subchannel set E_j .

Packet reception rate for a subchannel is related to a particular SINR (signal-to-interference and noise ratio), γ , requirement. Similar to [115], the packet successful transmission probability conditioned on $\{h_1, h_2, \dots, h_{n_c}\}$ is

$$\begin{aligned} P_s\{h_1, h_2, \dots, h_{n_c}\} &= \Pr[\gamma \geq \gamma_{th}] \\ &= \exp\left(-\frac{\gamma_{th}\mathcal{G}_n}{G_0 r_0^{-\alpha}}\right) \prod_{t=h_1}^{h_{n_c}} \left(1 - \frac{\gamma_{th}q_c}{\gamma_{th} + \left(\frac{r_t}{r_0}\right)^\alpha}\right) \end{aligned} \quad (6.4.4)$$

where r_0 is the distance between the desired transmitter and the receiver, r_t is the distance between interferer t and the receiver, and γ_{th} is the signal-to-noise-ratio threshold.

Because the random distribution of node position, integrating (6.4.4) with respect to node location probability density function f_{r_i} in (6.4.3), we obtain the average packet reception rate on a path, or path throughput, \bar{P}_s , in a given subchannel as

$$\begin{aligned} \bar{P}_s &= \int_{\rho_0-\ell}^{\rho_0+\ell} \dots \int_{\rho_{h_c}-\ell}^{\rho_{h_c}+\ell} P_s\{h_1, \dots, h_{n_c}\} dr_0 \dots dr_{h_c} \\ &= \int_{\rho_0-\ell}^{\rho_0+\ell} \exp\left(-\frac{\gamma_{th}\mathcal{G}_n}{G_0 r_0^{-\alpha}}\right) \\ &\quad \times \prod_{t=h_1}^{h_c} \int_{\rho_t-\ell}^{\rho_t+\ell} \left(1 - \frac{\gamma_{th}q_c}{\gamma_{th} + \left(\frac{r_t}{r_0}\right)^\alpha}\right) f_{r_0}(r_0) f_{r_t}(r_t) dr_t dr_0 \end{aligned} \quad (6.4.5)$$

where ρ_i is the distance from the torus centre $(0, 0)$ to the centre of the cluster in which node i is located.

6.4.5 Average End-to-End Packet Reception Rate

First, we calculate the average packet reception rate at each (single-hop) cooperation transmission, and single receiver is considered. In the proposed system, each intermediate node Rx at hop h , $\{1 < h \leq \mathcal{H}\}$, can receive at most M i.i.d. faded copies of a packet from different transmitters Tx_i , $\{1 \leq i \leq M\}$, in previous-hop cluster. Assume selection diversity [116] is adopted at the receiver to pick the signal with maximum SINR for decoding. Using random variable β denotes the selected signal, with $\beta = \mathbf{max}(\gamma_1, \dots, \gamma_M)$, where γ_i is the SINR of the signal from Tx_i . Assume γ_i is independent and identically distributed, the CDF (cumulative density function) of β is given by

$$\begin{aligned} F_\beta(x) &= F_\gamma^M(x) \\ F_\gamma(x) &= 1 - \bar{P}_s \end{aligned} \quad (6.4.6)$$

where M is the maximum number of allowed relays in each hop, and \bar{P}_s is given in (6.4.5).

Now we consider the average packet reception rate of end-to-end cooperative transmission. With regrade to the proposed cooperative system, the average number of nodes in each cluster is $n_d = \varepsilon V$, where ε is the node density. The cluster head chooses M relays with best SINRs from the n_d nodes, and each relay transmits the packet with different accumulated packet error rate. Using random variable ξ_i represents the SINR of the i th best relay node in the cluster, $\{1 \leq i \leq M\}$, e.g., $\xi_1 = \mathbf{max}(\beta_1, \dots, \beta_{n_d})$. The CDF of ξ_i is given by

$$F_{\xi_i}(x) = F_\beta^{n_d - i + 1}(x). \quad (6.4.7)$$

The average packet reception rate, δ_h^i , at the i th selected relay node at hop h , is

$$\begin{aligned} \delta_h^i &= \frac{\sum_{m=1}^M \delta_{h-1}^m}{M} (1 - F_{\xi_i}(x)) \\ &= \frac{\sum_{m=1}^M \delta_{h-1}^m}{M} (1 - F_\gamma^{M(n_d - i + 1)}(x)). \end{aligned} \quad (6.4.8)$$

At the first hop with $h = 1$, δ_1^i is given by

$$\delta_1^i = 1 - F_\gamma^{n_d - i + 1}(x). \quad (6.4.9)$$

At the destination, where $h = \mathcal{H}$, the average end-to-end packet reception rate, $\delta_{\mathcal{H}}$,

Table 6.2: Simulation parameters for OFDMA physical layer

number of subchannels	128
number of subcarriers in each subchannels	1
FFT size	128
Modulation	QPSK
Path loss coefficient (α)	2
Symbol rate per carrier	250ksymbol/sec
Packet length	512 bits
Doppler frequency	150 Hz
Channel fading	flat fading

is given by

$$\delta_{\mathcal{H}} = \frac{\sum_{m=1}^M \delta_{\mathcal{H}-1}^m}{M} (1 - F_{\gamma}^M(x)). \quad (6.4.10)$$

6.5 Simulation Results

We developed simulation scenarios in Matlab to evaluate the performance of the proposed cooperative system. Nodes were uniformly distributed over a 1500m \times 1500m area. In each slot, a node generated a data packet with a probability of $q_d = 1\%$, to a randomly chosen destination node. The C/I (carrier-to-noise) was given as the ratio of the received signal power on a given subcarrier when the receiver was located 250m away from the transmitter to that of the noise. The maximum number of relays at each hop was $M = 3$. We assume nodes are synchronized in time and frequency. The parameters of OFDMA are shown in Table 6.2. Each scenario was run for 5 seconds, and repeated for 100 rounds.

6.5.1 Approximate for Theoretical Analysis

We numerically evaluated the average end-to-end packet reception rate of the proposed cooperative system based on (6.4.10). Because sometimes it is difficult to get a close form of (6.4.3), in the simulations, we approximated that the average location of a node was at its cluster centre, to calculate the theoretical values.

6.5 Simulation Results

Varying C/I

The number of nodes and cluster radius were fixed at 100 and 145m, respectively. We increased C/I from 2 to 10 dB to evaluate the average end-to-end packet reception rate, $\delta_{\mathcal{H}}$, using (6.4.10). The theoretical and simulation results of $\delta_{\mathcal{H}}$ are plotted as a function of C/I in Figure 6.4. The figure shows an improvement on $\delta_{\mathcal{H}}$ with increasing

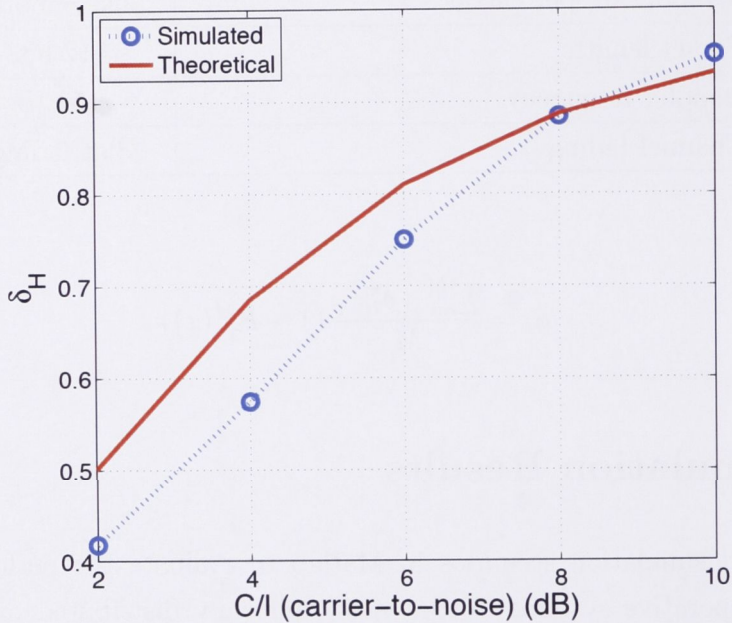


Figure 6.4: Average end-to-end packet reception rate, $\delta_{\mathcal{H}}$, comparison between theoretical and simulated results with increasing C/I from 2 to 10 dB, where the theoretical values were evaluated from (6.4.10).

C/I, and the theoretic values are approximately matched with the simulated ones.

Varying Cluster Radius

Then, we fixed C/I at 4 dB while varied cluster radius from 60 to 300 m. There were 250 nodes in the network. Figure 6.5 displays $\delta_{\mathcal{H}}$ vs. cluster radius for both theoretical and simulation results. It can be seen that the theoretic values are closely matched with the simulated ones.

Figure 6.5 also illustrates that if cluster size is too small or too large, $\delta_{\mathcal{H}}$ will drop dramatically. This is because that $\delta_{\mathcal{H}}$ is determined by average packet success rate at each hop and the average number of hops to deliver packets to destinations. If

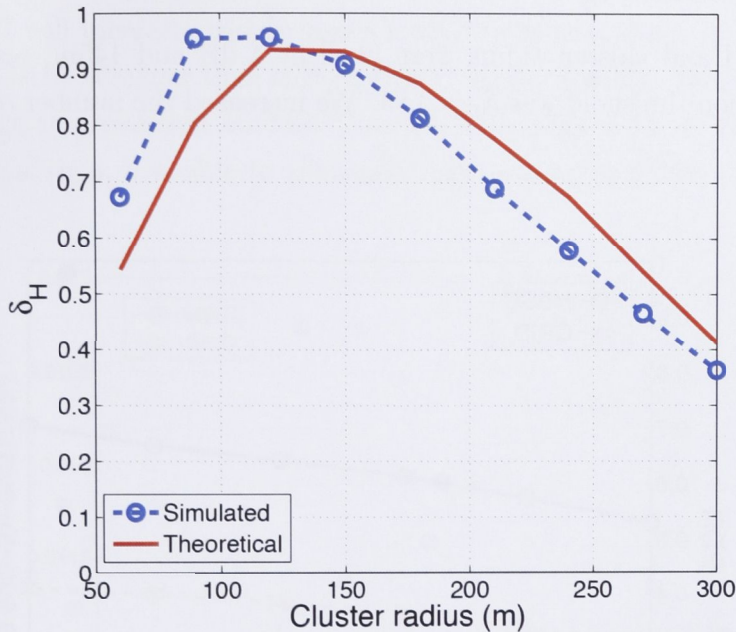


Figure 6.5: Average end-to-end packet reception rate comparison between theoretical and simulated results with increasing cluster radius from 60 to 300 m, where the theoretical values were evaluated from (6.4.10).

the cluster radius is too small, though single-hop reception rate of a packet is high, the packet will be transmitted via more hops to reach the destination. Moreover, decreasing cluster size will reduce the available relays at each cluster, and increase the number of co-channel clusters as there are more clusters in the network to share the bandwidth. However, if the cluster radius is too large, single-hop packet propagation distance is long, resulting in low packet reception rate at each transmission.

6.5.2 Comparing MSCC with GRID

We implemented the GRID protocol [110] into the OFDM multicarrier system to compare its performance with that of MSCC. In the simulations, the maximum number of retransmission at each hop was 2. We considered the following properties to assess the performance of routing protocols: (1) Packet delivery ratio (PDR), which is the ratio of the number of data packets successfully received at the destinations to the number of data packets generated by the sources; (2) Average end-to-end delay, which is the average time taken to transfer a data packet from a source to a destination.

6.5 Simulation Results

Varying node density

First, the C/I and cluster radius were fixed at 4 dB and 145m, respectively. The packet reception threshold was $\delta_0 = 0.85$. We increased the number of nodes from 80 to 280.

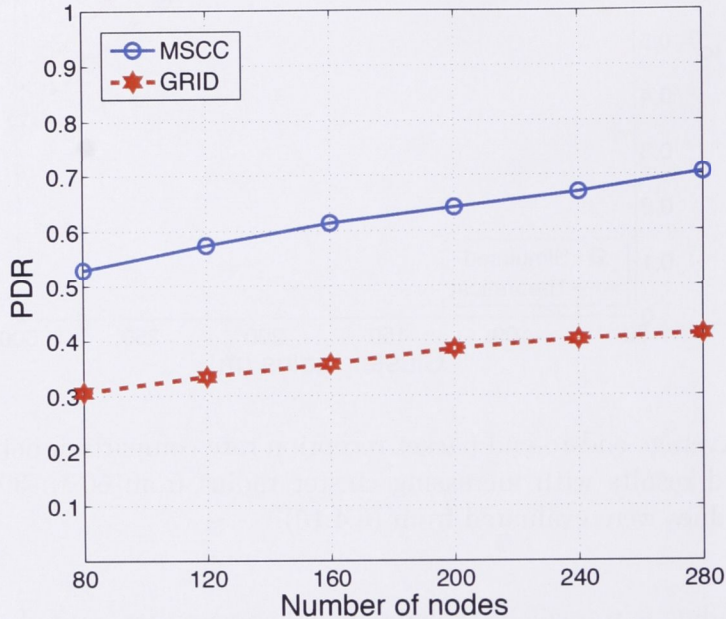


Figure 6.6: PDR comparison between MSCC and GRID with increasing nodes in the network from 80 to 280.

In regard of PDR plotted in Figure 6.6, MSCC outperforms GRID, especially in the scenarios with higher node density. We can notice an improvement of approximate 75% in the PDR of network using MSCC. Thus, MSCC is able to achieve diversity gain. Figure 6.6 also illustrates an increase on PDR with the rise of node density in both protocols, due to the presence of more sources of diversity in the network.

Figure 6.7 plots the average end-to-end delay against the number of nodes. It can be seen that when the number of nodes is smaller (than 100), GRID has a lower average end-to-end delay than that of MSCC. In low node density scenarios, the available nodes in each cluster are very small, which leads to a low probability of packet success reception. Thus, only the packets propagated via paths with short-length can reach their destinations. The reduction of path length contributes to the low packet delay in GRID. As node density increases, the average packet delay in

both protocols rises rapidly. This is because that, when more nodes are present in the network, CCI will increase, which causes a high retransmissions. In these scenarios, the delay of GRID is higher than that of MSCC. In the scenario with 280 nodes, there is about a 10% improvement for MSCC over GRID. This is due to MSCC employing multiple relays, thus, it is able to efficiently resist fading and CCI.

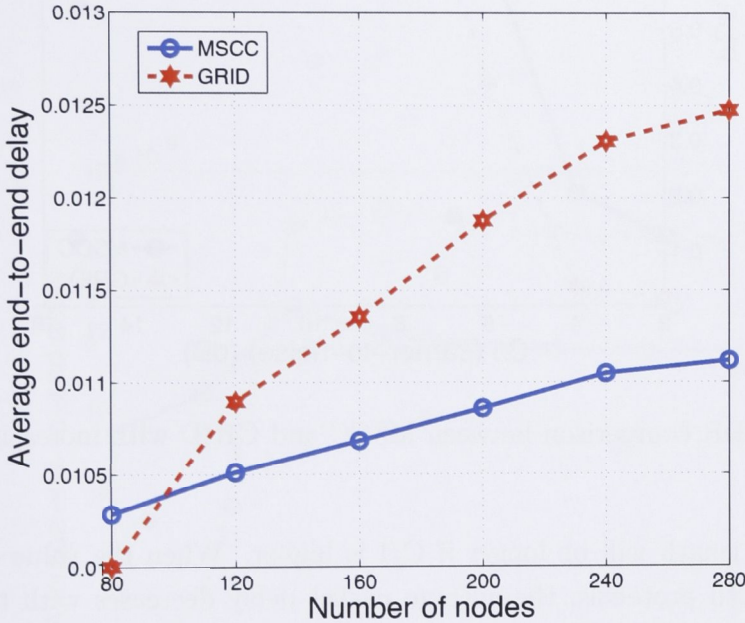


Figure 6.7: Average end-to-end delay comparison between MSCC and GRID with increasing nodes in the network from 80 to 280.

Varying C/I

Then, we fixed 250 nodes in the network, while increased C/I from 2 to 16 dB. The cluster radius was 120m, and the packet reception threshold was $\delta_0 = 0.95$. The PDR and average end-to-end delay are plotted in Figure 6.8 and Figure 6.9, respectively.

Figure 6.8 shows that higher C/I yields higher PDR, because increasing C/I can improve packet success probability. Generally, MSCC outperforms GRID. When C/I = 6 dB, there is about a 60% improvement for MSCC over GRID. This contributes to its capability to exploit network diversities.

When C/I is low, Figure 6.9 shows that increasing C/I leads to a longer delay for both protocols. This is because that, in lower (than 6 dB in Figure 6.9 C/I conditions,

6.6 Conclusion

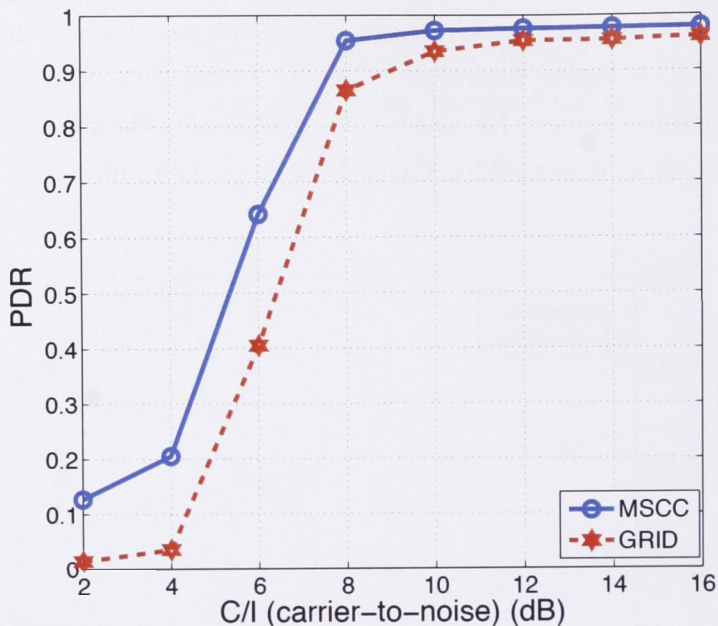


Figure 6.8: PDR comparison between MSCC and GRID with increasing C/I from 2 to 16 dB.

average path length will be longer if C/I is higher. When the value of C/I is high enough, in both protocols, the average packet delay decreases with the increase of C/I. This is due to increasing C/I can improve packet success rate and reduce the number of retransmissions. In comparison with MSCC, GRID has a lower delay when C/I is lower (than 5 dB), due to GRID has a shorter average path length. However, in high C/I scenarios, the delay in GRID is higher than that of MSCC. When C/I is 8 dB, there is about a 20% improvement for MSCC over GRID.

6.6 Conclusion

We have proposed a Multiple Shared Channels Cooperative (MSCC) routing protocol for OFDMA wireless networks. MSCC allows cooperative packet transmission to exploit network diversities. Moreover, a clustering infrastructure is combined with bandwidth reuse to reduce co-channel interference (CCI). The simulation results show that MSCC is able to improve packet delivery ratio and average end-to-end delay.

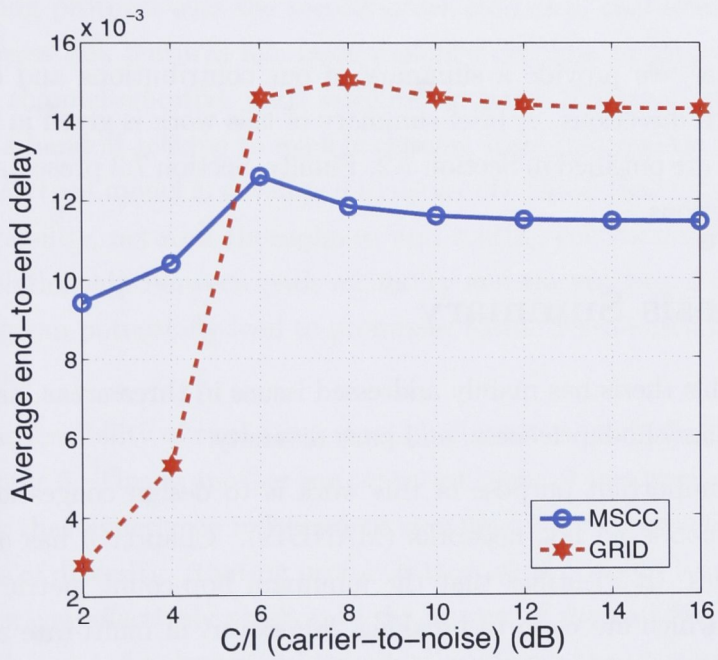


Figure 6.9: Average end-to-end delay comparison between MSCC and GRID with increasing C/I from 2 to 16 dB.

Chapter 7

Conclusions and Future Work

In this chapter, we provide a summary of our contributions and discuss potential future research directions. A brief summary of this work is given in Section 7.1. Our contributions are outlined in Section 7.2. Finally, Section 7.3 presents other promising research directions.

7.1 Thesis Summary

Research in this thesis has mainly addressed issues in three areas, namely congestion awareness, channel adaptiveness, and path diversity.

The first important purpose of this work is to design congestion-aware routing schemes for mobile ad hoc networks (MANETs). Chapter 3 has analysed existing routing metrics. It identifies that the minimum hop-count metric tends to favour fragile paths which are close to breaking. Moreover, in multi-rate ad hoc networks, the long term per packet fairness feature of IEEE 802.11 DCF leads to the solution of giving priority to higher data-rate links to build a route. However, this approach will prefer selecting paths with a greater number of short-distance hops. The increased number of hops can result in an increase in channel access contention. Thus, it is necessary to provide awareness of congestion to avoid bottleneck regions. Chapter 3 has presented a new routing approach which tackles congestion via several approaches, taking into account causes, indicators and effects. The simulation results demonstrate that the resulting protocol can improve network performance in a variety of situations due to its adaptability to congestion.

The second purpose of the thesis is to investigate the interrelationship between path reliability and channel fading. The traditional solutions to multihop routing problems in MANETs are mostly based on knowledge of topology which is built by

assigning each link with a cost of “1” or “0”, which is generally directly related to the link geometric distance. This model neglects the impact of channel variations. However, in MANETs, network connectivity is inexorably linked to channel fading. Both Chapter 4 and Chapter 5 have addressed the issue of reliable path selection based on channel-adaptive schemes. Chapter 4 has proposed to measure link reliability by incorporating the impacts of large-scale and small-scale fading. The simulation results show that the routing protocol implemented with the proposed metric can cope well with channel unreliability and achieve higher network performance than the conventional topology-based routing protocols. Next, in Chapter 5, the proposed channel-adaptive routing protocol uses the second-order statistical characteristics of channel fading to address link features like node mobility and link distance. In addition to adopting the channel-adaptive path selection in route discovery, the protocol also makes use of a handoff scheme to exploit channel state information in route maintenance. An analytical model is developed to derive the theoretical expressions for path breakage probability, network throughput, and routing control overhead. The study on the interrelationship between path reliability and the statistical characteristics of channel fading can potentially lead to promising future research on channel-adaptive routing schemes.

Finally, the feasibility of exploiting network diversities to combat fading is investigated in Chapter 6. This is another important purpose of this work. The presence of multiple users that experience independent channel fading means that MANETs are rich in sources of diversity. Routing protocols that allow cooperative transmission via multiple relays can effectively ameliorate the impact of channel fading. Particularly, Chapter 6 makes use of a clustering hierarchy to perform local relay selection and dynamic channel assignment. Then, at each hop, packets are transmitted cooperatively by several relays via different subchannels. A theoretical analysis is then presented to model the behaviours of the protocol. The simulation results demonstrate that it achieves diversity gains across a variety of scenarios. The theoretical analysis is consistent with the simulation results. It is expected that these channel-aware designs will give insights on future studies in MANETs.

7.2 Thesis Contributions

In this thesis, we mainly focus on designing congestion-aware routing protocols and channel-aware routing protocols. Specifically, we have made the following original

7.2 Thesis Contributions

contributions:

- We have introduced a congestion-aware routing metric, the Weighted Channel Delay (WCD), which employs data transmission delay, the Media Access Control (MAC) overhead and buffer queuing delay, to give preference to less congested high throughput links.

Then we have proposed the Congestion-Aware Routing protocol for MANETs (CARM). The new routing approach tackles congestion via several approaches, taking into account causes, indicators and effects. The localised routing decisions support to diffuse traffic evenly among the nodes to combat congestion. The simulation results demonstrate that CARM can improve network performance across a wide range of scenarios due to its adaptability to congestion.

- Secondly, we have proposed an innovative channel-adaptive routing metric, the Effective Link Operation Duration (ELOD), which particularly considers link reliability. Applying the ELOD as a routing metric can address node mobility as well as channel fading.

We then incorporated the ELOD into a routing protocol to perform channel-adaptive routing. The simulation results show that the routing protocol combined with the channel-adaptive metric can cope well with the channel unreliability in a variety of scenarios, and achieve higher network performance than the conventional topology-based routing protocols.

- Thirdly, we have designed a novel channel-adaptive routing protocol which extends the Ad-hoc On-Demand Multipath Distance Vector routing protocol (AOMDV) [31] with multiple channel adaptation schemes to fully exploit channel state information and improve routing decisions. Specifically, the proposed routing protocol, Channel-Aware AOMDV (CA-AOMDV), attempts to improve path stability by making use of the CSI in both route discovery and route maintenance phases.

Furthermore, we have developed an analytical model for MANETs. This model derives the theoretical expressions of routing control overhead and throughput for both AOMDV and CA-AOMDV. Simulation results show that CA-AOMDV can improve network performance in terms of packet delivery ratio, routing control overhead, and end-to-end packet delay, by decreasing the amount of path re-establishment. The simulations verify the theoretical results.

- The final contribution of this thesis is to propose a new diversity-based routing protocol, Multiple Shared Channels Cooperative Routing (MSCC). MSCC makes use of a clustering hierarchy and a bandwidth reuse scheme to reduce the CCI. In MSCC, packets are transmitted cooperatively: at each hop there are several relays simultaneously attending packet forwarding via different sub-channels. The protocol takes advantage of diversity in a multiple shared channel environment.

We then derive theoretical expressions to analyse the performance of this protocol. The simulation results demonstrate that MSCC can improve network performance.

7.3 Topics for Future Research

This section provides promising future research that can be directed from the work presented in this thesis.

- The proposed congestion-aware routing protocol solely uses information from the MAC layer to mitigate congestion. However, the measurement of congestion status involves various parameters (buffer size, channel occupation, packet drop rate, etc.), and congestion control mechanisms should be present in multiple layers (the data link layer, the application layer, etc.). It is beneficial to enhance the current congestion-aware routing protocol to react to congestion measurement from more layers, or to combine the routing scheme flexibly with congestion control mechanisms from other layers. Potentially more effective congestion management solutions are available by merging information from multiple layers.
- Channel adaptation is very environment-sensitive. That is, not all networks that use the same channel-adaptive scheme have the same performance, and different network conditions should use different adaptive schemes. Thus, various channel-adaptive schemes should be developed to meet the specific needs of particular types of networks. The theoretical model for path break probability can be used to indicate whether a channel-adaptive routing protocol can improve the performance of a particular network. In the proposed model, the analysis is only applied to the networks with independently flat fading links. Further research can be carried out for other channel models.

7.3 Topics for Future Research

- The proposed channel-adaptive schemes make use of channel state information to choose the best relays. Routing efficiency is greatly dependent on an accurate description of channel statistics. How often the channel statistics varies with node movement, and how long the statistics remains valid, are of great importance to the performance of channel adaptation schemes. It is necessary to develop research on these issues.
- Diversity is a promising technique to combat fading. The proposed scheme exploits multi-user diversity and frequency diversity. However, MANETs are inherently abundant in sources of diversity. It is attractive to devise enhanced routing mechanisms to achieve more diversity gain.
- We have proposed congestion-aware and channel-aware (including channel-adaptive and diversity-based) routing schemes to combat congestion and channel fading, respectively. Since both congestion control and accommodation of fading are major concerns in routing protocol design, it is appealing to integrate the various concepts (e.g., congestion control, channel-adaptive and diversity schemes) proposed in this work into a single routing framework, to improve routing efficiency. Such a routing framework can have applications in a wider range of network scenarios. Moreover, it is a more suitable routing solution for future MANETs which are built on next generation wireless communications systems. Future networks will have more massive traffic flows (e.g., new multimedia services and video on demand) and higher bandwidth, thus, they are more vulnerable to congestion and multi-path fading. In these environments, congestion mostly happens concurrently with channel fading.

There are a couple of practical issues involved in designing such a framework. First, the routing framework should be a multi-dimensional function of various factors including congestion information, CSI, diversity information, and so on. Such an integrated framework will be required to collect the massive volume of information. Therefore, it will incur a number of control messages. Secondly, the impact of each factor on network performance will be different, and there are interactions among these factors, thus, the weighted coefficient for each factor should be carefully decided.

Appendix A

Review of OFDMA

Orthogonal Frequency Division Multiplexing (OFDM) [117, 118] is a spectrally efficient digital modulation technique that splits a frequency band into a set of mutually orthogonal narrowband subcarriers, so as to transform a frequency selective fading channel into multiple flat fading channels. Data symbols are transmitted on these subcarriers in parallel. Moreover, each OFDM symbol is extended in length by containing a cyclic prefix (CP) to compensate for intersymbol interference (ISI) on a multipath channel. Consequently, the ability to resist multipath fading and narrow-band interference supports OFDM to be a promising candidate for future mobile communication systems. An illustration of a baseband OFDM system is shown in Figure A.1.

The Orthogonal Frequency Division Multiple Access (OFDMA) [119, 120] builds on OFDM. It groups the multiple subcarriers into subchannels, and allows a user to use all the subcarriers (as in OFDM), or only a particular set of subcarriers. In OFDMA ad hoc networks, a node may utilize a particular set of subchannels that with good channel conditions, and leaving the rest for use by other neighbouring nodes. By providing multiple orthogonal subchannels in each link, OFDMA takes a multi-radio advantage with a single radio [24]. Combining with dynamic subchannel allocation, OFDMA can be used to exploit frequency diversity. However, in MANETs, as the radio is shared among the nodes, a larger number of nodes mean higher co-channel interference (CCI), which results from the simultaneous transmissions using the same subchannel.

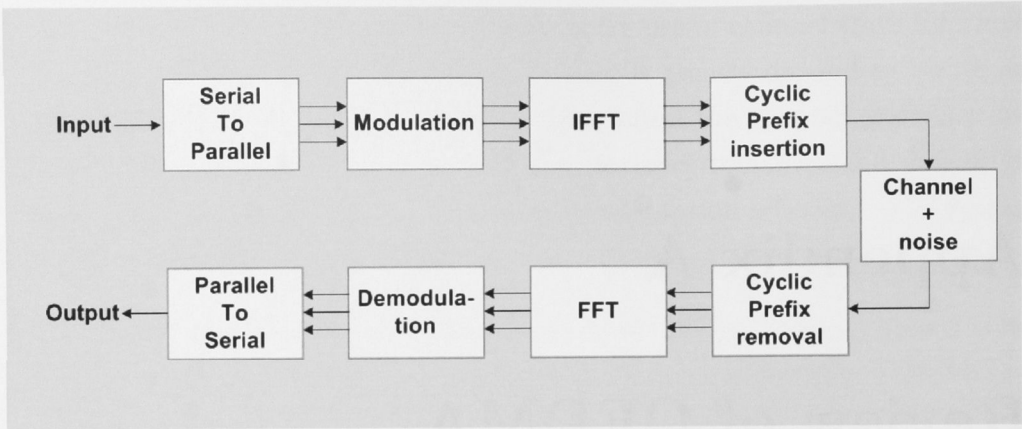


Figure A.1: A Baseband OFDM system

A.0.1 OFDMA Modulation

In this section, we briefly describe the OFDMA modulation scheme, based on the model in [121, 122]. First, we illustrate some descriptions in this section:

- Bold letter: denotes matrix or column vector,
- $(\cdot)^T$: transpose,
- $(\cdot)^H$: Hermitian transpose,
- I_N : the $N \times N$ identity matrix,
- $[\mathbf{A}]_{ij}$: the (i, j) th entry of a matrix \mathbf{A} ,

In OFDMA ad hoc networks, a node can communicate simultaneously with several neighbouring nodes. Assume ψ_l is the number of subcarriers allocated to subchannel l , and ϕ_b is the set of nodes with which a node, b , communicates. A size up to $K = \sum_{l \in \phi_b} \psi_l$ subcarrier sequence is passed to a serial-to-parallel (S/P) converter of b , which maps the sequence to transmitting signal vector $\mathbf{u}^b[n]$, with $\mathbf{u}^b[n] = (u^b[n, 1], \dots, u^b[n, K])^T$, where n denotes the discrete time.

The transmitting vector is then processed by a K -point discrete-time inverse Fourier transform (IFFT) and the IFFT operation at node b can be depicted in matrix form as

$$\tilde{\mathbf{u}}^b[n] = \mathbf{F}^H \mathbf{u}^b[n] \quad (\text{A.0.1})$$

where $\tilde{\mathbf{u}}^b[n] = (\tilde{u}^b[n, 1], \dots, \tilde{u}^b[n, K])^T$, and \mathbf{F} is the $K \times K$ FFT (fast Fourier transform) matrix with $[\mathbf{F}]_{wk} = \frac{1}{\sqrt{K}} \exp(-j2\pi \frac{wk}{K})$, $\{w, k = 1, \dots, K\}$. Next, the cyclic

prefix is incorporated and this extended sequence is mapped by a parallel-to-serial (P/S) converter before being transmitted over the wireless channel.

Bibliography

- [1] D. Cox, "Portable digital radio communications-an approach to tetherless access," *IEEE Communications Magazine*, pp. 30–40, July 1989.
- [2] R. Prasad, *Universal Wireless Personal Communications*. Boston, London: Artech House Publishers, 1998.
- [3] R. E. Kahn, S. A. Gronemeyer, J. Burchfiel, and R. Kunzelman, "Advances in packet radio technology," in *Proceedings of the IEEE*, vol. 66, no. 11, pp. 1468–1496, November 1978.
- [4] J. A. Freebersyser and B. Leiner, *A DoD Perspective on Mobile Ad Hoc Networks*, In *Ad Hoc Networking*. Addison-Wesley, 2001, ch. 2, pp. 29–51.
- [5] R. Berezdivin, R. Breinig, and T. Topp, "Next-generation wireless communications concepts and technologies," *IEEE Communications Magazine*, vol. 40, no. 3, pp. 108–116, March 2002.
- [6] W. C. Jakes, *Microwave mobile communications*, 2nd ed. WILEY INTERSCIENCE, 2001.
- [7] G. L. Stuber, *Principles of mobile communication*, 2nd ed. Kluwer Academic Publishers, 2001.
- [8] J. Kang, Y. Zhang, and B. Nath, "Accurate and energy-efficient congestion level measurement in ad hoc networks," in *Proceedings of WCNC*, vol. 4, pp. 2258–2263, March 2005.
- [9] H. Takagi and L. Kleinrock, "Optimal transmission ranges for randomly distributed packet radio terminals," *IEEE Transactions on Communications*, vol. COM-32, no. 3, pp. 246–257, March 1984.

-
- [10] M. Grossglauser and D. Tse, "Mobility increases the capacity of ad-hoc wireless networks," in *Proceedings of IEEE Information Communications (INFOCOM)*, pp. 477–486, April 2001.
- [11] M. Haenggi, "Link modeling with joint fading and distance uncertainty," in *Proceedings of 4th International Symposium on Modeling and Optimization in Mobile, Ad Hoc and Wireless Networks*, pp. 1–6, April 2006.
- [12] E. S. Sousa and J. A. Silvester, "Optimum transmission ranges in a direct-sequence spread-spectrum multihop packet radio network," *IEEE Journal on Selected Areas in Communications*, vol. 8, no. 5, pp. 762–771, June 1990.
- [13] R. Punnose, P. Nitkin, J. Borch, and D. Stancil, "Optimizing wireless network protocols using real time predictive propagation modeling," in *Proceedings of RAWCON*, pp. 39–44, August 1999.
- [14] E. Cianca, A. D. Luise, M. Ruggieri, and R. Prasad, "Channel-adaptive techniques in wireless communications: an overview," *Wireless Communications and Mobile Computing*, vol. 2, no. 8, pp. 799–813, December 2002.
- [15] J. Cavers, "Variable-rate transmission for Rayleigh fading channels," *IEEE Transactions on Communications*, vol. COM-20, pp. 15–22, February 1972.
- [16] T. Ekman, "Prediction of mobile radio channels: Modeling and design," *thesis, Uppsala University*, 2002.
- [17] A. Bletsas, A. Khisti, D. P. Reed, and A. Lippman, "A simple cooperative diversity method based on network path selection," *IEEE Journal on Selected Areas in Communications*, vol. 24, no. 3, pp. 659–672, March 2006.
- [18] J. Ai, A. A. Abouzeid, and Z. Ye, "Cross-layer optimal decision policies for spatial diversity forwarding in wireless ad hoc networks," in *Proceedings of Mobile Adhoc and Sensor Systems (MASS)*, pp. 150–159, October 2006.
- [19] M. R. Souryal, B. R. Vojcic, and R. L. Pickholtz, "Information efficiency of multihop packet radio networks with channel-adaptive routing," *IEEE Journal on Selected Areas in Communications*, vol. 23, no. 1, pp. 40–50, January 2005.
- [20] S. N. Diggavi, N. Al-Dhahir, A. Stamoulis, and A. R. Calderbank, "Great expectations: The value of spatial diversity in wireless networks," in *Proceedings of THE IEEE*, vol. 92, no. 2, pp. 219–270, February 2004.

BIBLIOGRAPHY

- [21] J. N. Laneman and G. W. Wornell, "Distributed space-time coded protocols for exploiting cooperative diversity in wireless networks," *IEEE Transactions on Information Theory*, vol. 49, no. 10, pp. 2415–2525, October 2003.
- [22] J. N. Laneman, D. N. C. Tse, and G. W. Wornell, "Cooperative diversity in wireless networks: Efficient protocols and outage behavior," *IEEE Transactions on Information Theory*, vol. 51, no. 12, pp. 3062–3080, December 2004.
- [23] R. Knopp and P. A. Humblet, "Information capacity and power control in a single cell multiuser environment," *In Proceedings of IEEE ICC 1995*, vol. 1, pp. 331–335, June 1995.
- [24] K. Karakayali, J. H. Kang, M. Kodialam, and K. Balachandran, "Joint resource allocation and routing for OFDMA-based broadband wireless mesh networks," *in Proceedings of ICC*, pp. 5088–5092, June 2007.
- [25] L. Hanzo, C. Wong, and M. Yee, *Adaptive Wireless Transceivers: Turbo-Coded, Turbo-Equalised and Space-Time Coded TDMA, CDMA, MC-CDMA and OFDM Systems*. Wiley, Europe Publishers, 2002.
- [26] E. S. Lo, P. W. Chan, V. K. N. Lau, R. S. C. abd K. B. Letaief, R. D. Murch, and W. H. Mow, "Adaptive resource allocation and capacity comparison of down-link multiuser MIMO-MC-CDMA and MIMO-OFDMA," *IEEE Transactions on Wireless Communications*, vol. 6, no. 2, pp. 1083–1093, March 2007.
- [27] T. S. Rappaport, *Wireless communications, principles and practice*, 2nd ed. Prentice Hall, 2000.
- [28] X. Chen, H. M. Jones, and D. Jayalath, "Congestion-aware routing protocol for mobile ad hoc networks," *in Proceedings of VTC-Fall 2007*, pp. 21–25, October 2007.
- [29] D. Johnson and D. Maltz, *Dynamic source routing in ad hoc wireless networks*. Mobile Computing, Kluwer Academic Publishers, 1996, ch. 5, pp. 153–181.
- [30] X. Chen, H. M. Jones, and D. Jayalath, "Effective link operation duration: a new routing metric for mobile ad hoc networks," *in Proceedings of ICSPCS*, pp. 315–320, December 2007.

- [31] M. K. Marina and S. R. Das, "On-demanding multipath distance vector routing in ad hoc networks," in *Proceedings of International Conference on Network Protocols (ICNP)*, pp. 14–23, November 2001.
- [32] X. Chen, H. M. Jones, and D. Jayalath, "Channel-aware routing in MANETs with route handoff," *submitted to IEEE Transactions on mobile computing*, 2008.
- [33] X. Chen, D. Jayalath, and L. Hanlen, "Multiple shared channels cooperative routing for ad hoc networks," *accepted by 2009 International Symposium on Intelligence, Context-Awareness and Autonomy in Wireless Networks*, 2009.
- [34] C. E. Perkins and P. Bhagwat, "Highly dynamic destination-sequenced distance-vector routing (DSDV) for mobile computers," in *Proceedings of ACM SIGCOMM*, vol. 24, no. 4, pp. 234–244, October 1994.
- [35] T. Clausen and P. Jacquet, "Optimized link state routing protocol (OLSR)," *IETF Request For Comment: RFC 3626*, 2003.
- [36] D. Bertsekas and R. Gallager, Eds., *Data Networks*. Prentice-hall, Englewood Cliffs, N.J, 1987, pp. 297–333.
- [37] C. E. Perkins and E. M. Royer, "Ad-hoc on-demand distance vector routing," in *Proceedings of Mobile Computing Systems and Applications (WMCSA '99)*, pp. 90–100, February 1999.
- [38] M. S. Corson and A. Ephremides, "a distributed routing algorithm for mobile wireless networks," *ACM/Baltes Wireless Networks Journal*, vol. 1, no. 1, pp. 61–82, February 1995.
- [39] V. Park and M. S. Corson, "A highly adaptive distributed routing algorithm for mobile wireless networks," in *Proceedings of IEEE INFOCOM '97*, vol. 3, pp. 1405–1413, April 1997.
- [40] C. K. Toh, "a novel distributed routing protocol to support ad hoc mobile computing," in *Proceedings of 15th IEEE annual international phoenix conference on computers and communications, phoenix*, pp. 480–486, November 1996.
- [41] Z. Haas and M. R. Pearlman, "The performance of query control schemes for the zone routing protocol," *IEEE/ACM Transactions on Networking (TON)*, vol. 9, no. 4, pp. 427–438, August 2001.

BIBLIOGRAPHY

- [42] B. Karp and H. T. Kung, "GPSR: greedy perimeter stateless routing for wireless networks," in *Proceedings of the sixth annual ACM/IEEE International Conference on Mobile computing and networking*, pp. 243–254, August 2000.
- [43] Y.-B. Ko and N. Vaidya, "Location-aided routing (LAR) in mobile ad hoc networks," in *proceedings of the fourth ACM/IEEE international conference on mobile computing and networking (MOBICOM'98)*, pp. 66–75, October 1998.
- [44] K. Wu and J. Harms, "Load-sensitive routing for mobile ad hoc networks," in *Proceedings of the IEEE International Conference on Computer Communications and Networks (ICCCN)*, pp. 540–546, October 2001.
- [45] H. Hassanein and A. Zhou, "Routing with load balancing in wireless ad hoc networks," in *Proceedings of the 4th ACM International Workshop on Modeling, Analysis and Simulation of Wireless and Mobile Systems*, pp. 89–96, July 2001.
- [46] D. A. Tran and H. Raghavendra, "Congestion adaptive routing in mobile ad hoc networks," *IEEE Transactions on Parallel and Distributed Systems*, vol. 17, no. 11, pp. 1294–1305, November 2006.
- [47] S. Lee and M. Gerla, "Dynamic load-aware routing in ad hoc networks," in *Proceedings of the IEEE International Conference on Communications (ICC)*, pp. 3206–3210, June 2001.
- [48] A. BOUKERCHE and S. K. DAS, "Congestion control performance of R-DSDV protocol in multihop wireless ad hoc networks," *Wireless Networks, Kluwer Academic Publishers*, vol. 9, pp. 261–270, May 2003.
- [49] R. Dube, C. Rais, K. Y. Wang, and S. K. Tripathi, "Signal stability-based adaptive routing (SSA) for ad hoc networks," *IEEE Personal Communications*, vol. 4, no. 1, pp. 36–45, February 1997.
- [50] M. Park, J. Andrews, and S. Nettles, "Wireless channel-aware ad hoc cross-layer protocol with multi-route path selection diversity," in *Proceedings of Vehicular Technology Conference (VTC 2003-Fall)*, vol. 4, pp. 2197–2201, October 2003.
- [51] Y. Yuan, Z. He, and M. Chen, "Virtual MIMO-based cross-layer design for wireless sensor networks," *IEEE Transactions on Vehicular Technology*, vol. 55, no. 3, pp. 856–864, May 2006.

- [52] B. Awerbuch, D. Holer, and H. Rubens, "High throughput route selection in multi-rate ad hoc wireless networks," in *Proceedings of the First working conference on wireless on-demand network systems (WONS 2004)*, pp. 251–269, March 2004.
- [53] S. Zhao, Z. Wu, A. Acharya, and D. Raychaudhuri, "PARMA: a PHY/MAC aware routing metric for ad-hoc wireless networks with multi-rate radios," in *Proceedings of WoWMoM 2005*, pp. 286–292, June 2005.
- [54] M. Zorzi and S. Pupolin, "Optimum transmission ranges in multihop packet radio networks in the presence of fading," *IEEE Transactions on Communications*, vol. 43, no. 7, pp. 2201–2205, July 1995.
- [55] T. Goff, N. Abu-Ghazaleh, D. Phatak, and R. Kahvecioglu, "Preemptive routing in ad hoc networks," in *Proceedings of the 7th annual international conference on Mobile computing and networking*, pp. 43–52, July 2001.
- [56] J. Zhao and R. Govindan, "Understanding packet delivery performance in dense wireless sensor networks," in *Proceedings of SenSys*, pp. 1–13, November 2003.
- [57] L. Wang, Y. T. Shu, O. W. W. Yang, M. Dong, and L. F. Zhang, "adaptive multipath source routing in wireless ad hoc networks," in *Proceedings of the IEEE International Conference on Communications (ICC)*, pp. 867–871, June 2001.
- [58] X. Lin, Y. K. Kwok, and V. K. N. Lau, "RICA: A receiver-initiated approach for channel-adaptive on-demand routing in ad hoc mobile computing networks," in *Proceedings of the 22nd International Conference on Distributed Computing Systems (ICDCS02)*, pp. 84–91, July 2002.
- [59] P. Sambasivam, A. Murthy, and E. M. Belding-Royer, "Dynamically adaptive multipath routing based on AODV," in *Proceedings of 3rd Annual Mediterranean Ad Hoc Networking Workshop*, pp. 27–30, June 2004.
- [60] X. Lin, Y. K. Kwok, and V. K. N. Lau, "BGCA: Bandwidth guarded channel adaptive routing for ad hoc networks," in *Proceedings of Wireless Communications and Networking Conference (WCNC2002)*, vol. 1, pp. 433–439, March 2002.

BIBLIOGRAPHY

- [61] M. R. Souryal and N. Moayeri, "Channel-adaptive relaying in mobile ad hoc networks with fading," in *Proceedings of Sensor and Ad Hoc Communications and Networks (SECON 2005)*, pp. 142–152, September 2005.
- [62] J. Wang, H. Zhai, W. Liu, and Y. Fang, "Reliable and efficient packet forwarding by utilizing path diversity in wireless ad hoc networks," in *Proceedings of Military Communications Conference (MILCOM)*, pp. 258–264, October 2004.
- [63] J. W. Lee, R. R. Mazumdar, and N. B. Shroff, "Joint opportunistic power scheduling and end-to-end rate control for wireless ad hoc networks," *IEEE Transactions on Vehicular Technology*, vol. 56, no. 2, pp. 801–809, March 2007.
- [64] D. S. J. D. Couto, D. Aguayo, J. Bicket, and R. Morris, "A high-throughput path metric for multi-hop wireless routing," in *Proceedings of the Ninth Annual International Conference on Mobile Computing and Networking (MobiCom '03)*, pp. 134–146, September 2003.
- [65] R. Draves, J. Padhye, and B. Zill, "Comparison of routing metrics for static multi-hop wireless networks," in *Proceedings of ACM Special Interest Group on Data Communications (SIGCOMM)*, pp. 133–144, August 2004.
- [66] S. Jain and S. R. Das, "Exploiting path diversity in the link layer in wireless ad hoc networks," in *Proceedings of the 6th IEEE WoWMoM Symposium*, pp. 22–30, June 2005.
- [67] P. Larsson, "Selection diversity forwarding in a multihop packet radio network with fading channel and capture," in *Proceedings of ACM MOBIHOC*, vol. 1, pp. 47–54, October 2001.
- [68] T. Hou and V. Li, "Transmission range control in multihop packet radio networks," *IEEE TRANSACTIONS ON COMMUNICATIONS*, vol. 34, no. 1, pp. 38–44, January 1986.
- [69] J. A. Silvester and L. Kleinrock, "On the capacity of multihop slotted ALOHA networks with regular structure," *IEEE Transactions on Communications*, vol. COM-31, no. 8, pp. 974–982, August 1983.
- [70] M. Qin and R. S. Blum, "Capacity of wireless ad hoc networks with cooperative diversity: A warning on the interaction of relaying and multi-hop routing," in

- Proceedings of International Conference on Communications (ICC)*, vol. 2, pp. 1128–1131, May 2005.
- [71] K. Azarian, H. E. Gamal, and P. Schniter, “On the achievable diversity-vs-multiplexing tradeoff in cooperative channels,” *IEEE Transactions on Information Theory*, vol. 51, pp. 4152–4172, December 2005.
- [72] P. Kyasanur and N. H. Vaidya, “Routing and interface assignment in multi-channel multi-interface wireless networks,” in *Proceedings of WCNC*, pp. 2051–2056, March 2005.
- [73] V. Kanodia, A. Sabharwal, and E. Knightly, “MOAR: a multichannel opportunistic auto-rate media access protocol for ad hoc networks,” in *Proceedings of IEEE BROADNETS*, pp. 600–710, October 2004.
- [74] A. S. Akki and F. Haber, “A statistical model of mobile-to-mobile land communication channel,” *IEEE Transactions on Vehicular Technology*, vol. VT-35, pp. 2–10, February 1986.
- [75] F. Vatalaro and A. Forcella, “Doppler spectrum in mobile-to-mobile communications in the presence of three-dimensional multipath scattering,” *IEEE Transactions on Vehicular Technology*, vol. 46, no. 1, pp. 213–219, February 1997.
- [76] A. S. Akki, “Statistical properties of mobile-to-mobile land communication channel,” *IEEE Transactions on Vehicular Technology*, vol. 43, no. 4, pp. 826–831, November 1994.
- [77] M. Heusse, F. Rousseau, G. Berger-Sabbatel, and A. Duda, “Performance anomaly of 802.11b,” in *Proceedings of INFOCOM*, vol. 2, pp. 836–843, March 2003.
- [78] A. Raniwala, K. Gopalan, and T. Chiueh, “Centralized algorithms for multi-channel wireless mesh networks,” *ACM SIGMOBILE Mobile Computing and Communications Review (MC2R)*, vol. 8, no. 2, pp. 50–65, April 2004.
- [79] Y. J. Lee and G. F. Riley, “A workload-based adaptive load balancing technique for mobile ad hoc networks,” in *Proceedings of WCNC*, vol. 4, pp. 2002–2007, March 2005.

BIBLIOGRAPHY

- [80] "IEEE Std 802.11 Wireless LAN Medium Access Control (MAC) and Physical Layer (PHY) Specifications," 1999.
- [81] B. Ohara and A. Petrick, *IEEE 802.11 Handbook, A Designer's Companion*. IEEE Press, 1999.
- [82] A. Kamerman and L. Monteban, "WaveLAN II: A high-performance wireless LAN for the unlicensed band," *Bell Labs Technical Journal*, pp. 118–133, 1997.
- [83] G. Holland, N. Vaidya, and P. Bahl, "A rate-adaptive MAC protocol for multi-hop wireless networks," in *Proceedings of the 7th annual international conference on Mobile computing and networking*, pp. 236–251, July 2001.
- [84] M. Lacage, M. H. Manshaei, and T. Turetletti, "IEEE 802.11 rate adaptation: A practical approach," in *Proceedings of MSWiM'04*, pp. 126–134, October 2004.
- [85] <http://www.isi.edu/nsnam/ns>.
- [86] J. Broch et al, "A performance comparison of multi-hop wireless adhoc network routing protocols," in *Proceedings of MOBICOM'98*, pp. 85–97, October 1998.
- [87] C. E. Perkins, E. M. Royer, S. R. Das, and M. K. Marina, "Performance comparison of two on-demand routing protocols for ad hoc networks," *IEEE Personal Communications*, vol. 8, pp. 16–28, February 2001.
- [88] C. Toh, "Associativity-based routing for ad-hoc mobile networks," *Wireless Personal Communications*, vol. 4, pp. 103–139, March 1997.
- [89] A. B. McDonald and T. Znati, "A path availability model for wireless ad-hoc networks," in *Proceedings of Wireless Communications and Networking Conference, 1999*, vol. 1, pp. 35–40, September 1999.
- [90] S. Agarwal, A. Ahija, J. P. Singh, and R. Shorey, "Route-lifetime assessment based routing (RABR) protocol for mobile ad-hoc networks," In *Proceedings of IEEE International Conference on Communications 2000*, vol. 3, pp. 1697–1701, June 2000.
- [91] W. Su and M. Gerla, "IPv6 flow handoff in ad hoc wireless networks using mobility prediction," in *Proceedings of GLOBECOM*, vol. 1a, pp. 271–275, December 1999.

- [92] S. Jiang, D. He, and J. Rao, "A prediction-based link availability estimation for routing metrics in MANETs," *IEEE/ACM Transactions on Networking*, vol. 13, no. 6, pp. 1302–1312, December 2005.
- [93] M. Gerharz, C. de Waal, M. Frank, and P. Martini, "Link stability in mobile wireless ad hoc networks," in *Proceedings of the 27th IEEE Conference on Local Computer Networks (LCN)*, pp. 30–39, November 2002.
- [94] S. Panichpapiboon, G. Ferrari, and O. K. Tonguz, "Optimal transmit power in wireless sensor networks," *IEEE Transactions on Mobile Computing*, vol. 5, no. 10, pp. 1432–1447, October 2006.
- [95] R. J. Punnoose, P. V. Nikitin, and D. D. Stancil, "Efficient simulation of Ricean fading within a packet simulator," in *Proceedings of Vehicular Technology Conference (VTC)*, vol. 2, pp. 764–767, September 2000.
- [96] M. Haenggi, "Routing in ad hoc networks—a wireless perspective," in *Proceedings of BroadNets*, pp. 652–660, December 2004.
- [97] L. L. Scharf, *Statistical Signal Processing: Detection, Estimation, and Time Series Analysis*. Addison-Wesley, 1991.
- [98] O. Tickoo, S. Raghunath, and S. Kalyanaraman, "Route fragility: A novel metric for route selection in mobile ad hoc networks," in *Proceedings of the 11th IEEE International Conference on Networks (ICON2003)*, pp. 537–542, September 2003.
- [99] P. Pham, S. Perreau, and A. Jayasuriya, "New cross-layer design approach to ad hoc networks under Rayleigh fading," *IEEE Journal on Selected Areas in Communications*, vol. 23, no. 1, pp. 28–39, January 2005.
- [100] A. Nasipuri and S. R. Das, "On-demand multi-path routing for mobile ad hoc networks," in *Proceedings of Eight International Conference on Computer Communications and Networks*, pp. 64–70, October 1999.
- [101] J. S. daSilva and S. Mahmoud, "Capacity degradation of packet radio fading channels," In *Proceedings of the sixth symposium on Data communications*, pp. 97–101, 1979.

BIBLIOGRAPHY

- [102] I. S. Gradshteyn and I. M. Ryzhik, *Tables of integrals, serials, and products*, 7th ed. Academic press, 2007.
- [103] C. S. Patel, G. L. Stuber, and T. G. Pratt, "Simulation of Rayleigh-faded mobile-to-mobile communication channels," *IEEE Transactions on Communications*, vol. 53, no. 11, pp. 1876–1884, 2005.
- [104] R. U. Nabar, H. Bolcskei, and F. W. Kneubuhler, "Fading relay channels: performance limites and space-time signal design," *IEEE Journals on Selected Areas in Telecommunications*, vol. 22, no. 6, pp. 1099–1109, August 2004.
- [105] P. Soldati and M. Johansson, "Network-wide resource optimization of wireless OFDMA mesh networks with multiple radios," in *Proceedings of ICC 2007*, pp. 4979–4984, June 2007.
- [106] "IEEE Std 802.16e," *IEEE Standard for Local and Metropolitan Area Networks Part 16*, February 2006.
- [107] B. Kim, S. W. Kim, and R. L. Ekl, "OFDMA-based reliable multicasting MAC protocol for WLANs," *IEEE Transactions on Vehicular Technology*, vol. 57, no. 5, pp. 3136–3145, September 2008.
- [108] S. Valentin, T. Freitag, and H. Karl, "Integrating multiuser dynamic OFDMA into IEEE 802.11 WLANs-LLC/MAC extensions and system performance," in *Proceedings of ICC*, pp. 3328–3334, 2008.
- [109] B. Hofmann-Wellenhof, H. Lichtenegger, and J. Collins, *Global Positioning System: Theory and Practice*, 4th ed. Springer-Verlag, 1997.
- [110] W. H. Liao, Y. C. Tseng, and J. P. Sheu, "GRID: A fully location-aware routing protocol for mobile ad hoc networks," *Telecommunication Systems*, vol. 18, no. 1-3, pp. 37–60, October 2001.
- [111] G. Fodor, "Performance analysis of a reuse partitioning technique for OFDM based evolved UTRA," in *Proceedings of 14th IEEE International Workshop on Quality of Service*, pp. 112–120, 2006.
- [112] M. Sichitiu and C. Veerarittiphan, "Simple, accurate time synchronization for wireless sensor networks," in *Proceedings of IEEE Wireless Communications and Networking Conference*, vol. 2, pp. 1266–1273, March 2003.

- [113] Z. Zhang, W. Zhang, and C. Tellambura, "Improved OFDMA uplink frequency offset estimation via cooperative relaying: AF or DcF?" in *Proceedings of ICC'08*, pp. 3313–3317, May 2008.
- [114] M. Penrose, *Random Geometric Graphs*. Oxford University Press, 2003.
- [115] X. Liu and M. Haenggi, "The impact of the topology on the throughput of interference-limited sensor networks with rayleigh fading," in *Proceedings of IEEE SECON 2005*, pp. 317–327, September 2005.
- [116] D. G. Brennan, "Linear diversity combining techniques," in *Proceedings of the IEEE*, vol. 91, no. 2, pp. 331–356, February 2003.
- [117] T. J. Hwang, H. S. Hwang, and H. Baik, "Adaptive OFDM with channel predictor over frequency-selective and rapid fading channel," in *Proceedings of PIMRC 2003*, vol. 1, pp. 859–863, September 2003.
- [118] D. Schafhuber and G. Matz, "MMSE and adaptive prediction of time-varying channels for OFDM systems," *IEEE Transactions on Wireless Communications*, vol. 4, no. 2, pp. 593–602, March 2005.
- [119] R. V. Nee and R. Prasad, *OFDM for Wireless Multimedia Communications*. Artech House Publishers, 1999.
- [120] S. Yun, S. Y. Park, Y. Lee, E. Alsusa, and C. G. Kang, "Spectrum efficient region-based resource allocation with fractional loading for FH-OFDMA cellular systems," *Electronics Letters*, vol. 41, no. 13, pp. 752–754, June 2005.
- [121] Y. Li, L. J. Cimini, Jr., and N. R. Sollenberger, "Robust channel estimation for OFDM systems with rapid dispersive fading channels," *IEEE Transaction on Communications*, vol. 46, no. 7, pp. 902–915, July 1998.
- [122] Y. Li, N. Seshadri, and S. Ariyavisitakul, "Channel estimation for OFDM systems with transmitter diversity in mobile wireless channels," *IEEE Journal on Selected Areas in Communications*, vol. 17, no. 3, pp. 461–471, March 1999.